

Introduction to Integrability

Lecture Notes

ETH Zurich, HS16

PROF. N. BEISERT

© 2013–2017 Niklas Beisert

This document as well as its parts is protected by copyright.
This work is licensed under the Creative Commons
“Attribution-NonCommercial-ShareAlike 4.0 International”
License (CC BY-NC-SA 4.0).



To view a copy of this license, visit:

<https://creativecommons.org/licenses/by-nc-sa/4.0>

The current version of this work can be found at:

<http://people.phys.ethz.ch/~nbeisert/lectures/>

Contents

Contents	3
Overview	5
0.1 Introduction	5
0.2 Contents	6
0.3 Literature	6
0.4 Acknowledgements	6
1 Integrable Mechanics	1.1
1.1 Hamiltonian Mechanics	1.1
1.2 Integrals of Motion	1.2
1.3 Liouville Integrability	1.4
1.4 Comparison of Classes	1.9
2 Structures of Classical Integrability	2.1
2.1 Lax Pair	2.1
2.2 Classical r-matrix	2.2
2.3 Spectral Parameter	2.3
2.4 Spectral Curve	2.4
2.5 Dynamical Divisor	2.8
2.6 Reconstruction	2.10
3 Integrable Field Theory	3.1
3.1 Classical Field Theory	3.1
3.2 Structures of Integrability	3.5
3.3 Inverse Scattering Method	3.8
3.4 Spectral Curves	3.16
4 Integrable Spin Chains	4.1
4.1 Heisenberg Spin Chain	4.1
4.2 Spectrum of the Closed Chain	4.4
4.3 Coordinate Bethe Ansatz	4.7
4.4 Bethe Equations	4.13
4.5 Generalisations	4.16
5 Long Chains	5.1
5.1 Magnon Spectrum	5.1
5.2 Ferromagnetic Continuum	5.3
5.3 Anti-Ferromagnetic Ground State	5.6
5.4 Spinons	5.9
5.5 Spectrum Overview	5.13

6	Quantum Integrability	6.1
6.1	R-Matrix Formalism	6.1
6.2	Charges	6.6
6.3	Other Types of Bethe Ansätze	6.12
7	Quantum Algebra	7.1
7.1	Lie Algebra	7.1
7.2	Classical Integrability	7.3
7.3	Quantum Algebras	7.6
7.4	Yangian Algebra	7.9
8	Integrable Statistical Mechanics	8.1
8.1	Models of Statistical Mechanics	8.1
8.2	Integrability	8.7
	Schedule of Lectures	7

0 Overview

0.1 Introduction

What is integrability?

- ... a peculiar feature of some theoretical physics models.
- ... makes calculations in these models much more feasible in principle and in practice; it is also known as (complete) solvability.
- ... often can be used to map a physical problem to a problem of complex functional analysis.
- ... allows to compute some quantities exactly and analytically rather than approximately and numerically.
- ... is a hidden enhancement of symmetries which constrain the motion substantially or completely.
- ... is the absence of chaotic motion.
- ... is a colourful mixture of many subjects and techniques from mathematics to physical phenomena.
- ... a lot of fun.

Which classes of models are integrable?

- some classical mechanics models, e.g.: free particle, harmonic oscillator, spinning top, planetary motion, ... ,¹
- some $(1 + 1)$ -dimensional classical field theories, e.g.: Korteweg–de Vries (KdV), sine-Gordon, Einstein gravity, sigma models on coset spaces, classical magnets, string theory,
- some quantum mechanical models, e.g. the quantum versions of the above classical mechanics models,
- some $(1 + 1)$ -dimensional quantum field theories, e.g. most of the quantum counterparts of the above classical field theories, except cases where integrability is spoiled by quantum effects,
- some 2-dimensional models of statistical mechanics, e.g. 6-vertex model, 8-vertex model, alternating sign matrices, loop models, Ising model, ... ,
- $D = 4$ self-dual Yang–Mills theory,
- $D = 4$, $N = 4$ maximally supersymmetric Yang–Mills theory in the planar limit and the AdS/CFT dual string theory on $AdS_5 \times S^5$,

One observes that integrability is a phenomenon largely restricted to two-dimensional systems. There are some higher-dimensional exceptions, but most of them have some implicit two-dimensionality (self-duality, planar limit).

¹Most models discussed in lectures and textbooks are in fact integrable, most likely because they can be solved easily and exactly.

0.2 Contents

1. Integrable Mechanics (120 min)
2. Structures of Classical Integrability (140 min)
3. Integrable Field Theory (270 min)
4. Integrable Spin Chains (245 min)
5. Long Chains (150 min)
6. Quantum Integrability (140 min)
7. Quantum Algebra (185 min)
8. Integrable Statistical Mechanics (90 min)

0.3 Literature

- G. Arutyunov, “Students Seminar: Classical and Quantum Integrable Systems”
- O. Babelon, D. Bernard, M. Talon, “Introduction to Classical Integrable Systems”, Cambridge University Press (2003)
- M. Dunajski, “Solitons, Instantons and Twistors”, Oxford University Press (2010).
- A. Torrielli, “Lectures on Classical Integrability”,
<http://arxiv.org/abs/1606.02946>.
- N. Beisert, “The Dilatation Operator of $\mathcal{N} = 4$ super Yang-Mills Theory and Integrability”, Phys. Rept. 405, 1–202 (2004),
<http://arxiv.org/abs/hep-th/0407277>.
- N. Reshetikhin, “Lectures on the integrability of the 6-vertex model”,
<http://arxiv.org/abs/1010.5031>.
- L.D. Faddeev, “How Algebraic Bethe Ansatz Works for Integrable Model”,
<http://arxiv.org/abs/hep-th/9605187>.
- P. Zinn-Justin, “Six-Vertex, Loop and Tiling Models: Integrability and Combinatorics”
- D. Bernard, “An Introduction to Yangian Symmetries”, Int. J. Mod. Phys. B7, 3517–3530 (1993), <http://arxiv.org/abs/hep-th/9211133>.
- V. Chari, A. Pressley, “A Guide to Quantum Groups”, Cambridge University Press (1995).
- C. Gómez, M. Ruiz-Altaba, G. Sierra, “Quantum Groups in Two-Dimensional Physics”, Cambridge University Press (1996).
- N. Beisert et al., “Review of AdS/CFT Integrability: An Overview”,
<http://arxiv.org/abs/1012.3982>.
- ...

0.4 Acknowledgements

I am grateful to Elias Furrer and Florian Loebbert for a list of corrections on an earlier version of these lecture notes.

1 Integrable Mechanics

In the first chapter we introduce and discuss the notion of integrability for a system of classical mechanics with finitely many degrees of freedom. In this situation there is a very clean definition of integrability due to Liouville. This lays the foundations for the more elaborate cases of integrability in $(1 + 1)$ -dimensional field theory and quantum mechanics discussed in later chapters.

1.1 Hamiltonian Mechanics

We start by defining a classical mechanics system in Hamiltonian formulation. It consists of a phase space M of dimension $2n$ ¹ and a Hamiltonian function $H : M \rightarrow \mathbb{R}$. Phase space is defined by a set of coordinates q^k and momenta p_k with $k = 1, \dots, n$.²

A solution of the system is a curve $(q^k(t), p_k(t))$ in phase space which obeys the Hamiltonian equations of motion

$$\dot{q}^k = \frac{\partial H}{\partial p_k}, \quad \dot{p}_k = -\frac{\partial H}{\partial q^k}. \quad (1.1)$$

The ultimate goal for a system of Hamiltonian mechanics is to find the solutions $(q^k(t), p_k(t))$ given generic initial conditions (q_0^k, p_k^0) at $t = t_0$. However, for most systems this goal cannot be achieved,³ and the explicit time evolution might provide more information than one is actually interested in. In most cases, one would rather like to understand some generic properties of the solution like conserved quantities, periodic motion or asymptotic behaviour.

It is convenient to introduce Poisson brackets which map a pair of functions F, G on phase space to another function on phase space⁴

$$\{F, G\} := \frac{\partial F}{\partial q^k} \frac{\partial G}{\partial p_k} - \frac{\partial F}{\partial p_k} \frac{\partial G}{\partial q^k}. \quad (1.2)$$

¹Ordinarily, the phase space must have even dimension. A phase space of odd dimension is also conceivable with some restrictions on the structures of Hamiltonian mechanics, such as the canonical two-form.

²The coordinate q^k is canonically conjugate to the coordinate p_k in the Hamiltonian equations of motion and the Poisson brackets. Due to this duality it makes sense to assign the indices of q and p to be upper and lower, respectively. However, one may just as well ignore their vertical position.

³In other words, the set of established mathematical functions does not suffice to formulate the solution. Evidently, one can define new abstract functions that solve precisely the given system of equations, but since their properties are unknown, this does not help towards understanding the physical behaviour of the system at hand.

⁴The Poisson brackets are often defined by specifying the canonical relations $\{q^k, p_l\} = \delta_l^k$ along with the trivial ones $\{q^k, q^l\} = \{p_k, p_l\} = 0$ instead of the fully general form.

The Poisson brackets are anti-symmetric, and they obey the Jacobi identity for any three phase space functions F, G, K

$$\{\{F, G\}, K\} + \{\{G, K\}, F\} + \{\{K, F\}, G\} = 0. \quad (1.3)$$

The Poisson brackets allow us to write the equations of motion in a compact and uniform fashion as

$$\frac{d}{dt} q^k = -\{H, q^k\}, \quad \frac{d}{dt} p_k = -\{H, p_k\}. \quad (1.4)$$

More generally, the time-dependence of a function $F(q, p, t)$ evaluated on a solution $(q^k(t), p_k(t))$ reads⁵

$$\frac{d}{dt} F = \frac{\partial F}{\partial t} - \{H, F\}. \quad (1.5)$$

Finally, the concept of *canonical transformations* $(q, p) \mapsto (\tilde{q}, \tilde{p})$ plays an important role. For a transformation to be canonical, the new coordinates $\tilde{q}(q, p)$ and $\tilde{p}(q, p)$ as functions of the old ones, must be canonically conjugate

$$\{\tilde{q}^k, \tilde{p}_l\} = \delta_l^k, \quad \{\tilde{q}^k, \tilde{q}^l\} = \{\tilde{p}_k, \tilde{p}_l\} = 0. \quad (1.6)$$

One goal is to find phase space coordinates in which the transformed Hamiltonian \tilde{H} takes a simpler form. Ideally, one would make \tilde{H} a function of the new momenta \tilde{p}_k only. In this case, the new momenta are constants and the new positions depend linearly on time.

1.2 Integrals of Motion

For a time-independent Hamiltonian, $\partial H / \partial t = 0$, the function $H(q, p)$ is an *integral of motion* or a *conserved quantity*

$$\frac{d}{dt} H = \frac{\partial H}{\partial t} - \{H, H\} = 0. \quad (1.7)$$

The immediate benefit is that solutions are constrained to a hyper-surface of M with constant energy E defined by $H(q, p) = E$. This makes it somewhat easier to find solutions.

Depending on the model, further (time-independent)⁶ integrals of motion $F_k(q, p)$ can exist

$$\frac{d}{dt} F_k = -\{H, F_k\} \stackrel{!}{=} 0. \quad (1.8)$$

⁵To compare this to the above equations of motion one should introduce the coordinate functions $Q^k(q, p, t) := q^k$, $P_k(q, p, t) := p_k$.

⁶Throughout this course we will implicitly assume that functions of phase space have no explicit time dependence unless specified otherwise.

This gives additional constraints $F_k(q, p) = f_k = \text{const}$ and motion takes place on an even lower-dimensional hyper-surface which is called a *level set*

$$M_f := \{(q, p) \in M; F_k(q, p) = f_k \text{ for all } k\}. \quad (1.9)$$

The restriction of motion to level sets is not the only benefit of an integral of motion; it furthermore corresponds to a symmetry of the system, a fact which can be used to generate new solutions from existing ones. To that end, one associates a *flow* $-\{F, \cdot\}$ on phase space to the phase space function F .⁷ Note that the flow of the Hamiltonian H describes time evolution. The flow of an integral of motion F_k shifts a solution $(q(t), p(t))$ infinitesimally to another solution⁸

$$(q(t), p(t)) + \epsilon \delta(q(t), p(t)) + \dots \quad (1.10)$$

with

$$\delta q(t) = -\{F_k, q(t)\}, \quad \delta p(t) = -\{F_k, p(t)\}. \quad (1.11)$$

This solution carries the same energy E as well as the conserved charge f_k (but not necessarily the conserved charges f_l of the other integrals of motion).

Additional simplifications come about when all integrals of motion are *in involution* or (*Poisson commute*)

$$\{F_k, F_l\} = 0. \quad (1.12)$$

In this case, all solutions deformed by the flows of the F_k belong to the same level set M_f . Moreover, all flows mutually commute.

By construction, the Hamiltonian H is among the integrals of motion and often one identifies $F_1 = H$. In other cases, it may be more convenient to write H as a more complicated function of the conserved quantities $H = H(F_k)$.

Finding further integrals of motion is all but straight-forward:

- They are often found by trial and error based on a suitable ansatz.
- Noether's theorem implies the existence of a conserved quantity for each global symmetry of the system.
- Additional conserved quantities can be viewed to generate additional hidden symmetries of the system. Finding all integrals of motion is thus tantamount to identifying all (hidden) symmetries.

Example. Let us consider as an example a particle of mass m moving in a two-dimensional rotationally symmetric potential $V(r)$, $r = \sqrt{x^2 + y^2}$. The Lagrange function reads

$$L = \frac{1}{2}m\dot{x}^2 + \frac{1}{2}m\dot{y}^2 - V(r). \quad (1.13)$$

⁷A flow is a vector field describing an infinitesimal shift $\delta(q, p) = -\{F, (q, p)\}$ of the phase space points. Alternatively, it can be viewed as a derivative operator $G \mapsto -\{F, G\}$ for phase space functions.

⁸This construction is closely related to Noether's theorem: A continuous global symmetry gives rise to an integral of motion. In the Hamiltonian framework, there is a natural inversion of this statement: The flow of an integral of motion generates precisely the associated symmetry.

Due to the rotational symmetry, it makes sense to go to radial coordinates, $x = r \cos \varphi$, $y = r \sin \varphi$. The transformed Lagrange function reads

$$L = \frac{1}{2}m\dot{r}^2 + \frac{1}{2}mr^2\dot{\varphi}^2 - V(r). \quad (1.14)$$

A rotation shifts φ by a constant amount and leaves L invariant. We go to the Hamiltonian formulation by means of a Legendre transformation. The momenta read $p = m\dot{r}$ and $\psi = mr^2\dot{\varphi}$ and we find the Hamiltonian

$$H = \frac{p^2}{2m} + \frac{\psi^2}{2mr^2} + V(r). \quad (1.15)$$

The equations of motion read

$$\begin{aligned} \dot{r} &= \frac{\partial H}{\partial p} = \frac{p}{m}, & \dot{p} &= -\frac{\partial H}{\partial r} = \frac{\psi^2}{mr^3} - V'(r), \\ \dot{\varphi} &= \frac{\partial H}{\partial \psi} = \frac{\psi}{mr^2}, & \dot{\psi} &= -\frac{\partial H}{\partial \varphi} = 0. \end{aligned} \quad (1.16)$$

The Hamiltonian does not depend on φ , consequently $F = \psi$ is an integral of motion. Towards finding a solution, it makes sense to express the momentum p through the energy E and the conserved quantity ψ ⁹

$$P(r, E, \psi) = \sqrt{2m(E - V(r)) - \frac{\psi^2}{r^2}}. \quad (1.17)$$

We know that $dr/dt = P/m$ which we solve by separation of variables

$$\int_{r_0}^r \frac{m dr'}{P(r', E, \psi)} = t. \quad (1.18)$$

By integrating and solving this relationship we obtain the solution $r(t)$ depending further on E , ψ and the integration constants r_0 and t_0 . Finally, we can integrate the angular dependence

$$\varphi(t) = \varphi_0 + \int_0^t \frac{\psi dt}{m r(t)^2} = \varphi_0 + \int_{r_0}^{r(t)} \frac{\psi dr'}{r'^2 P(r', E, \psi)}. \quad (1.19)$$

In principle, this solves the class of models, but the remaining integrals and inversions typically cannot be done using elementary functions except in special cases such as a harmonic potential $\sim r^2$ or an inverse quadratic potential $\sim 1/r^2$.

1.3 Liouville Integrability

A system with $2n$ -dimensional phase space M is called (Liouville) *integrable* if it has

⁹The function P gives one branch of the solution. The other branch has the opposite sign for the square root. Here we focus on a local solution; the global solution is obtained by properly taking the branching points into account.

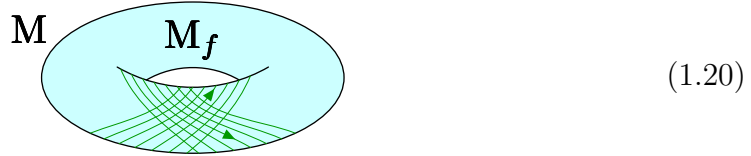
- n independent¹⁰
- everywhere differentiable
- integrals of motion F_k
- in involution, $\{F_k, F_l\} = 0$.

Such a system is solvable by “quadratures”, i.e. it suffices to solve a finite number of equations and integrals (instead of solving the equations of motion, which are differential equations). In order to understand this statement better, let us first investigate some of the resulting structures.

Phase Space Structure. For an integrable system, the level sets M_f have a particularly nice structure:

- M_f has dimension n ;
- there are n independent commuting flows acting on it.

The flows therefore locally define a complete set of n coordinates.



Considering the fact that the Hamiltonian is one of the integrals of motion, the coordinates will be called *time functions* T^k . They are specified by the differential equations $\{F_k, T^l\} = -\delta_k^l$ while picking a particular point as the origin. These differential equations define the T^k within a level set. Furthermore, the time functions can be defined across the level sets by imposing the additional differential equations $\{T^k, T^l\} = 0$. The Jacobi identity then ensures that suitable functions T^k can be constructed. Altogether we have

$$\{T^k, F_l\} = \delta_l^k, \quad \{F_k, F_l\} = \{T^k, T^l\} = 0, \quad (1.21)$$

which tells us that the map $(q, p) \mapsto (T, F)$ is a canonical transformation.

A useful corollary of integrability is that motion on the level set is linear because H is an integral of motion and thus a function $H(F)$ of the F_k only

$$\begin{aligned} \frac{d}{dt} F_k &= -\{H, F_k\} = 0, \\ \frac{d}{dt} T^k &= -\{H, T^k\} = -\sum_l \frac{\partial H}{\partial F_l} \{F_l, T^k\} = \frac{\partial H}{\partial F_k} = \text{const}. \end{aligned} \quad (1.22)$$

In other words, the solution in the new coordinates reads

$$T^k = T_0^k + t \frac{\partial H}{\partial F_k}(f), \quad F_k = f_k = \text{const}. \quad (1.23)$$

¹⁰A function of phase space is called independent of a set of functions if it cannot be written as a function of the values of the other functions. For instance, the total angular momentum $J^2 = J_x^2 + J_y^2 + J_z^2$ is dependent on the components $\{J_x, J_y, J_z\}$ of the angular momentum. Moreover, a constant function is always dependent, even on the empty set of functions.

Diagram (1.24) consists of two parts. On the left, a light blue oval represents a level set in phase space. Inside, a blue curve oscillates vertically, with a dashed blue line below it. A blue arrow labeled t points to the right. On the right, a 2D plot shows a grid of red lines with a positive slope. The horizontal axis is labeled T^1 and the vertical axis is labeled T^2 . A blue arrow labeled t points to the right, parallel to the T^1 axis.

(1.24)

Note that the time functions T^k are only defined locally. If one extends them globally to level sets with non-trivial cycles, they become multiple-valued functions. Going around a non-trivial cycle $C_l(f)$ of a level set, the times jump by a definite amount¹¹ determined by the so-called *period matrix*

$$\Omega_l^k(f) = \oint_{C_l(f)} dT^k. \quad (1.25)$$

In that sense, the time functions T^k are uniquely defined on the universal cover of the level sets.

Diagram (1.26) consists of two parts. On the left, a light blue oval represents a level set in phase space. Inside, a green curve oscillates vertically, with a dashed green line below it. A green arrow labeled T^1 points to the right, and a green arrow labeled T^2 points upwards. On the right, a 2D plot shows a grid of red lines with a positive slope. The horizontal axis is labeled T^1 and the vertical axis is labeled T^2 . Two points on the T^1 axis are labeled ω_1 and ω_2 .

(1.26)

Quadrature. The above merely describes the resulting picture, but the transformation $(q, p) \mapsto (T, F)$ is described by means of differential equations. Let us now show explicitly how the desired transformation can be constructed by quadrature amounting to a complete solution of the system.

As the first step, we solve the coordinates p_k for the values of the charges f_k at fixed positions q^k .¹² In other words, we construct a set of functions $P_k(q, f)$ such that

$$P_k(q, F(q, p)) \stackrel{!}{=} p_k. \quad (1.27)$$

As the second step, we fix some arbitrary point q_0^k in position space and introduce a function $S(q, f)$

$$S(q, f) := \int_{q_0}^q P_k(q', f) dq'^k. \quad (1.28)$$

Effectively, this is the integral of the canonical one-form $p_k dq^k$ over the level set M_f written out in the coordinates q^k . Importantly, this integral only depends on the endpoint q and not on the path between q_0 and q because the canonical

¹¹The differential equations determine the time functions locally up to a constant shift.

¹²For a general point in phase space this transformation is invertible. However, there may be points for which the transformation is singular. In these cases, one might proceed by interchanging the roles of some p_k and q^k .

one-form is closed when restricted to the level set M_f . To see this, we consider the derivative of the integrand one-form

$$dP_k \wedge dq^k = df_l \wedge dq^k \frac{\partial P_k}{\partial f_l} + dq^l \wedge dq^k \frac{\partial P_k}{\partial q^l}. \quad (1.29)$$

Here, the involutive property $\{F_k, F_l\} = 0$ implies the symmetry $\partial F_k / \partial q^l = \partial F_l / \partial q^k$ making use of the above relationship $P(q, F(q, p)) = p$. Therefore the latter term vanishes and $dp_k \wedge dq^k = 0$ when restricted to M_f .

As the third and final step, we use the function $S(q, f)$ as a generator for a canonical transformation.¹³ We notice that S was constructed to correctly reproduce the coordinate maps $P_k(q, f)$

$$\frac{\partial S}{\partial q^k}(q, f) = P_k(q, f). \quad (1.30)$$

We can thus define the time functions $T^k(q, p)$ as

$$T^k(q, p) := \frac{\partial S}{\partial f_k}(q, F(q, p)) = \int_{q_0}^q \frac{\partial P_l}{\partial f_k}(q', F(q', p)) dq'^l. \quad (1.31)$$

Consequently, the map $(q, p) \mapsto (T, F)$ is a canonical transformation.

In the above construction of the canonical transformation we merely used inversion of a relationship and elementary integration which formally solves our mechanical system. Nevertheless, it deserves being mentioned that neither of the above steps is trivial. Only for very special integrable mechanical systems, the solutions can actually be expressed in terms of elementary mathematical functions.

Nevertheless, the various structures we have already discussed can be used to infer useful qualitative information on the solution. For instance, it may be possible to derive the periodicity of solutions (as functions of the integrals of motion) without explicitly finding the underlying solutions.

Example. In the above example of a radial potential $V(r)$ in two dimensions, we are just as before led to solve for p at given positions and integrals of motion

$$P(r, E, \psi) = \sqrt{2m(E - V(r)) - \frac{\psi^2}{r^2}}. \quad (1.32)$$

The momentum ψ is already an integral of motion, and no coordinate transformation is required. The generating function of the canonical transformation reads

$$\begin{aligned} S(r, \varphi, E, \psi) &= \int_{(r_0, \varphi_0)}^{(r, \varphi)} (P(r', E, \psi) dr' + \psi d\varphi') \\ &= \int_{r_0}^r P(r', E, \psi) dr' + \psi(\varphi - \varphi_0). \end{aligned} \quad (1.33)$$

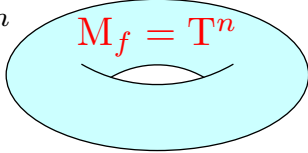
¹³We refer to textbooks of Hamiltonian mechanics for the notion of generating functions of canonical transformations.

From this we can read off the time variables t and τ conjugate to E and ψ , respectively

$$\begin{aligned} t &:= \frac{\partial S}{\partial E} = \int_{r_0}^r \frac{m \, dr'}{P(r', E, \psi)}, \\ \tau &:= \frac{\partial S}{\partial \psi} = \varphi - \varphi_0 - \int_{r_0}^r \frac{\psi \, dr'}{r'^2 P(r', E, \psi)}. \end{aligned} \quad (1.34)$$

Notice that these are precisely the integrals we obtained earlier. The time variable τ is another conserved quantity essentially because t is the actual time and the two are independent. The inversion of this canonical transformation solves the system completely.

Compact Level Sets. The following theorem holds for a Liouville integrable system: If the level set M_f is compact, it is diffeomorphic to the n -dimensional torus T^n , the so-called *Liouville torus*.

$$M = M^{2n} \quad \text{with} \quad M_f = T^n \quad (1.35)$$


The theorem follows from the above structure of flows: it is well-known that a compact manifold of dimension n which admits n commuting vector fields is diffeomorphic to the torus T^n .

In the case of compact level sets, it makes sense to introduce *action-angle variables*: So far, we have merely characterised the integrals of motion F_k as independent, differentiable and in involution. However, any invertible transformation on the F_k would lead to an equivalent set of integrals of motion. The corresponding time variables T^k as constructed above would transform accordingly. However, here we can introduce the action-angle variables as a standardised set of phase space coordinates. One defines the action variables I_k as the periods of the n independent non-trivial cycles $C_k(f)$ on the level set

$$I_k(f) := \frac{1}{2\pi} \oint_{C_k(f)} p_l \, dq^l. \quad (1.36)$$

These are (non-local) functions of the level set M_f , and thus they are integrals of motion.¹⁴ Based on these, we can construct associated time variables which are called the angle variables Θ^k . The period matrix for the angle variables takes a particularly simple form

$$\oint_{C_l(f)} d\Theta^k = 2\pi \delta_l^k, \quad (1.37)$$

i.e. each angle variable increases by 2π over its associated cycle. The action-angle variables are a particularly useful concept towards quantisation because the action variables are quantised in multiples of \hbar . E.g., for a harmonic oscillator the action variable is E/ω which is indeed quantised in units of \hbar .

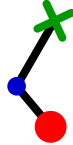
¹⁴The choice of cycles leaves some remaining freedom in the definition of action variables.

1.4 Comparison of Classes

Independently of integrability, we can always *locally* define functions (T^k, F_k) such that $\{T^k, F_l\} = \delta_l^k$ and $\{F_k, F_l\} = \{T^k, T^l\} = 0$ with the Hamiltonian H a function of the F_k only. This means that any system of classical mechanics can be considered integrable in a sufficiently small patch of phase space. However, for a system to be integrable, the functions F_k must be global diffeomorphisms on phase space. Moreover, in order to perform the quadrature they must be known functions rather than being defined implicitly through differential equations. In that sense, integrability is a property which depends strongly on the global structure of phase space and the explicit knowledge of the integrals of motion.

Chaos. In the generic situation, it is almost always impossible to continue the integrals of motion F_k as defined above consistently to all regions of phase space. In other words, when following the level set by means of the defining differential equations, one may end up in the initial region with the shifted level set misaligned with the original one. This leads to *chaotic motion*.

A hallmark feature of chaotic motion is the exponential divergence of solutions, where a minor change in the initial conditions can lead to a radical deviation in the long-term evolution. Tracing out initially nearby solutions would lead to highly complicated hyper-surfaces spread out wildly across phase space. The latter could not possibly be described as level sets of globally differentiable functions F_k . Most dynamical systems with more than one degree of freedom, i.e. a phase space of dimension 4 or higher, are chaotic. A reasonably simple example of a chaotic system is the double pendulum.



(1.38)

Its two constituent pendulums will alternate between oscillatory and rotational motion with a seemingly random pattern of repetitions. For example, mass of the secondary pendulum may sweep out the following irregular trajectory:



(1.39)

Integrability. For an integrable system the hyper-surfaces match up well globally due to their definition as a level set of differentiable functions F_k . As discussed above, one finds linear motion on the level set. Since the level set typically has several periods which are rationally incompatible, the motion of the system is quasi-periodic. All (time-independent) dynamical systems with one degree of freedom are integrable. Further examples include the multi-dimensional HO, the spinning top, planetary motion and classical integrable spin chains.

Super-Integrability. Some systems have more than n integrals of motion, but evidently only n of them can be in involution. These systems are called *super-integrable*. Here, some of the periods of the tori are rationally compatible and therefore the orbits partially close. For a maximally super-integrable system with $2n - 1$ integrals of motion the orbits close and the motion is truly periodic. Dynamical systems with one degree of freedom are in fact maximally super-integrable and therefore have periodic motion. Further examples are Kepler's planetary motion,¹⁵ the spinning top¹⁶ and multi-dimensional harmonic oscillators with rationally compatible frequencies.

For non-integrable systems, there may be further useful distinctions that could be made:

- n integrals of motion which are not (all) in involution,
- less than n (but more than one) integrals of motion,
- regions of phase space of a chaotic system which show regular behaviour.

In this lecture series we will only be interested in the fully integrable cases. Super-integrability may occur accidentally, but we will not pay attention to it.

¹⁵In addition to the angular momentum there is the Runge–Lenz vector which is orthogonal to the angular momentum vector. This amounts to 5 integrals of motion and maximal super-integrability.

¹⁶The spinning top has 3 integrals of motion in involution H , J^2 and J_z and is therefore integrable. Among the two further components of the angular momentum vector only one is independent of J^2 and J_z .

2 Structures of Classical Integrability

In this chapter we shall introduce several important structures for integrable models that will help us investigate and solve the model. In some form or another, they will reappear for integrable field theories and quantum integrable models.

2.1 Lax Pair

Integrable systems are often formulated in terms of a *Lax pair*. A Lax pair is a pair of square matrices L, M whose entries are functions of phase space. The characteristic property of Lax pairs is that the *Lax equation*

$$\frac{d}{dt} L = [M, L] \quad (2.1)$$

is equivalent to the complete set of equations of motion.

If a Lax pair exists for a classical mechanics system, the matrix L can be used to generate a tower of integrals of motion F_k

$$F_k = \text{tr } L^k. \quad (2.2)$$

These quantities are trivially conserved due to the cyclicity of the trace

$$\frac{d}{dt} F_k = k \text{tr } L^{k-1} [M, L] = 0. \quad (2.3)$$

Although there are infinitely many F_k , at most N of them can be independent for an $N \times N$ Lax matrix.

Alternatively, one can say that the Lax equation is equivalent to the statement that time evolution of L is generated by a similarity transformation. Therefore the characteristic polynomial and eigenvalue spectrum of L are conserved. Note that these are functions of the F_k .

Having a Lax pair formulation of integrability is very convenient, but

- inspiration is needed to find it,
- its structure is hardly transparent,
- it is not at all unique,
- the size of the matrices is not immediately related to the dimensionality of the system.

Therefore, the concept of Lax pairs does not provide a means to decide whether any given system is integrable (unless one is lucky to find a sufficiently large Lax pair).

Example. Consider a harmonic oscillator with frequency ω . Its Hamiltonian takes the form

$$H = \frac{1}{2m} p^2 + \frac{\omega^2}{2m} q^2. \quad (2.4)$$

A Lax pair is given by

$$L = \begin{pmatrix} +p & \omega q \\ \omega q & -p \end{pmatrix}, \quad M = \begin{pmatrix} 0 & -\frac{1}{2}\omega \\ +\frac{1}{2}\omega & 0 \end{pmatrix}. \quad (2.5)$$

The Lax equation is equivalent to the equation of motion of the harmonic oscillator

$$\dot{p} = -\omega^2 q, \quad \omega \dot{q} = \omega p. \quad (2.6)$$

The resulting integrals of motion read

$$\begin{aligned} F_1 &= 0, \\ F_2 &= 2p^2 + 2\omega^2 q^2 = 4mH, \\ F_3 &= 0, \\ F_4 &= 2(p^2 + \omega^2 q^2)^2 = 8m^2 H^2, \\ &\dots \end{aligned} \quad (2.7)$$

Here F_1 and F_3 are trivial and can be ignored. The first and only independent integral of motion F_2 is the Hamiltonian. The higher even powers are merely powers of the Hamiltonian which are not independent integrals of motion.

2.2 Classical r-matrix

For integrability we not only need sufficiently many global integrals of motion F_k , but they must also be in involution, $\{F_k, F_l\} = 0$. In the formulation of a Lax pair $L, M \in \text{End}(V)$, this property is equivalent to the statement

$$\{L_1, L_2\} = [r_{12}, L_1] - [r_{21}, L_2]. \quad (2.8)$$

The statement is defined on the tensor product space $\text{End}(V \otimes V)$ of two matrices, and the *classical r-matrix* r_{12} is a particular element of this space whose entries are functions on phase space.¹ Furthermore, $L_1 := L \otimes 1$, $L_2 := 1 \otimes L$, and $r_{21} := P(r_{12})$ denotes the permutation of the two spaces for the r-matrix. Note that the r-matrix is by no means uniquely defined by the equation.² Much like for the Lax pair, there is no universal method to obtain the r-matrix.

However, there is a method due to Sakharov and Shabat to construct Lax pairs and r-matrices from scratch without reference to a physics model, the idea being that an integrable physics model can be built upon these structures.

¹The tensor product $A \otimes B$ of two matrices with elements A^a_c, B^b_d has the elements $(A \otimes B)^{ab}_{cd} = A^a_c B^b_d$, where ab and cd are combined indices enumerating a basis for the tensor product space.

²For example, one can add an operator of the form $1 \otimes X + L \otimes Y$ where X and Y are arbitrary matrices.

From the above equation it follows straight-forwardly that

$$\begin{aligned} \{\text{tr } L^k, \text{tr } L^l\} &= kl \text{tr}_{1,2} (L_1^{k-1} L_2^{l-1} [r_{12}, L_1] - L_1^{k-1} L_2^{l-1} [r_{21}, L_2]) \\ &= 0. \end{aligned} \quad (2.9)$$

There is a useful graphical representation of the equation where matrices are objects with one ingoing and one outgoing leg. Connecting two legs corresponds to a product of matrices, whereas two matrices side by side correspond to a tensor product. Consequently, the classical r-matrix will be an object with two ingoing and outgoing legs, and the above equation reads

$$\begin{aligned} \left\{ \begin{array}{c} 1 \\ \text{---} L \text{---} 1, 2 \\ \text{---} L \text{---} 2 \end{array} \right\} &= \begin{array}{c} \begin{array}{c} 1 \\ \text{---} L \text{---} 1 \\ \text{---} r \text{---} 2 \end{array} - \begin{array}{c} 1 \\ \text{---} L \text{---} 2 \\ \text{---} r \text{---} 1 \end{array} \\ - \begin{array}{c} 2 \\ \text{---} L \text{---} 1 \\ \text{---} r \text{---} 2 \end{array} + \begin{array}{c} 2 \\ \text{---} L \text{---} 2 \\ \text{---} r \text{---} 1 \end{array} \end{array}. \end{aligned} \quad (2.10)$$

Many relationships can be conveniently expressed and proved using this graphical notation. We shall make extensive use of it in the context of integrable spin chains.

Example. For the above harmonic oscillator, a suitable classical r-matrix is given by

$$r_{12} = \frac{1}{q} \begin{pmatrix} 0 & 0 \\ 1 & 0 \end{pmatrix} \otimes \begin{pmatrix} 0 & 1 \\ 0 & 0 \end{pmatrix} - \frac{1}{q} \begin{pmatrix} 0 & 1 \\ 0 & 0 \end{pmatrix} \otimes \begin{pmatrix} 0 & 0 \\ 1 & 0 \end{pmatrix}. \quad (2.11)$$

The above commutators with the Lax matrix L then agrees precisely with the Poisson brackets

$$\{L_1, L_2\} = \omega \begin{pmatrix} 0 & 1 \\ 1 & 0 \end{pmatrix} \otimes \begin{pmatrix} 1 & 0 \\ 0 & -1 \end{pmatrix} - \omega \begin{pmatrix} 1 & 0 \\ 0 & -1 \end{pmatrix} \otimes \begin{pmatrix} 0 & 1 \\ 1 & 0 \end{pmatrix}. \quad (2.12)$$

2.3 Spectral Parameter

In many cases, Lax pairs depend on an auxiliary variable, the so-called *spectral parameter*, which is not directly related to the dynamics of the model. The Lax pair $L(u)$, $M(u)$ then obeys the Lax equation at all values of $u \in \mathbb{C}$

$$\frac{d}{dt} L(u) = [M(u), L(u)] \quad \text{for all } u \in \mathbb{C}. \quad (2.13)$$

The Lax pair must be constructed such that this equation is equivalent to the complete set of equations of motion. As a functional equation it is, in principle, much more constraining than the Lax equation without spectral parameter.³ This feature is useful for mechanical systems with infinitely many degrees of freedom whose equations of motion could thus be formulated by a finite-dimensional Lax pair. Even for a finite-dimensional system, Lax pairs with spectral parameter often

³Expanding the equation as a series in the spectral parameter yields infinitely many equations.

exist. While the spectral parameter is not essential to encode finitely many equations of motion, it is nevertheless useful in several respects. For example, in some cases, the above construction of conserved quantities misses some of the conserved quantities. More importantly, one can make use of the analytical structure of $L(u)$ in the complex spectral parameter u . This transforms the mechanical system to a problem of complex analysis which provides us with powerful tools to investigate the dynamics.

Also the classical r-matrix can be generalised to admit spectral parameters. It then becomes a function $r_{12}(u_1, u_2)$ of two spectral parameters $u_1, u_2 \in \mathbb{C}$ associated to each of the two related Lax matrices. The defining equation now reads

$$\{L_1(u_1), L_2(u_2)\} = [r_{12}(u_1, u_2), L_1(u_1)] - [r_{21}(u_2, u_1), L_2(u_2)]. \quad (2.14)$$

Example. A Lax pair with spectral parameter for the harmonic oscillator is given by

$$L(u) = \begin{pmatrix} +p + u\omega q & \omega q - up \\ \omega q - up & -p - u\omega q \end{pmatrix}, \quad M = \begin{pmatrix} 0 & -\frac{1}{2}\omega \\ +\frac{1}{2}\omega & 0 \end{pmatrix}. \quad (2.15)$$

Here, M does not depend on u for some reason, but the non-trivial dependence of L on u is what matters most.

The integrals of motion $F_k(u)$ now become functions of u as well. We find

$$\begin{aligned} F_1(u) &= 0, \\ F_2(u) &= 4(1 + u^2)mH = (1 + u^2)F_2(0), \\ F_3(u) &= 0, \\ F_4(u) &= 8(1 + u^2)^2m^2H^2 = (1 + u^2)^2F_4(0), \\ &\dots \end{aligned} \quad (2.16)$$

In our case, the presence of the spectral parameter does not change much, as there is only one integral of motion H in the first place. In systems with infinitely many degrees of freedom, however, the expansion of the $F_k(u)$ in u can yield infinitely many independent integrals of motion which are needed for integrability of such a model.

2.4 Spectral Curve

We know that the $F_k(u)$ are integrals of motion, but, in fact, there is much more information encoded into the eigensystem of the Lax matrix $L(u)$ and its analytic dependence on the spectral parameter u . In the following we shall investigate the analytic structure of the Lax eigensystem in detail. Even though somewhat abstract, the observed structures can tell us much about the physics of the model.

Singularities. First of all, the Lax equation $dL/dt = [M, L]$ tells us that the time evolution of $L(u)$ is iso-spectral, i.e. the set of eigenvalues $\lambda_k(u)$ is an integral of motion for all $u \in \mathbb{C}$.

Let us analyse the dependence of the eigenvalues on the spectral parameter u : Suppose, the Lax matrix $L(u)$ is analytic (holomorphic) in u on the compactified complex plane $\bar{\mathbb{C}}$ except for some finite set of points $\{\tilde{u}_k\}$ where $L(u)$ has pole singularities.⁴ One might expect the same to hold for the eigenvalues $\lambda_k(u)$, but interestingly this is not always true. Namely, the eigenvalues are the solutions of the characteristic equation, and solving algebraic equations may introduce further singularities. One can convince oneself that this can happen only when two eigenvalues coincide at certain points $u = \hat{u}_k$.

Let us study the *generic* singular behaviour at coincident eigenvalues of a 2×2 matrix⁵

$$L(u) = \begin{pmatrix} a(u) & b(u) \\ c(u) & d(u) \end{pmatrix}. \quad (2.17)$$

The eigenvalues of this matrix read

$$\lambda_{1,2}(u) = \frac{1}{2}(a(u) + d(u)) \pm \sqrt{\frac{1}{4}(a(u) - d(u))^2 + b(u)c(u)}. \quad (2.18)$$

Now suppose that at a point $u = \hat{u}$ the eigenvalues degenerate $\lambda_1(\hat{u}) = \lambda_2(\hat{u})$ implying the relationship

$$\frac{1}{4}(a(\hat{u}) - d(\hat{u}))^2 + b(\hat{u})c(\hat{u}) = 0. \quad (2.19)$$

Expanding around $u = \hat{u}$ we find the leading correction term for the eigenvalues at order $(u - \hat{u})^{1/2}$

$$\begin{aligned} \lambda_{1,2}(u) &= \frac{1}{2}(a(\hat{u}) + d(\hat{u})) \pm \alpha \sqrt{u - \hat{u}} + \mathcal{O}(u - \hat{u}), \\ \alpha^2 &= \frac{1}{2}(a(\hat{u}) - d(\hat{u}))(a'(\hat{u}) - d'(\hat{u})) \\ &\quad + b(\hat{u})c'(\hat{u}) + b'(\hat{u})c(\hat{u}). \end{aligned} \quad (2.20)$$

This means that one may generically expect a square root singularity at a point $u = \hat{u}$ where two eigenvalues degenerate.

We thus learn that in addition to the manifest pole singularities at $u = \tilde{u}_k$ inherited from $L(u)$, there can be arbitrarily many square root singularities at $u = \hat{u}_k$. Their positions often depend on the integrals of motion, and thus they encode some of the time-independent data of the solution.

Riemann Sheets. A square root singularity \hat{u} is a special point for a complex function: When following the function analytically along a small circle around such

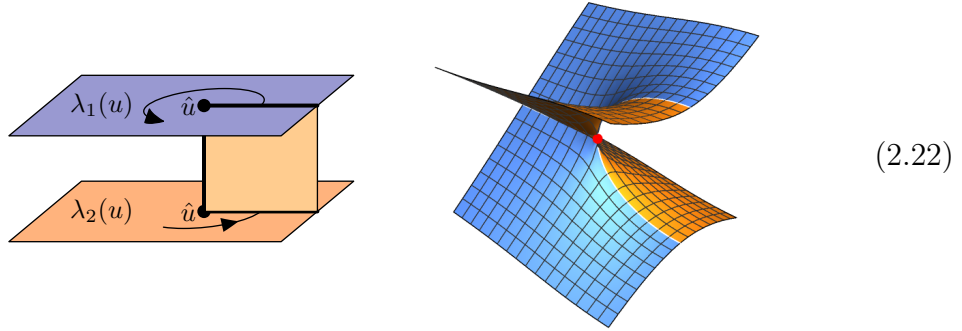
⁴By multiplying $L(u)$ by a scalar function $\omega(u)$, these poles may be shifted to different locations without changing the relevant relationships. Hence the location of the \tilde{u}_k may not be physically relevant.

⁵More complicated singular situations can arise for bigger matrices, but these may be viewed as the coincidence of several singularities and thus not generic behaviour.

a point, the function does not return to its original value. For example, we can follow the function $\lambda(u) = \alpha + \beta\sqrt{u - \hat{u}}$ around the circle $u(\tau) = \hat{u} + \epsilon e^{i\tau}$, to obtain

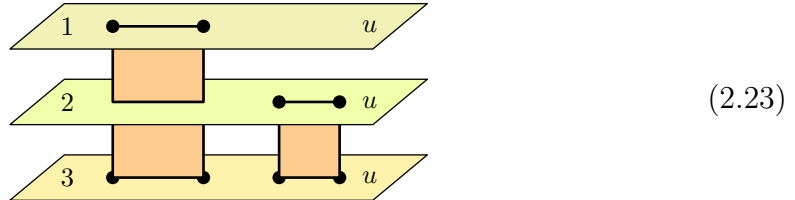
$$\lambda(u(\tau)) = \alpha + \beta\sqrt{\epsilon} e^{i\tau/2} + \mathcal{O}(\epsilon). \quad (2.21)$$

For a square root singularity, it takes an angle of 4π rather than 2π to let the function return to its value before rotation. The rotation of 2π interchanges the branches of the complex square root function, i.e. it flips the sign in front of the square root term. For the square root singularity arising from the spectral decomposition this means that the rotation interchanges two eigenvalues, as can be seen explicitly in the above example of a 2×2 matrix.



Generically, the N eigenvalue functions $\lambda_k(u)$ form an N -sheeted cover of the compactified complex plane (without the punctures at \tilde{u}_k). At the square root branch points \hat{u}_k , two Riemann sheets coincide; taking a full circle of angle 2π around these points interchanges the two sheets. There is nothing wrong with such a behaviour because all eigenvalues are equivalent by all means. A rotation by 2π merely changes our labelling of the eigenvalues which is inconsequential.

Consequently, branch points should be connected in pairs by some branch cuts. These branch cuts have no a priori physical meaning, they merely specify the location of some (unavoidable) discontinuities of the functions $\lambda_k(u)$ in the coordinate u . When passing through such branch cuts, the function $\lambda_k(u)$ is analytically continued by some other eigenvalue $\lambda_l(u)$.



Spectral Curve. In functional analysis, it is common to reinterpret a function $\lambda_k(u)$, $u \in \bar{\mathbb{C}}$, with several Riemann sheets $k = 1, \dots, N$ over the compactified complex plane $\bar{\mathbb{C}}$ as a single-valued analytic function $\lambda(z)$, $z \in X$, on a single Riemann surface X . A Riemann surface is a one-dimensional complex (or two-dimensional real) manifold with a potentially non-trivial topology. To each point $z \in X$ on the Riemann surface there corresponds a point $u(z) \in \bar{\mathbb{C}}$ on one of

the sheets $k(z)$ such that the value of the function at z equals the value of the function at u on sheet k

$$\lambda(z) = \lambda_{k(z)}(u(z)). \quad (2.24)$$

The branch cuts then correspond to the inevitable discontinuities of the (discrete) sheet function $k(z)$ whereas the branch points are singularities of the coordinate transformation $z \rightarrow u$.



$$(2.25)$$

For the above eigenvalue problem, we find that the Lax matrix $L(u)$ as well as the set of eigenvalues $\{\lambda_k(u)\}$ are non-singular functions of u , whereas the particular eigenvalue functions $\lambda_k(u)$ are not. The latter are only analytic as a function $\lambda(z)$ on the Riemann surface $z \in X$. The appropriate Riemann surface corresponding to the Lax matrix $L(u)$ is called the *spectral curve*.⁶ Note that the latter not only depends on the physical model, but its moduli typically depend on (the conserved charges of) the solution. In fact, in many cases, the action variables are the periods of a suitable one-form around the non-trivial cycles of the spectral curve X . This shows that the genus g of the spectral curve X is related to the dimensionality n of the mechanical system, roughly $g \approx n$.

Example. For concreteness, we consider the harmonic oscillator again. The eigenvalue functions read

$$\lambda_{1,2}(u) = \pm \sqrt{(p + u\omega q)^2 + (\omega q - up)^2} = \pm \sqrt{2mE} \sqrt{1 + u^2}. \quad (2.26)$$

Clearly, this function has square root singularities at $\hat{u}_{1,2} = \pm i$. Furthermore, it has a pole at $\tilde{u} = \infty$.

Next we would like to understand the spectral curve. We choose the map⁷

$$u(z) = -i \frac{z - 1/z}{z + 1/z}. \quad (2.27)$$

in order to resolve the square root singularities at $\pm i$ and find

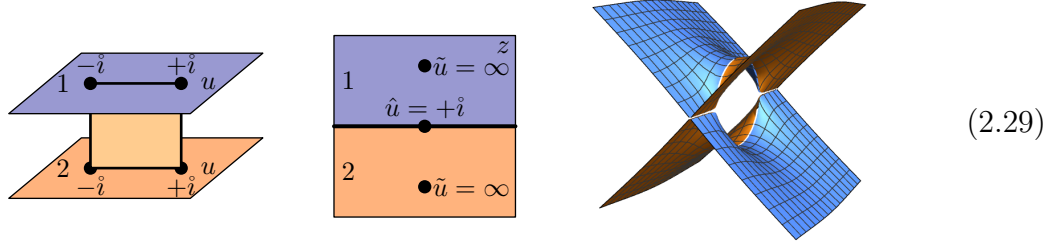
$$\lambda(z) = \sqrt{2mE} \frac{2}{z + 1/z}. \quad (2.28)$$

The resulting function is rational. The square root singularities $\hat{u}_{1,2} = \pm i$ have been mapped to the regular points $\hat{z}_{1,2} = 0, \infty$ on the Riemann surface. The pole at $\tilde{u} = \infty$ has two pre-images $\tilde{z}_{1,2} = \pm i$, one for each Riemann sheet. The eigenvalue

⁶The spectral curve X is a one-dimensional complex submanifold of two-dimensional complex space $(u, \lambda) \in \tilde{\mathbb{C}}^2$ expressed by the eigenvalue equation $\det(L(u) - \lambda) = 0$.

⁷A standard trick to resolve the square root singularities of $\sqrt{1 + u^2}$ is to take the combination $u = (x - x^{-1})/2$. Comparing the binomial formulas, one finds $\sqrt{1 + u^2} = \pm(x + x^{-1})/2$. The sign can be fixed at will and corresponds to the map $x \mapsto -x^{-1}$ which leaves u invariant.

function has two sheets, one branch cut and two poles. Therefore the resulting Riemann surface has genus 0; it is a Riemann sphere with two punctures $\tilde{z}_{1,2}$.



2.5 Dynamical Divisor

The spectral curve encodes information about the conserved charges of a solution. However, this only tells us about half of phase space; the other half is dynamical information which is in fact encoded into the eigenvectors of the Lax matrix. Let us therefore investigate the analytic behaviour of the eigenvectors $\psi_k(u)$.

Branch Points. We have already established that the eigenvalues are analytic in u except for poles in $L(u)$ at $\{\tilde{u}_k\}$ and square root singularities at $\{\hat{u}_k\}$ due to diagonalisation of $L(u)$. The former do not necessarily play a role for the eigenvectors, but the latter will also be square root singularities for them. Another source of singularities is the (arbitrary) normalisation of eigenvectors. We will discuss the normalisation later, and focus on the square root singularities.

We have learned that a rotation of angle 2π around a square root singularity exchanges two eigenvalues. Correspondingly, the eigenvectors are also exchanged. Importantly, there is a unique eigenvector at the singularity \hat{u} , even though there are two degenerate eigenvalues $\lambda_k(\hat{u}) = \lambda_l(\hat{u})$. In order to understand this issue, we reconsider the above 2×2 matrix at $u = \hat{u}$

$$L(\hat{u}) = \begin{pmatrix} a(\hat{u}) & b(\hat{u}) \\ c(\hat{u}) & d(\hat{u}) \end{pmatrix}. \quad (2.30)$$

We know that the matrix has two degenerate eigenvalues. However, for the matrix to have two independent eigenvectors as well, it would have to be proportional to the unit matrix

$$a(\hat{u}) = d(\hat{u}) = \lambda_{1,2}(\hat{u}), \quad b(\hat{u}) = c(\hat{u}) = 0. \quad (2.31)$$

In this case, the coefficient $\alpha = (a' - d')(a - d) + bc' + b'c$ of the square root term $\sqrt{u - \hat{u}}$ in the expansion of $\lambda_{1,2}(u)$ around \hat{u} is zero. Therefore, the square root singularity exists only for $\alpha \neq 0$ in which case the matrix is not diagonalisable, and has only a single eigenvector.⁸ In other words, square root singularities indicate points where the Lax matrix becomes non-diagonalisable.

⁸In physics, specifically in quantum mechanics, one typically encounters hermitian or unitary matrices which are always diagonalisable. The matrix $L(u)$ is often chosen to be hermitian, but only for a subset of spectral parameters. In our case, we have the reality condition $L(u)^\dagger = L(u^*)$, which is hermitian for real u only.

For a generic Lax matrix $L(u)$, the two distinct eigenvectors $\psi_k(u)$ and $\psi_l(u)$ therefore approach a common direction $\psi_k(\hat{u}) = \psi_l(\hat{u})$ at the point $u = \hat{u}$. This implies that, just like the eigenvalues, the eigenvectors can be viewed as a single-valued function $\psi(z)$ on the spectral curve X

$$\psi(z) = \psi_{k(z)}(u(z)). \quad (2.32)$$

Dynamical Divisor. We know that the eigenvector function $\psi(z)$ is analytic on the spectral curve X except for a set of poles. This analytical behaviour highly constrains the function and makes it constructible from a small set of data. Unfortunately, the length of eigenvectors is not determined by the eigenvalue equation and can be chosen at will. Given some scalar function $\omega(z)$ on the spectral curve X , the eigenvectors $\psi(z)$ can just as well be rescaled by this function

$$\psi(z) \equiv \omega(z)\psi(z). \quad (2.33)$$

In particular, the eigenvalue function $\psi(z)$ may inherit unphysical singularities from the scaling function $\omega(z)$.

In order to eliminate these unphysical degrees of freedom, it makes sense to pick a particular normalisation for the vectors $\psi(z)$. A reasonable choice is to fix one of the components of $\psi(z)$ to a constant for all $z \in X$. To that end, pick some constant vector v and demand

$$v \cdot \psi(z) = 1. \quad (2.34)$$

This choice eliminates the scaling degrees of freedom completely and fixes the function $\psi(z)$ uniquely.

We can now investigate the poles of $\psi(z)$. A pole z_k^\times of the vector-valued function $\psi(z)$ is defined as a point $z \in \mathbb{C}$ where *any* of the components of $\psi(z)$ diverges like $1/(z - z_k^\times)$.⁹ The set of poles $\{z_k^\times\}$ is called the *dynamical divisor*. One can show that it consists of $N + g - 1$ points, where N is the size of the Lax matrix and g the genus of the spectral curve X . Unlike the spectral curve, the dynamical divisor consists of the time-dependent information of the solution. As time progresses, the poles of $\psi(z)$ move around on X (in a well-prescribed fashion).

Example. Let us again consider the example of the harmonic oscillator. The eigenvectors of $L(u)$ take the form

$$\psi_{1,2}(u) \sim \begin{pmatrix} up - \omega q \\ u\omega q + p - \lambda_{1,2}(u) \end{pmatrix}, \quad (2.35)$$

where the branch points are inherited from the eigenvalues $\lambda_{1,2}(u)$. Expressing the eigenvectors as a function on the Riemann sphere X we find a rational dependence on z

$$\psi(z) \sim \begin{pmatrix} -iz(p - i\omega q) + iz^{-1}(p + i\omega q) \\ z(p - i\omega q) + z^{-1}(p + i\omega q) - 2\sqrt{2mE} \end{pmatrix}. \quad (2.36)$$

⁹In our normalisation, the poles are precisely the points where the direction of $\psi(z)$ is orthogonal to v (after rescaling by an infinite amount). Therefore, the set of poles crucially depends on the vector v we chose for the normalisation.

Noting the constraint $(p + i\omega q)(p - i\omega q) = p^2 + \omega^2 q^2 = 2mE$ we can rewrite this expression up to normalisation as

$$\psi(z) \sim \begin{pmatrix} i(p + i\omega q + \sqrt{2mE} z) \\ p + i\omega q - \sqrt{2mE} z \end{pmatrix}. \quad (2.37)$$

Finally we can fix the normalisation such that the first component of the eigenvector is constrained to 1

$$\psi(z) = \begin{pmatrix} 1 \\ -i \frac{p + i\omega q - \sqrt{2mE} z}{p + i\omega q + \sqrt{2mE} z} \end{pmatrix}. \quad (2.38)$$

This function has a single pole ($N + g - 1 = 1$) at

$$z^\times = -\frac{p + i\omega q}{\sqrt{2mE}}, \quad (2.39)$$

which is also the zero of the first component of $\psi(z)$ in a previous normalisation.

A solution of the harmonic oscillator is given by the path

$$q(t) = \frac{\sqrt{2mE}}{\omega} \sin(\omega t), \quad p(t) = \sqrt{2mE} \cos(\omega t). \quad (2.40)$$

The eigenvalue function reads

$$\psi(z) \sim \begin{pmatrix} i(e^{i\omega t} + z) \\ e^{i\omega t} - z \end{pmatrix}, \quad (2.41)$$

and the divisor is given by $z^\times = -e^{i\omega t}$.¹⁰

2.6 Reconstruction

Finally let us wrap up the insights gained in this chapter and discuss the applications.

Suppose we have an integrable model and an explicit solution of its equations of motion. Suppose further we know a Lax pair with spectral parameter for this model. Then the Lax pair obeys the Lax equation which tells us that the eigenvalue spectrum of $L(u)$ is conserved in time. The eigenvalues as a function of u define the spectral curve X for this model and our solution. The moduli of the spectral curve describe the conserved quantities of the solution. A particular set of marked points on the curve X , the dynamical divisor, describes the position variables of the model. These points move around on the spectral curve X in a particular fashion as time progresses.

¹⁰In view of this, it might make sense to divide $L(u)$ by the function $\sqrt{1 + u^2}$. This would shift the poles from $\tilde{z}_{1,2} = \pm i$ to $\tilde{z}_{1,2} = 0, \infty$ around which the divisor rotates.

A particularly nice feature of this construction is that it is reversible: Given a Riemann surface obeying a particular set of properties and a suitable set of marked points on it, we can reconstruct a unique state of the physical system that corresponds to it. The construction can thus be viewed as a transformation of the solution to a set of abstract data. As we shall see later in the case of integrable field theories, the transformed data sometimes is not abstract but has a useful interpretation in physical terms. The transformation is thus somewhat similar to a Fourier transformation which just as well produces data with a particular physical interpretation.

$$\begin{array}{ccc}
 \text{Diagram 1} & \longleftrightarrow & \text{Diagram 2}
 \end{array} \tag{2.42}$$



Furthermore, the transformation clearly separates integrals of motion from time-dependent variables. In many cases, one might only be interested in the former but not the latter. Then it is sufficient to construct a suitable spectral curve. This has several applications:

- Gain some understanding on the structure of general solutions.
- Determine relevant properties of the solution, such a periodicities, as a function of the integrals of motion.
- In quantum mechanics, the integrals of motion and the conjugate time-dependent variables cannot be determined simultaneously. An eigenstate is thus specified by only half of phase space, typically the integrals of motion.

3 Integrable Field Theory

Next we consider classical mechanics of a one-dimensional field $\phi(x)$. Together with time-evolution, this amounts to a problem of $(1+1)$ -dimensional fields $\phi(t, x)$. The phase space for such models is infinite-dimensional,¹ thus integrability requires infinitely many integrals of motion in involution. Comparing infinities is subtle, so defining integrability requires care. Since there is no clear notion of integrability for field theories, we will be satisfied with the availability of efficient constructive methods for solutions. Whether or not a model is formally integrable will be of little concern.

3.1 Classical Field Theory

Most random field theory models are clearly non-integrable, but there are several well-known models that are integrable:

- The Korteweg–de Vries (KdV) equation²

$$\dot{h} = 6hh' - h''' \quad (3.1)$$

arguably is the prototype integrable field theory. After a suitable transformation and adjustment of parameters, it can be used to model surface waves in shallow water.

- The non-linear Schrödinger equation

$$i\dot{\psi} = -\psi'' + 2\kappa|\psi|^2\psi \quad (3.2)$$

is the standard differential equation of non-relativistic quantum mechanics, albeit with a term non-linear in the wave function.

- The sine-Gordon equation

$$\ddot{\phi} - \phi'' + m^2 \sin \phi = 0 \quad (3.3)$$

is similar to the Klein–Gordon equation of a free scalar relativistic particle, but the mass term $m^2\phi$ is replaced by a term periodic in the value of the field.

- Non-linear sigma models

$$\partial^\alpha (G_{\mu\nu}(X) \partial_\alpha X^\nu) = 0 \quad (3.4)$$

describe the geodesic dynamics of the embedding $X^\mu(x)$ of a submanifold into a curved target space described by the metric $G_{\mu\nu}(X)$. If the submanifold is

¹Note that a time slice is a field which can be Taylor or Fourier expanded leading to infinitely many independent coefficients.

²The values of the coefficients are inessential, they can be adjusted by rescaling x , t and h .

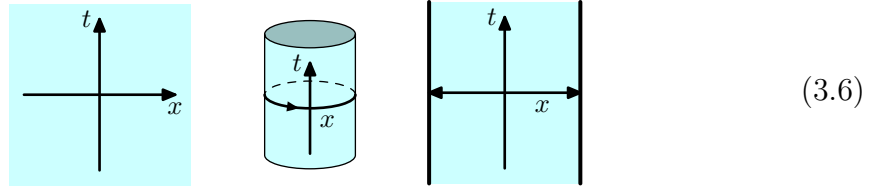
two-dimensional and the target space has certain symmetries, this model can be integrable. In the two-dimensional case, there are furthermore close connections to string theory.

- The classical Heisenberg magnet (Landau–Lifshitz equation)

$$\dot{\vec{S}} = -\kappa \vec{S} \times \vec{S}'', \quad \vec{S}^2 = 1. \quad (3.5)$$

In addition to the bulk equations of motion, a complete definition of the model also requires the specification of *boundary conditions*. The most common choices are:

- infinite spatial extent with rapidly decaying fields (or derivatives) as $x \rightarrow \infty$,
- closed or periodic boundary conditions with $x \equiv x + L$,
- open boundaries with Dirichlet or Neumann conditions $\phi = \text{const}$ or $\phi' = 0$.



Boundary conditions may also be twisted in some way or combined differently.

In this chapter we will discuss methods of integrability for field theories in $1 + 1$ dimensions using two of these models as examples. Let us therefore consider some of their properties in more detail.

Korteweg–de Vries Equation. The KdV equation can be derived from an action

$$S = \int dt dx \left[\frac{1}{2} \dot{\phi} \phi' - \phi'^3 - \frac{1}{2} \phi''^2 \right]. \quad (3.7)$$

Its Euler–Lagrange equation reads $\dot{\phi}' = 6\phi'\phi'' - \phi'''' = 0$ which is the KdV equation upon substitution $h = \phi'$. In the Hamiltonian formulation h is the momentum conjugate to ϕ .³ For the canonical structure one finds a slightly unusual form

$$\{h(x), h(y)\} = \delta'(x - y), \quad (3.8)$$

and the total momentum and Hamiltonian (total energy) read

$$P = \int dx \frac{1}{2} h^2, \quad H = \int dx \left[h^3 + \frac{1}{2} h'^2 \right]. \quad (3.9)$$

In addition to these evident conserved charges,⁴ there is an infinite tower of conserved *local* charges F_k in involution

$$F_0 = - \int dx h, \quad F_3 = \int dx \left[5h^4 + 10hh'^2 + h''^2 \right], \quad \dots \quad (3.10)$$

The existence of this infinite tower of conserved charges is due to integrability, and it leads to interesting behaviour in the solutions as we shall see shortly.

³The factor of $1/2$ in the canonical definition of momentum must be dropped because the above action is in first order form with ϕ being its own conjugate variable (up to a derivative).

⁴The momentum P and energy H correspond to translations in x and t .

Solitons and Factorised Scattering. A characteristic solution of the KdV equation is the *solitonic wave*

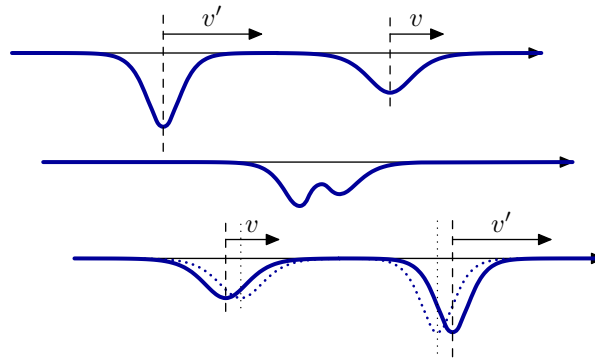
$$h(t, x) = -\frac{1}{2}v \operatorname{sech}^2\left[\frac{1}{2}\sqrt{v}(x - x_0 - vt)\right], \quad \begin{array}{c} \text{Graph of } h \text{ vs } x \\ \text{The curve is a negative sech-squared wave moving to the right with velocity } v. \\ \text{The width of the wave is indicated as } \sim 1/\sqrt{v}. \end{array} \quad (3.11)$$

which represents a wave packet moving at constant velocity v with several curious features: The wave packet never changes its shape, it neither disperses nor does it build up and eventually break; the non-linearity of the model is perfectly balanced against the dispersive effects of wave packets. Conservation of the shape of the soliton is related to integrability. Namely, the shape is determined by the infinite tower of local charges. As the latter are conserved, the shape must be conserved as well. The first few charges for the soliton read

$$\begin{aligned} P &= \frac{1}{3}v^{3/2}, & H &= -\frac{1}{5}v^{5/2}, \\ F_0 &= 2v^{1/2}, & F_3 &= \frac{2}{7}v^{7/2}. \end{aligned} \quad (3.12)$$

Furthermore, one can see that the amplitude of the wave is coupled to the velocity and width, and that the wave decays exponentially away from its centre. Moreover, this soliton can only propagate towards the right.

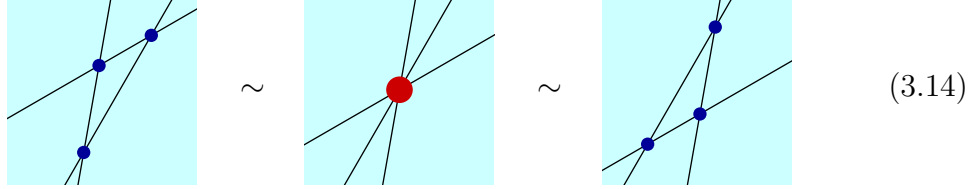
The most interesting effect occurs when one constructs a solution from two such solitons: We assume that initially the soliton centres are widely separated. Then they will largely evolve as if they were on their own because the interactions due to non-linear effects are strongly suppressed. If, however, a faster wave packet is to the right of a slower one, their distance will decrease until they come close and interact via the non-linear term. The colliding solitons then yield some complicated wave form. After some more time elapses, the two wave packets separate again and, most curiously, they emerge from the collision with precisely the same shapes and velocities. Merely the fast soliton has overtaken the slower one. Furthermore, the centres of the solitons have shifted by some amount. This suggests that the wave packets behave as two material particles which collide and scatter completely elastically.



$$(3.13)$$

Even more interestingly, the scattering of more than two solitons behaves in exactly the same way: Normally one can expect the solitons to scatter in a sequence of

pairwise interactions. Even if three or more solitons happen to come close at some point, their shapes are precisely restored after the collision. Moreover, the displacements of the centres of the solitons turn out to be independent of the sequence in which they scatter. To that end it also makes no difference whether the process involved a collision of three or more solitons. This curious effect is called *factorised scattering* and it is a hallmark feature of integrable models.



Heisenberg Magnet. The classical Heisenberg magnet is a model of a one-dimensional magnetic material with a magnetisation or spin vector field $\vec{S}(t, x)$. The spin vector has a constant length, $\vec{S}^2 = 1$.⁵



The energy depends on the alignment of nearby spins, the simplest ansatz is^{6 7}

$$H = \int dx \frac{1}{2} \vec{S}'^2. \quad (3.16)$$

A suitable Poisson structure is⁸

$$\{S^a(x), S^b(y)\} = -\varepsilon^{abc} S^c(x) \delta(x - y). \quad (3.17)$$

The equations of motion are the so-called Landau–Lifshitz equations

$$\dot{\vec{S}}(x) = -\{H, \vec{S}(x)\} = -\vec{S}(x) \times \vec{S}''(x). \quad (3.18)$$

Alternatively, this model is often formulated in terms of spherical variables ϑ, φ to parametrise the unit vector \vec{S} . As an aside, let us state the Hamiltonian,

$$H = \int dx \left[\frac{1}{2} \vartheta'^2 + \frac{1}{2} \sin^2 \vartheta \varphi'^2 \right], \quad (3.19)$$

⁵The field $\vec{S}(t, x)$ can also be viewed as the evolution of a one-dimensional curve on a two-dimensional sphere S^2 .

⁶Note that $\vec{S} \cdot \vec{S}' = 0$ due to $\vec{S}^2 = 1$.

⁷We conveniently fix the parameter κ of the above equation of motion to 1. This corresponds to a rescaling of time and energy.

⁸The above Hamiltonian along with the Poisson structure follows from a Lagrange function which is somewhat subtle.

the canonical structure

$$\{\varphi(x), \vartheta(y)\} = \frac{\delta(x-y)}{\sin \vartheta(x)}, \quad (3.20)$$

and the resulting equations of motion

$$\begin{aligned} \dot{\vartheta} &= 2 \cos \vartheta \vartheta' \varphi' + \sin \vartheta \varphi'', \\ \dot{\varphi} &= \cos \vartheta \varphi'^2 - \frac{\vartheta''}{\sin \vartheta}. \end{aligned} \quad (3.21)$$

The system is formulated without making reference to a preferred vector. Therefore it has a global rotational symmetry $\vec{S}(x) \mapsto R\vec{S}(x)$ with $R \in \text{SO}(3)$. This leads to a Noether current \vec{J}_α and associated Noether charge \vec{Q}

$$\vec{J}_t = \vec{S}, \quad \vec{J}_x = -\vec{S} \times \vec{S}', \quad \vec{Q} = \int dx \vec{S}. \quad (3.22)$$

The current and charge are conserved $\vec{J}_x - \dot{\vec{J}}_t = 0$ and $\dot{\vec{Q}} = 0$ provided the field \vec{S} satisfies the equations of motion. The total momentum is not easily expressed using the field \vec{S} ; instead we can use the spherical coordinates and write

$$P = \int dx (1 - \cos \vartheta) \varphi'. \quad (3.23)$$

This model is integrable, therefore there are infinitely many additional integrals of motion such as

$$F_3 = \frac{1}{2} \int dx \vec{S}'' \cdot (\vec{S} \times \vec{S}'). \quad (3.24)$$

3.2 Structures of Integrability

We want to set up a Lax pair to describe the integrals of motion for the field theory. There, integrability requires infinitely many conserved quantities, so the Lax pair should have a spectral parameter u .

Lax Connection. In field theory, we prefer to formulate quantities in terms of local objects. A suitable object is the *Lax connection* $A_\alpha(u; t, x)$. The Lax connection satisfies the flatness or zero-curvature condition

$$\dot{A}_x(u) - A'_t(u) + [A_x(u), A_t(u)] = 0 \quad \text{for all } u \in \mathbb{C} \quad (3.25)$$

if and only if the equations of motion hold. This method of specifying an integrable field theory is also called the *zero-curvature representation*.

A Lax connection for the KdV equation reads

$$\begin{aligned} A_x(u) &= \begin{pmatrix} 0 & -1 \\ u^{-1} - h & 0 \end{pmatrix}, \\ A_t(u) &= \begin{pmatrix} -h' & -4u^{-1} - 2h \\ 4u^{-2} - 2u^{-1}h + h'' - 2h^2 & h' \end{pmatrix}. \end{aligned} \quad (3.26)$$

A Lax connection for the Heisenberg magnet is given by a 2×2 matrix-valued field whose entries depend on u and are functions of phase space⁹

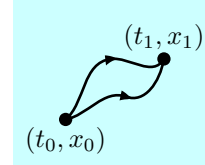
$$\begin{aligned} A_x(u) &= -\frac{i}{u} \vec{\sigma} \cdot \vec{S}, \\ A_t(u) &= \frac{i}{u} \vec{\sigma} \cdot (\vec{S} \times \vec{S}') + \frac{2i}{u^2} \vec{\sigma} \cdot \vec{S}. \end{aligned} \quad (3.27)$$

Here $\vec{\sigma}$ is the triplet of 2×2 traceless hermitian Pauli matrices.

It is convenient to work with the Lax connection using the language of differential forms. It is a matrix-valued connection one-form $A(u) = A_x(u)dx + A_t(u)dt$ which obeys the zero-curvature condition $dA(u) = A(u) \wedge A(u)$.

Given a one-form $A(u)$, one is tempted to construct a parallel transport operator (path-ordered integral, Wilson line) which translates between the vector spaces attached to the two endpoints of the path¹⁰

$$U(u; t_1, x_1; t_0, x_0) := \overleftarrow{\text{P}} \exp \int_{(t_0, x_0)}^{(t_1, x_1)} A(u). \quad (3.28)$$



The operator is the main ingredient for the construction of a Lax pair for our system.

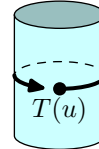
Due to flatness of $A(u)$ the parallel transport is invariant under continuous deformations of the path contour between (t_0, x_0) and (t_1, x_1) . Moreover, shifting the end points amounts to simple differential equations¹¹

$$\partial_\alpha^1 U^{10} = A_\alpha^1 U^{10}, \quad \partial_\alpha^0 U^{10} = -U^{10} A_\alpha^0. \quad (3.29)$$

Here the upper indices 0 and 1 represent the points (t_0, x_0) and (t_1, x_1) , respectively.

Lax Monodromy. The Lax pair is constructed from the parallel transport operator, but we have to take the boundary conditions into account. The simplest choice is periodic boundaries, $\phi(x + L) = \phi(x)$. In this case the Lax pair is defined as

$$\begin{aligned} T(u) &= \overleftarrow{\text{P}} \exp \int_0^L dx A_x(u), \\ M(u) &= A_t(u)|_{x=0}. \end{aligned} \quad (3.30)$$



⁹As usual, the Lax connection is not unique. However, a useful recipe to construct it is to make an ansatz in terms of the components of a Noether current and constrain the coefficients by means of the flatness condition. The Noether current for the $\mathfrak{su}(2)$ -symmetric Heisenberg magnet takes the form $J_t = \vec{\sigma} \cdot \vec{S}$ and $J_x = -\vec{\sigma} \cdot (\vec{S} \times \vec{S}')$.

¹⁰The path ordering operator $\overleftarrow{\text{P}}$ acts on the Taylor expansion of the exponent and sorts the integrand matrices according to their value of x in decreasing order from left to right.

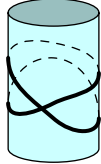
¹¹In fact, these equations can be viewed as the defining properties of U^{10} together with $U^{00} = 1$.

The path of integration winds once around the non-contractible cycle of periodic space, therefore there is no good reason for $T(u)$ to be trivial. The matrix $T(u)$ is also known as the *monodromy matrix*.

The above differential equations for U^{10} imply the Lax equation¹²

$$\dot{T}(u) = [M(u), T(u)]. \quad (3.31)$$

The eigenvalues or equivalently the traces of powers of T are conserved

$$F_k(u) = \text{tr } T(u)^k. \quad (3.32)$$


One can expand them around some point u_0 , e.g. $u_0 = \infty$, to obtain an infinite tower of conserved quantities

$$F_k(u) = \sum_{r=0}^{\infty} \frac{F_k^{(r)}}{u^r}. \quad (3.33)$$

For completeness, we need to show that they are in involution. This follows from a relationship involving the classical r-matrix

$$\{T_1(u_1), T_2(u_2)\} = [r_{12}(u_1, u_2), T_1(u_1) \otimes T_2(u_2)]. \quad (3.34)$$

This relationship is slightly different from the previous one,¹³ but it works just as well. A classical r-matrix for the Heisenberg model is given by

$$r_{12}(u_1, u_2) = \frac{\sigma^k \otimes \sigma^k}{2(u_1 - u_2)}. \quad (3.35)$$

The latter satisfies the classical Yang–Baxter equation¹⁴

$$\begin{aligned} & [r_{12}(u_1 - u_2), r_{13}(u_1 - u_3)] \\ & + [r_{12}(u_1 - u_2), r_{23}(u_2 - u_3)] \\ & + [r_{13}(u_1 - u_3), r_{23}(u_2 - u_3)] = 0. \end{aligned} \quad (3.36)$$

The above relations imply that the integrals of motion are involution

$$\{F_k(u_1), F_l(u_2)\} = \{F_k^{(r)}, F_l^{(s)}\} = 0. \quad (3.37)$$

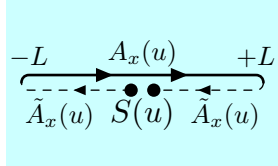
These are necessary conditions for the system to be integrable. As counting degrees of freedom vs. integrals of motion is ambiguous within a field theory, it is not clear whether the above conditions are sufficient to make the system integrable.

¹²Here we set $t_0 = t_1 = t$ and $x_0 = 0 \equiv x_1 = L$ so that the time derivative acts on both t_0 and t_1 and $A_t(u)$ is the same at x_0 and x_1 due to periodicity.

¹³The monodromy $T(u)$ can be viewed as an exponentiated Lax matrix $L(u)$ leading to a different but equivalent relationship.

¹⁴This is the simplest form of classical Yang–Baxter equation. There are various modifications for different types of integrable models.

Lax Scattering. For infinite boundary conditions, we should construct a different Lax pair. One may be tempted to use the parallel transport U from $x = -\infty$ to $x = +\infty$. This, however, does not work well because U still depends substantially on x as $x \rightarrow \pm\infty$. The crucial point for infinite boundary conditions is that the fields tend to fixed values as $x \rightarrow \pm\infty$. The Lax connection \tilde{A} at these fixed values is not necessarily zero, and therefore U does not have a proper limit on its own. In order to make the limit well-defined, we parallel transport the endpoints back to $x = 0$ with the asymptotic Lax connection¹⁵

$$\begin{aligned}
S(u) = & \lim_{L \rightarrow \infty} \exp[-L\tilde{A}_x(u)] \\
& \cdot \left[\overset{\leftarrow}{\text{P}} \exp \int_{-L}^L dx A_x(u) \right] \\
& \cdot \exp[-L\tilde{A}_x(u)], \\
M(u) = & \tilde{A}_t(u).
\end{aligned}
\tag{3.38}$$


Note that this construction is very similar to the scattering operator for a quantum mechanical wave function off a given potential; we will return to this point of view below. The outer factors account for the fact that the asymptotic wave function oscillates with a given momentum. They shift the wave function back to $x = 0$ with the free asymptotic momentum.

Again, the scattering matrix $S(u)$ obeys the Lax equation

$$\dot{S}(u) = [M(u), S(u)]. \tag{3.39}$$

and can be used to define an infinite tower of conserved charges

$$F_k(u) = \text{tr } S(u)^k. \tag{3.40}$$

3.3 Inverse Scattering Method

In the following we will solve an integrable field theory on the infinite line by means of the *inverse scattering method*. The method transforms between the field on a time slice and a set of abstract scattering data. Time evolution for this abstract data turns out to be very simple. As such, the method is somewhat analogous to a Fourier transformation for a linear wave equation. The method can be applied in two ways:

- Determine the complete time evolution of a time slice in position space by transforming the problem to the abstract space.
- Construct wave solutions by specifying the abstract data. Typically the waves are a collection of solitons scattering off each other.

We shall use KdV as an example model.

¹⁵We assume that the Lax connection has the same limit in both asymptotic regions, otherwise the below construction needs adjustments.

Auxiliary Linear Problem. A key element of the inverse scattering method is the so-called auxiliary linear problem which defines a scattering setup. Consider an N -component field ψ and an $N \times N$ matrix connection one-form A . One can then set up a linear equation of motion for ψ

$$\partial_\alpha \Psi = A_\alpha \Psi \quad \text{or} \quad d\Psi = A\Psi. \quad (3.41)$$

Note that this equation can have consistent solutions only if the connection A is flat, i.e. $dA = A \wedge A$. Using the parallel transport operator U discussed above we can write down a general solution

$$\Psi^1 = U^{10} \Psi^0. \quad (3.42)$$

Here, Ψ^1 denotes the solution at a generic position (t_1, x_1) whereas Ψ^0 is the field at a reference position (t_0, x_0) .

Let us now take A to be the Lax connection of the KdV equation. Furthermore, we consider only a specific time slice.¹⁶ The auxiliary linear problem $\Psi' = A_x \Psi$ then reads in components

$$\Psi'_1 = -\Psi_2, \quad \Psi'_2 = (u^{-1} - h)\Psi_1. \quad (3.43)$$

We can impose the first of these equations by the ansatz $\Psi = (\psi, -\psi')$. Then the two above differential equations combine into a single second-order differential equation

$$-\psi''(x) + h(x)\psi(x) = u^{-1}\psi(x). \quad (3.44)$$

Interestingly, this equation takes the form of a time-independent Schrödinger equation with potential $h(x)$ and energy eigenvalue u^{-1} . The Schrödinger equation can be viewed as a transformation between functions h and ψ : For a given function $h(x)$ and value of u there is a two-dimensional space of solutions $\psi(x)$. Alternatively, for a given $\psi(x)$ at a certain value of u there is a unique $h(x) = \psi''(x)/\psi(x) + u^{-1}$.

Scattering. As it stands, the above transformation creates a lot of auxiliary data in $\psi(x)$ which not only depends on x but also non-trivially on u . We now want to reduce the data so that the transformation is more one-to-one. The trick is to consider only the asymptotic data in $\psi(x)$ at $x \rightarrow \pm\infty$. At $x \rightarrow \pm\infty$, the potential $h(x)$ vanishes sufficiently fast such that the Schrödinger equation reduces to the one of a free particle

$$-\psi''(x) \simeq u^{-1}\psi(x) \quad \text{at } x \rightarrow \pm\infty. \quad (3.45)$$

Therefore the solutions $\psi(x)$ are asymptotically plane waves

$$\psi(x) \simeq c_-^{\text{R/L}} e^{-ikx} + c_+^{\text{R/L}} e^{ikx} \quad \text{with} \quad k^2 = \frac{1}{u} \quad \text{as } x \rightarrow \pm\infty. \quad (3.46)$$

¹⁶This can be any time slice, but more specifically it can be the time slice that supports the initial values of the KdV problem.

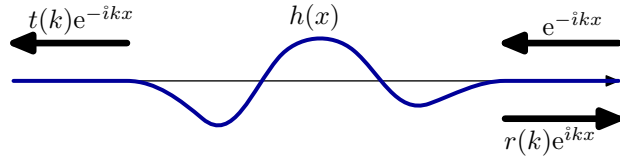
We know that the space of solutions is two-dimensional, and thus any solution $\psi(x)$ is parametrised by the values of c_{\pm} in one of the asymptotic regions. The coefficients c_{\pm} of the opposite asymptotic region are thus uniquely specified by the Schrödinger equation. As the Schrödinger equation is linear, the relationship between the asymptotic coefficients must be linear as well

$$\begin{pmatrix} c_-^R \\ c_+^R \end{pmatrix} = \tilde{S}(k) \begin{pmatrix} c_-^L \\ c_+^L \end{pmatrix} \quad (3.47)$$

with the 2×2 matrix $\tilde{S}(k)$ parametrised as

$$\tilde{S}(k) = \begin{pmatrix} 1/t(k) & r(-k)/t(-k) \\ r(k)/t(k) & 1/t(-k) \end{pmatrix}. \quad (3.48)$$

In fact, the above matrix represents the result of the quantum mechanical scattering problem of a particle off the potential $h(x)$. The functions $t(k)$ and $r(k)$ describe transmission and reflection as follows: Suppose there is an incoming wave $\sim e^{ikx}$ from the right with unit coefficient, $c_-^R = 1$, and no incoming wave $\sim e^{-ikx}$ from the left, $c_+^L = 0$. The remaining coefficients describe the amplitudes of the transmitted wave $t(k) = c_-^L$ and of the reflected wave $r(k) = c_+^R$.



$$(3.49)$$

We can now relate the matrix $\tilde{S}(k)$ to the Lax scattering matrix $S(u)$ introduced earlier. By construction, they must be related by a suitable similarity transformation, let us derive it: The asymptotic solutions of our scattering problem are of the form $\psi(x) \simeq c_- e^{-ikx} + c_+ e^{ikx}$ and they are represented by the vector (c_-, c_+) . To compare to the Lax scattering matrix $S(u)$, we should return to the two-component vector $\Psi(x) = (\psi(x), -\psi'(x))$ and shift it back to $x = 0$ with the asymptotic Lax matrix \tilde{A}_x . We thus find the relationship

$$\exp(-x\tilde{A}_x)\Psi(x) \simeq \begin{pmatrix} c_- + c_+ \\ ikc_- - ikc_+ \end{pmatrix} = D(k) \begin{pmatrix} c_- \\ c_+ \end{pmatrix} \quad (3.50)$$

with the transformation matrix

$$D(k) = \begin{pmatrix} 1 & 1 \\ ik & -ik \end{pmatrix}. \quad (3.51)$$

This matrix converts between the Lax scattering matrix and the scattering matrix of the Schrödinger equation

$$S(u) = D(k)\tilde{S}(k)D(k)^{-1}. \quad (3.52)$$

Scattering Data. We have now reduced the data of the auxiliary linear problem to the scattering data consisting of the functions $t(k)$ and $r(k)$. These depend on one variable k only and hence they contain a comparable amount of information as the wave function $h(x)$. It turns out that the transformation is invertible, and one can reconstruct $h(x)$ from the scattering data. We shall present the inverse transformation after investigating the scattering functions in more detail.

Several of the properties are easily derived by relating our scattering problem to the Lax scattering matrix $S(u)$. There are two evident properties of $S(u)$: First, tracelessness of the Lax connection, $\text{tr } A_x(u) = 0$, implies that $S(u)$ has unit determinant, $\det S(u) = 1$. This leads to a relationship between the transmission and reflection coefficients

$$\det \tilde{S}(k) = 1, \quad t(k)t(-k) + r(k)r(-k) = 1. \quad (3.53)$$

Furthermore, the complex conjugate of the Lax connection obeys the reality condition $A_x(u)^* = A_x(u^*)$ which directly implies that $S(u)^* = S(u^*)$. Noting that complex conjugation of the transformation matrix also flips the sign of k , $D(k)^* = D(-k)$, we find the relationship for the transmission and reflection coefficients

$$\tilde{S}(k)^* = \tilde{S}(-k^*), \quad t(k)^* = t(-k^*), \quad r(k)^* = r(-k^*). \quad (3.54)$$

These relationships can also be derived from the scattering problem of the Schrödinger equation.

Next we would like to discuss the analytic behaviour of the scattering matrix in k : If the potential $h(x)$ has compact support, the defining integral of the Lax scattering matrix $S(u)$ is over a finite domain, and as such it displays the same analytic behaviour as $A_x(u)$. In this case $\tilde{S}(k)$ is analytic on the whole complex plane except for the point $k = 0$ where the transformation $D(k)$ is singular and typically produces a pole in all elements. For a potential $h(x)$ supported on the whole line, the limit within $S(u)$ can spoil the analytic behaviour. This is related to the asymptotic behaviour of the wave function $\psi(x)$ which changes drastically at $\text{Im } k = 0$ from exponential decline to oscillations to exponential growth. One can argue that the transmission and reflection coefficients $t(k)$ and $r(k)$ are analytic on the upper half plane $\text{Im } k > 0$. In particular, they do not need to be analytic on the real axis, and thus the values on the real axis do not necessarily agree with the limit $\text{Im } k \rightarrow 0$. The behaviour in the lower half plane $\text{Im } k < 0$ shall not be of interest to us.

In the following we will discuss the spectrum of the above Schrödinger equation with *bounded* wave functions ψ . Since the Hamiltonian operator for the Schrödinger equation is hermitian, the energy eigenvalues u^{-1} corresponding to bounded eigenfunctions must be real. There are two different classes: Above the asymptotic value of the potential, i.e. for positive u^{-1} , there always exist two oscillating wave functions (distinguished by the sign of k). Due to their oscillatory behaviour, they are not square integrable. For negative u^{-1} the two solutions are usually unbounded in either of the asymptotic regions. Only for specific values of the energy u^{-1} there is one bounded solution which decays exponentially towards

both asymptotic regions due to the energy deficit. This mode is localised where the potential $h(x)$ is sufficiently negative. It is square integrable and thus normalisable. Let us discuss the continuum and discrete cases in more detail.

Continuum States. For real k the wave function oscillates as $x \rightarrow \pm\infty$, it is therefore naturally bounded. We then know that $t(k)^* = t(-k)$ and $r(k)^* = r(-k)$. This also implies the standard unitarity relationship between the transmission and reflection coefficients, $|t(k)|^2 + |r(k)|^2 = 1$. In other words, the absolute value of both functions $t(k)$ and $r(k)$ must be bounded by 1 on the real axis. Furthermore, one can argue that $r(k) \rightarrow 0$ as $k \rightarrow \pm\infty$.

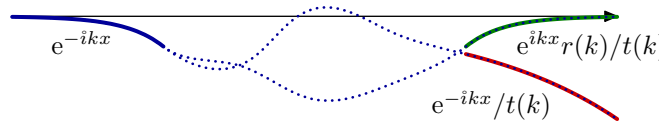
Discrete States. For complex k , the asymptotic wave function $\sim e^{\pm ikx}$ either displays exponential growth or exponential decline at $x \rightarrow \pm\infty$. A bounded wave function should decline in both asymptotic regions. The wave e^{-ikx} at $x \rightarrow -\infty$ declines if and only if $\text{Im } k > 0$. Let us consider a solution of the Schrödinger equation with asymptotic behaviour

$$\psi(x) \simeq e^{-ikx} \quad \text{at } x \rightarrow -\infty, \quad (3.55)$$

a so-called *Jost solution*. The asymptotic behaviour of this solution at $x \rightarrow +\infty$ is a linear combination of e^{-ikx} and e^{+ikx} which is determined by the scattering matrix

$$\psi(x) \simeq \frac{1}{t(k)} e^{-ikx} + \frac{r(k)}{t(k)} e^{+ikx} \quad \text{at } x \rightarrow +\infty, \quad (3.56)$$

The former of these two terms grows while the latter declines. In order for the wave function to be bounded, the coefficient of the former factor must be zero. The corresponding element of the scattering matrix is $1/t(k)$ and therefore a pole of $t(k)$ indicates the existence of a normalisable state.



$$(3.57)$$

Now unitarity of the Schrödinger equation implies that for normalised states u^{-1} must be negative. Therefore all the poles of $t(k)$ in the upper half plane $\text{Im } k > 0$ must lie on the imaginary axis. For a potential $h(x)$ with N normalisable states, we deduce that $t(k)$ has N poles at some $k = i\kappa_n$ with $\kappa_n > 0$. Due to analyticity of $r(k)/t(k)$, the reflection coefficient $r(k)$ shares the set of poles, albeit with different residues. From the above properties we furthermore know that both functions $t(k)$ and $r(k)$ must be real on the imaginary axis. From scattering theory one can furthermore deduce that all residues of $r(k)$ at $k = i\kappa_n$ are positive imaginary numbers $i\lambda_n$

$$r(k) \sim \frac{i\lambda_n}{k - i\kappa_n} \quad \text{for } k \rightarrow i\kappa_n \quad \text{with } \lambda_n > 0. \quad (3.58)$$

Inverse Scattering Transformation. Above, we have transformed the function $h(x)$ to the set of scattering data $t(k)$, $r(k)$ with some specific properties. This is called the *scattering transformation*. Interestingly, the function $h(x)$ can be reconstructed completely from the scattering data, this is called the *inverse scattering transformation*. In the following, we will write out the inverse scattering transformation without derivation.

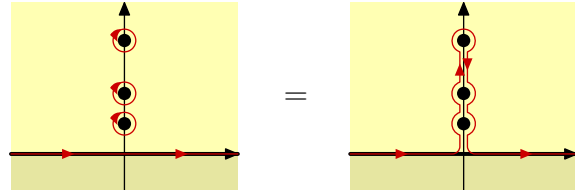

(3.59)

In order to carry out the inverse scattering transformation, we just require a subset of the data, namely the reflection function $r(k)$ for the continuum $k \in \mathbb{R}$ as well as the set of poles and residues $\{(\kappa_n, \lambda_n)\}$ of $r(k)$ on the imaginary axis corresponding to the discrete spectrum.

First, one performs the Fourier transformation of $r(k)$ dressed by the poles and residues

$$\hat{r}(x) = \int_{-\infty}^{\infty} \frac{dk}{2\pi} e^{ikx} r(k) + \sum_{j=1}^N \lambda_n e^{-\kappa_n x}. \quad (3.60)$$

Here, the contributions from the poles can be viewed as an extension of the integration contour away from the real axis to also encircle the poles on the positive imaginary axis.


(3.61)

The next step is to solve the Gelfand–Levitan–Marchenko (GLM) integral equation for the unknown function $K(x, y)$

$$K(x, y) + \hat{r}(x + y) + \int_x^\infty dz K(x, z) \hat{r}(z + y) = 0. \quad (3.62)$$

The solution then directly yields the potential as the expression

$$h(x) = -2 \frac{\partial}{\partial x} [K(x, x)]. \quad (3.63)$$

Time Evolution. Arguably, both the scattering transformation and its inverse are highly non-trivial, and one may wonder whether they simplify or complicate the solution. The major benefit of the transformation, however, is that time evolution becomes almost trivial in the scattering data. To that end, we already know that

time evolution of the Lax scattering matrix is governed by the Lax equation. Transforming to the basis of the Schrödinger equation the Lax equation reads

$$\dot{\tilde{S}}(k) = [D(k)^{-1}M(u)D(k), \tilde{S}(k)] \quad (3.64)$$

with the transformed time evolution matrix

$$D(k)^{-1}M(u)D(k) = \begin{pmatrix} -4ik^3 & 0 \\ 0 & 4ik^3 \end{pmatrix}. \quad (3.65)$$

For the transmission and reflection coefficients this implies

$$\dot{t}(k) = 0, \quad \dot{r}(k) = 8ik^3 r(k). \quad (3.66)$$

These equations have the immediate solutions

$$t(k, t) = t(k), \quad r(k, t) = e^{8ik^3 t} r(k). \quad (3.67)$$

For the poles and residues of the discrete spectrum, we infer the time-dependence

$$\kappa_n(t) = \kappa_n, \quad \lambda_n(t) = \lambda_{n,0} e^{8\kappa_n^3 t}. \quad (3.68)$$

Altogether this implies a simple linear equation of motion for \hat{r}

$$\dot{\hat{r}}(x) = -\hat{r}'''(x). \quad (3.69)$$

In conclusion, we can easily evolve the scattering data from the initial time slice at $t = 0$ to any other time slice. By means of the scattering transformations this solves the time evolution in the original KdV equation.

Example. As an instructive example, we reconstruct the potential $h(x)$ from a given reflection function $r(k)$. We assume that there is no contribution from the continuum, $r(k) = 0$ for $k \in \mathbb{R}$, and just a single pole specified by κ and $\lambda(t)$. We can immediately write our ansatz in the function $\hat{r}(x)$

$$\hat{r}(x) = \lambda e^{-\kappa x}. \quad (3.70)$$

In order to solve the GLM equation, we make use of the special property

$$\hat{r}(x+y) = \hat{r}(x) e^{-\kappa y}$$

$$K(x, y) + \hat{r}(x) e^{-\kappa y} + e^{-\kappa y} \int_x^\infty dz K(x, z) \hat{r}(z) = 0. \quad (3.71)$$

Now we observe that the y -dependence implies that $K(x, y) = K(x) e^{-\kappa y}$, and we can perform the integral

$$K(x) + \lambda e^{-\kappa x} + \frac{\lambda}{2\kappa} e^{-2\kappa x} K(x) = 0. \quad (3.72)$$

This equation is solved by

$$K(x) = -\frac{2\kappa\lambda e^{-\kappa x}}{2\kappa + \lambda e^{-2\kappa x}}, \quad K(x, y) = -\frac{2\kappa\lambda e^{-\kappa x - \kappa y}}{2\kappa + \lambda e^{-2\kappa x}}. \quad (3.73)$$

We can then read off the potential $h(x)$ as

$$\begin{aligned} h(x) &= -2 \frac{\partial}{\partial x} K(x, x) = -\frac{16\kappa^3 \lambda e^{-2\kappa x}}{(2\kappa + \lambda e^{-2\kappa x})^2} \\ &= -2\kappa^2 \operatorname{sech}^2 \left[\kappa x - \frac{1}{2} \log \frac{\lambda}{2\kappa} \right]. \end{aligned} \quad (3.74)$$

This expression has the same form as the soliton solution. Finally, we identify the soliton velocity v with the location of the pole κ and its centre x_0 with the residue λ as follows

$$\kappa = \frac{1}{2}\sqrt{v}, \quad \lambda(t) = 2\kappa e^{2\kappa x_0 + 8\kappa^3 t} = \sqrt{v} e^{\sqrt{v}x_0 + v^{3/2}t}. \quad (3.75)$$

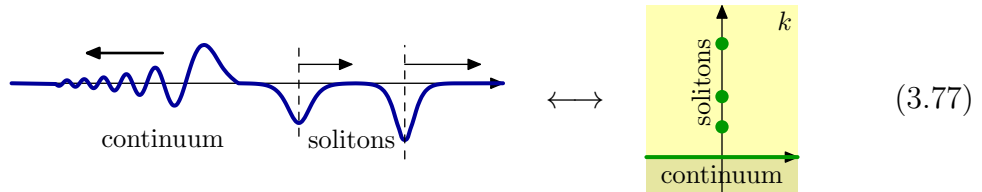
Note that the time-dependence of $\lambda(t)$ follows from the general formula. We recover the soliton solution

$$h(t, x) = -\frac{1}{2}v \operatorname{sech}^2 \left[\frac{1}{2}\sqrt{v}(x - x_0 - vt) \right]. \quad (3.76)$$

Physics of the Scattering Data. To conclude the treatment of the inverse scattering method, let us illustrate the physics of the scattering data. The latter consists of two distinct parts, the discrete states specified by poles and residues $\{(\kappa_n, \lambda_n)\}$, and the continuum specified by the reflection function $r(k)$.

It does not take much imagination that each discrete state corresponds to one soliton. The position κ specifies the velocity $v = 4\kappa^2$ while λ specifies the centre.¹⁷ The velocity is a constant while the centre is time-dependent. In the scattering data, the moduli of the solitons are separated very cleanly. The inverse scattering transformation maps these data to a physical wave form $h(x)$. When the individual wave packets are widely separated, it produces approximately their superposition. However, the non-linearity of the inverse scattering transformation also reproduces the collision process in an exact fashion.

The continuum is specified by a continuous function $r(k)$. Its absolute value is time-independent while the phase oscillates in time. The associated wave form is somewhat similar to a collection of many solitons. However, as time evolves, the continuum will never dissociate like solitons, but rather disperse. The function $r(k)$ can be viewed as a kind of Fourier transformation such that $r(k)$ specifies the amplitude and phase of a component of the wave moving at velocity $v = -4k^2$. This shows that the continuum propagates towards the left while the solitons always propagate to the right.

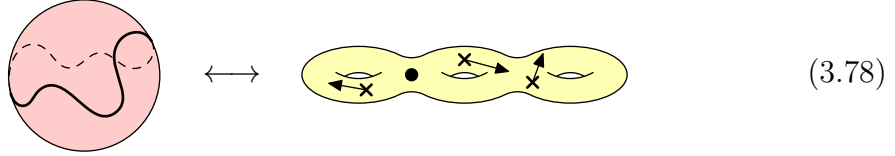


¹⁷Note that the scattering data allows for each velocity to be present at most once. The interactions between solitons make sure that two of them cannot have precisely the same velocity. This property shows that solitons are governed by Fermi-statistics. In fact, it is a common feature of integrable systems that the elementary excitations behave like fermions.

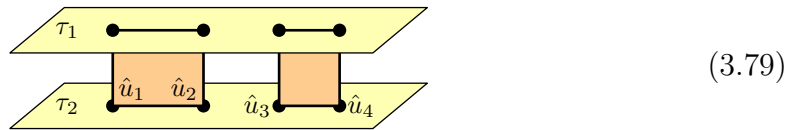
3.4 Spectral Curves

Above we have sketched a method to solve an integrable field theory with infinite boundary conditions. In the following we sketch an analogous method for periodic boundary conditions. It is similar in the structures it uses and the type of the final result, but there are also crucial differences due to the different topology. In this case, we shall use the Heisenberg magnet as an example to illustrate the method.¹⁸

For any solution $\vec{S}(t, x)$ of the equations of motion we know how to compute the monodromy matrix $T(u)$. It contains a lot, perhaps all, information on the integrals of motion. Let us therefore investigate $T(u)$. In particular, the dependence on the spectral parameter $u \in \mathbb{C}$ reveals many properties of the solution by means of the so-called spectral curve. This information is very useful because it allows to construct suitable spectral curves from scratch and thus learn about the conserved charges of a solution without constructing the latter. One can even reconstruct the solution from the spectral curve with the dynamical divisor.



Riemann Sheets. The monodromy matrix obeys the Lax equation, and therefore the spectrum $\tau_k(u)$ of eigenvalues of $T(u)$ constitutes integrals of motion. Even though $T(u)$ is largely analytical in u , we argued previously that the diagonalisation of a matrix typically introduces further square root singularities $\{\hat{u}_j\}$. At these points, two eigenvalues $\tau_k(u)$ and the corresponding eigenvectors degenerate. The eigenvalue functions $\tau_k(u)$ can thus be considered the Riemann sheets of a function $\tau(u)$ on a Riemann surface. Importantly, the sheets are joined along branch cuts which connect the branch points \hat{u}_k in pairs.



The number and locations \hat{u}_k of the branch points depend on the underlying solution $\vec{S}(t, x)$ in a very non-trivial fashion. Conversely, the locations of the branch cuts determine the functions $\tau_k(u)$ as we shall show later. Therefore they determine many (if not all) of the integrals of motion and classify solutions $\vec{S}(t, x)$.

Let us determine further properties of the function $\tau(u)$.

Essential Singularities. Recall that the monodromy matrix $T(u)$ was constructed by means of the matrix

$$A_x(u) = -\frac{i}{u} \vec{\sigma} \cdot \vec{S}. \quad (3.80)$$

¹⁸The methods can be applied to the KdV equation with minor adjustments. Here we prefer a model with more manifest symmetries to illustrate their representation in the method.

It has a pole at $u = 0$ which leads to an essential singularity in $T(u)$. We would like to understand the nature of this singularity better.

To that end, we should diagonalise the connection $A_x(u, x)$ at all x by means of a similarity transformation $D(u, x)$

$$\partial_x + \tilde{A}_x(u, x) = D(u, x)^{-1}(\partial_x + A_x(u, x))D(u, x). \quad (3.81)$$

The rotation matrix is determined such that $\tilde{A}_x \sim \sigma^3$ is diagonal. This transformation matrix $D(u, x)$ can be perfectly regular at $u = 0$. To leading order in u a diagonal \tilde{A}_x is achieved by a rotation which satisfies

$$D(0, x)^{-1}(\vec{\sigma} \cdot \vec{S}(x))D(0, x) = \sigma^3 \|\vec{S}(x)\| = \sigma^3. \quad (3.82)$$

The resulting connection reads

$$\partial_x + \tilde{A}_x(u, x) = -\frac{i}{u} \sigma^3 + \mathcal{O}(u^0) \quad (3.83)$$

and the transformed monodromy matrix is now computed as a plain integral without path ordering

$$\tilde{T}(u) = \exp \int_0^L dx \tilde{A}_x(u, x). \quad (3.84)$$

Since the monodromy matrices are related by a plain similarity transformation

$$T(u) = D(u, L)^{-1} \tilde{T}(u) D(u, 0) = D(u, 0)^{-1} T(u) D(u, 0), \quad (3.85)$$

we can now easily read off the singular behaviour of the eigenvalues at $u = 0$

$$\tau_{1,2}(u) = \exp \left(\pm \frac{iL}{u} + \mathcal{O}(u^0) \right). \quad (3.86)$$

The higher orders at $u = 0$ can be obtained by a careful analysis involving a u -dependent transformation $D(u, x)$. This is somewhat laborious, and we shall skip the analysis and just state the first few terms

$$\tau_{1,2}(u) = \exp \pm i \left[u^{-1} L - \frac{1}{2} P + \frac{1}{4} u H - \frac{1}{8} u^2 F_3 + \dots \right]. \quad (3.87)$$

Importantly, the resulting conserved charges are *local integrals of motion*. The property of locality is closely related to the pole singularity in $A_x(u)$. In our case the lowest few charges are:

- the total momentum P at $\mathcal{O}(u^0)$,
- the total energy E at $\mathcal{O}(u^1)$,
- higher local charges F_k involving k spatial derivatives at $\mathcal{O}(u^{k-1})$.

Quasi-Momentum and Spectral Curve. For a later reconstruction of the function $\tau(u)$ the existence of essential singularities is inconvenient. They can be removed by considering the logarithm of the function $\tau(u)$ which is known as the *quasi-momentum* $q(u)$

$$q(u) := -i \log \tau(u). \quad (3.88)$$

Evidently, the quasi-momentum has single poles at $u = 0$ with residue $\pm L$.

Note that the quasi-momentum $q(u)$ has inherited the ambiguity of the complex logarithm, and is therefore defined only modulo shifts of 2π . Evidently, one will choose the function to be analytic almost everywhere, but in addition to switching sheets at the existing branch cuts of $\tau(u)$, it can jump by multiples of 2π

$$q_1 \leftrightarrow q_2 + 2\pi n. \quad (3.89)$$

The characteristic number n is constant along the branch cut.

To get rid of these ambiguities, it makes sense to consider the derivative of the quasi-momentum q' or dq as a differential form,

$$q'(u) = -i \frac{\tau'(u)}{\tau(u)}. \quad (3.90)$$

This function has only two sheets and algebraic type singularities. It can be viewed as a complex curve, the so-called *spectral curve*. It is therefore ideally suited for complex analysis and for construction purposes.

Note that the curve has inherited some properties from its construction via $\tau(u)$. Let us list them:

- All closed periods of $dq(u)$ on the Riemann surface must be multiples of 2π due to its definition as a logarithmic derivative

$$\oint dq = \oint du q'(u) \in 2\pi\mathbb{Z}. \quad (3.91)$$

- Any point-like singularities cannot have a residue, i.e. they must be poles of higher degree. A pole with a residue requires $q(u)$ to have a logarithmic singularity and thus $\tau(u)$ to have a pole or a zero. This is in conflict with the group nature of the monodromy $T(u)$.
- The essential singularity of τ implies a double pole at $u = 0$ without a residue for the single pole

$$q'_{1,2}(u) = \mp \frac{L}{u^2} + \frac{0}{u} + \dots \quad \text{at } u \rightarrow 0. \quad (3.92)$$

- The function $q'(u)$ has branch cuts which end in *inverse* square root branch points

$$q'_{1,2}(u) = \frac{\pm*}{\sqrt{u - \hat{u}_k}} + \dots \quad \text{at } u \rightarrow \hat{u}_k. \quad (3.93)$$

Special Properties. The matrix $T(u)$ has a further special property which follows from a property of $A_x(u)$ and which influences the behaviour of $\tau(u)$ and $q(u)$.

We know that $A_x \sim \vec{\sigma} \cdot \vec{S}$ is a traceless matrix. After integration and exponentiation we derive

$$\det T(u) = 1, \quad \tau_1(u) \tau_2(u) = 1. \quad (3.94)$$

For the quasi-momentum it implies that the two sheets differ merely by their sign and potentially by a shift of a multiple of 2π . In order to fix the shift ambiguity on one sheet, we can define the second sheet to be the negative of the first sheet without a shift

$$q_2 = -q_1. \quad (3.95)$$

Passing through a branch cut therefore must include a potential shift by 2π

$$q \leftrightarrow -q + 2\pi n. \quad (3.96)$$

The number n will henceforth characterise the branch cut.

Symmetry Points. Another distinguished point is $u = \infty$ where $A_x(u)$ vanishes. The expansion of $T(u)$ is therefore straight-forwardly

$$T(u) = \exp\left(-\frac{i}{u} \vec{\sigma} \cdot \vec{Q} + \mathcal{O}(1/u^2)\right), \quad (3.97)$$

where \vec{Q} is the Noether charge for rotations

$$\vec{Q} = \int_0^L dx \vec{J}_t, \quad \vec{J}_t = \vec{S}. \quad (3.98)$$

For the quasi-momentum it implies

$$q(u) = \pm \frac{1}{u} \|\vec{Q}\| \quad \text{at } u \rightarrow \infty. \quad (3.99)$$

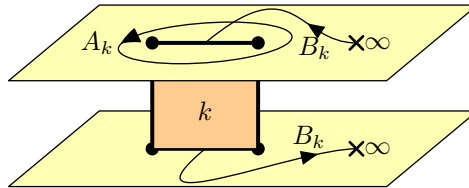
Here we have used and fixed the freedom to shift by multiples of 2π by setting $q(\infty) = 0$.

As an aside, the higher powers of $1/u$ in $T(u)$ correspond to multi-local conserved charges such as

$$\int_0^L dx \int_0^x dx' \vec{S}(x) \times \vec{S}(x'). \quad (3.100)$$

Periods and Moduli. The locations \hat{u}_k of the branch points determine the spectral curve, but they are not immediately telling much about the physical properties of the underlying solution. There are other quantities which are much more suitable: *periods*.

We know that the periods of dq are integer multiples of 2π . To be more concrete, we choose a convenient basis of cycles on the Riemann surface: There is a cycle around each branch cut, these are called the *A-cycles* A_k . Furthermore there is a cycle through each cut, these are called the *B-cycles* B_k .¹⁹



$$(3.101)$$

¹⁹The curve B_k is not actually a cycle, but the concatenation of two curves B_k is. Here we use the distinguished point $u = \infty$ whose value we have fixed to $q(\infty) = 0$ as the starting and ending point to simplify the enumeration of independent cycles.

Note that the combination of all A-cycles combines to an inverse cycle around the remaining singular point $u = 0$ and therefore all A-cycles are independent.

From the way we have defined the cuts and sheets of $q(u)$ it is evident that all A-periods vanish while the B-periods in general yield integers²⁰

$$\oint_{A_k} dq = 0, \quad \int_{B_k} dq = 2\pi n_k. \quad (3.102)$$

The integers n_k describe the jump of the quasi-momentum $q(u)$ at the branch cuts. They are called *mode numbers*.

We can measure another characteristic number for each branch cut as the A-period of $u dq$, the so-called *filling* I_k

$$I_k = \frac{1}{2\pi i} \oint_{A_k} u dq. \quad (3.103)$$

It is a measure of the length of the branch cut,²¹ and unlike n_k it takes continuous values. Note that quantisation of the classical theory renders these numbers to be quantised as integers, too.

Finite-Gap Construction. Let us summarise the properties of the spectral curve $q'(u)$:

- The function has two Riemann sheets, it is single-valued on the Riemann surface, the sum of the Riemann sheets is zero.
- The function has branch points \hat{u}_k of the type $1/\sqrt{u - \hat{u}_k}$.
- There is a fixed pole $\pm L/u^2 + 0/u$ at $u = 0$.
- The asymptotic behaviour at $u \rightarrow \infty$ is $\sim 1/u^2$.

For spectral curves with finitely many cuts (“finite-gap”) we can make a general ansatz as an algebraic curve

$$q'(u) = \pm \frac{P_N(u)}{u^2 \sqrt{Q_{2N}(u)}}, \quad (3.104)$$

where P_N and Q_{2N} are polynomials of degree N and $2N$, respectively, with $2N + 2$ free parameters in total. This ansatz automatically satisfies several of the above properties, the remaining properties constrain some of the parameters as follows:

- N A-periods $\oint dq = 0$,
- N B-periods $\int dq = 2\pi n_k$,
- N fillings $\oint u dq \sim I_k$,
- 1 coefficient of the $1/u^2$ pole at $u = 0$,
- 1 ambiguity of overall rescaling of P and \sqrt{Q} .

²⁰For integer periods one can always make at least half of them vanish by a suitable choice of independent cycles and thus of Riemann sheets and cuts.

²¹We can argue that I_k vanishes for very short cuts: Then u is approximated by a constant so that I_k is approximated by this constant times the vanishing A-period of the cut.

We learn that all degrees of freedom are fixed by the knowledge of the (discrete) mode numbers n_k and the (continuous) fillings I_k .²² All integrals of motion (momentum, energy, spin, higher charges) follow from this finite-gap solution.

This classifies solutions with finite genus N . One could view the more general spectral curves with infinitely many cuts as the limiting case $N \rightarrow \infty$.

Physics of Spectral Curves. Finite genus spectral curves are specified by one discrete mode number n_k and one continuous filling I_k for each cut. This matches qualitatively with the spectrum for $(1+1)$ -dimensional field theories with closed boundary conditions, such as string theory. Let us discuss the latter:

For solutions \vec{S} near a trivial vacuum solution \vec{S}_0 one could make an ansatz in terms of Fourier modes

$$\vec{S} = \vec{S}_0 + \sum_n \vec{\alpha}_n \exp(2\pi i n x / L). \quad (3.105)$$

Here, the mode numbers n are discrete whereas the amplitudes $\vec{\alpha}_n$ are continuous.


(3.106)

Finite-gap solutions represent solutions where only a finite number of Fourier modes n_k are active with a non-zero filling $I_k \sim |\alpha_k|^2 > 0$.²³ Note that for a non-linear problem²⁴ the Fourier mode expansion leads to complicated non-linear relationships of the α 's. The spectral curve automatically takes care of this complication. It can be viewed as a non-linear version of the Fourier transformation by means of complex analysis which is perfectly adapted to our physics model.

Here we have only discussed the spectral curve encoding the conserved quantities of the model. As discussed earlier, the dynamical degrees of freedom should be represented by the dynamical divisor. The latter consists of a set of marked points on the spectral curve which encodes a specific eigenvector of the transfer matrix and from which the complete solution can be reconstructed. Nevertheless, the spectral curve and the conserved charges arguably are the more relevant set of data for the physical behaviour of the solution.

This is even more so with a view to quantum mechanics:

- Due to the uncertainty principle, only half of the phase space variables can be measured simultaneously. The spectral curve does provide this part.
- The quantum mechanical system can be viewed as a collection of Fourier modes specified by the mode numbers n_k . Each mode behaves similarly to a

²²The residue at $u = 0$ is fixed to zero by the sum of A-periods.

²³Note that a vanishing filling I_k corresponds to no cut at all, and therefore only the cuts with non-zero filling I_k are present.

²⁴In our model, the constraint $\vec{S}^2 = 1$ is responsible for the non-linearity.

quantum mechanical harmonic oscillator where the filling I_k becomes quantised and corresponds to the excitation number. The main complication due to non-linearity is that the modes are not independent, but interact whenever the I_k are not small. This complication is solved by the spectral curve.

4 Integrable Spin Chains

We now proceed to integrable quantum mechanical models, particularly to integrable spin chains. They are instructive because:

- they form a large class of integrable models,
- they can be treated uniformly,
- they have many parameters to tune,
- short chains are genuine quantum mechanical models,
- long chains approximate $(1 + 1)$ D quantum field theories,
- for large quantum numbers they are approximated by classical models,
- they model magnetic materials.

Here we will focus on magnets. A magnetic material consists of many microscopic magnets, e.g. atoms with spin. The energy of the material depends on the configuration of nearby spins.

nearby spins	ferromagnet	anti-ferromagnet
opposite alignment $\uparrow\downarrow$	high energy	low energy
equal alignment $\uparrow\uparrow$	low energy	high energy

(4.1)

Two well known models of magnets are:

- Ising model, a model of statistical mechanics. It consists of a lattice of spins taking values \uparrow, \downarrow . The alignment of nearest neighbours determines the energy.
- Heisenberg chain, a quantum mechanical model. It consists of a chain of spin states $|\uparrow\rangle, |\downarrow\rangle$. The Hamiltonian acts on nearest neighbours.

In the following we shall discuss the Heisenberg spin chain in detail.

4.1 Heisenberg Spin Chain

Let us start by introducing the model.

Setup. A single spin state can be $|\downarrow\rangle$ or $|\uparrow\rangle$ or any complex linear combination of these two. In other words, a spin is described by an element of the vector space

$$\mathbb{V} = \mathbb{C}^2. \quad (4.2)$$

A spin chain of length L is the L -fold tensor product

$$\mathbb{V}^{\otimes L} = \mathbb{V}_1 \otimes \dots \otimes \mathbb{V}_L. \quad (4.3)$$

This space serves as the Hilbert space of our model. It has finite dimension 2^L . A basis is given by the “pure” states,¹ e.g.

$$|\uparrow\uparrow\downarrow\uparrow\uparrow\uparrow\downarrow\rangle. \quad (4.4)$$

The Hamiltonian operator $H : \mathbb{V}^{\otimes L} \rightarrow \mathbb{V}^{\otimes L}$ is homogeneous and acts on nearest neighbours

$$\mathcal{H} = \sum_k \mathcal{H}_{k,k+1}, \quad \mathcal{H}_{k,l} : \mathbb{V}_k \otimes \mathbb{V}_l \rightarrow \mathbb{V}_k \otimes \mathbb{V}_l. \quad (4.5)$$

The pairwise kernel $H_{k,l}$ for the Heisenberg chain reads

$$\mathcal{H}_{k,l} = \lambda_0(1 \otimes 1) + \lambda_x(\sigma^x \otimes \sigma^x) + \lambda_y(\sigma^y \otimes \sigma^y) + \lambda_z(\sigma^z \otimes \sigma^z). \quad (4.6)$$

It is integrable for all values of the coupling constants $\lambda_0, \lambda_x, \lambda_y, \lambda_z$. Several useful cases can be distinguished:

- The most general (and most complicated) case is $\lambda_x \neq \lambda_y \neq \lambda_z \neq \lambda_x$: This is the so-called “XYZ” model.
- Many simplifications occur for $\lambda_x = \lambda_y \neq \lambda_z$: This is the so-called “XXZ” model.
- Symmetry is enhanced for $\lambda_x = \lambda_y = \lambda_z$: This is the so-called “XXX” model.

We shall mainly use the XXX model with the choice²

$$\lambda_0 = -\lambda_x = -\lambda_y = -\lambda_z = \frac{1}{2}\lambda. \quad (4.7)$$

With this choice the Hamiltonian kernel reads

$$\mathcal{H}_{k,l} = \lambda(\mathcal{I}_{k,l} - \mathcal{P}_{k,l}), \quad (4.8)$$

where $\mathcal{I}_{k,l}$ is the identity operator and $\mathcal{P}_{k,l}$ the permutation on the two equivalent spaces \mathbb{V}_k and \mathbb{V}_l . Note that $\lambda > 0$ implies ferromagnetic behaviour whereas $\lambda < 0$ implies anti-ferromagnetic behaviour.³ As λ is merely an overall factor of the spectrum, we shall fix it to $\lambda = 1$ for convenience. The kernel of the XXX Hamiltonian thus reads

$$\mathcal{H}_{k,l} = \mathcal{I}_{k,l} - \mathcal{P}_{k,l}. \quad (4.9)$$

Boundary Conditions. To complete the definition of the model, we must specify the boundary conditions. Typical choices are

- open chain:

$$\mathcal{H} = \sum_{k=1}^{L-1} \mathcal{H}_{k,k+1}, \quad (4.10)$$

¹We do not attribute a particular meaning to pure states (and neither to entangled states), they merely serve to conveniently enumerate a basis.

²The value of λ_0 is largely irrelevant because it merely induces an overall shift of all energies. Our choice sets the energy of a reference state to zero.

³We shall be interested in all states of the model, hence the difference between the ferromagnetic and anti-ferromagnetic case is merely an overall sign of the energy spectrum. The distinction between the two cases becomes relevant only when considering the ground state and its low-energy excitations.

- closed chain: identify sites periodically such that $\mathbb{V}_{L+1} \equiv \mathbb{V}_1$

$$\mathcal{H} = \sum_{k=1}^L \mathcal{H}_{k,k+1}, \quad (4.11)$$

- infinite chain:

$$\mathcal{H} = \sum_{k=-\infty}^{+\infty} \mathcal{H}_{k,k+1}. \quad (4.12)$$

Other choices that are sometimes encountered include:

- twists of the closed boundary conditions,
- open boundary conditions with specific boundary Hamiltonians,
- semi-infinite chains.

Some of these boundary conditions are compatible with integrability, others may not.

Boundary conditions have a strong impact on the spectrum: Infinite chains generally have a continuous spectrum while finite chains have a discrete spectrum by definition. This makes the spectral problem more interesting for finite chains. Here, the closed chains are typically easier to handle than open chains, therefore we shall mainly consider the former.

Symmetry. The XXX Hamiltonian has a $SU(2)$ Lie group symmetry because the kernel $\mathcal{H}_{k,l}$ is formulated as a manifestly $SU(2)$ invariant operator.

We can set up a representation \mathcal{Q}^α , $\alpha = x, y, z$, of the Lie algebra $\mathfrak{su}(2)$ on spin chains

$$\mathcal{Q}^\alpha = \sum_{k=1}^L \frac{1}{2} \sigma_k^\alpha. \quad (4.13)$$

- This is a tensor product representation of L spin- $1/2$ irreps of $\mathfrak{su}(2)$ given by the Pauli matrices σ_k^α acting on site k .
- The Hamiltonian is invariant

$$[\mathcal{Q}^\alpha, \mathcal{H}] = 0. \quad (4.14)$$

- The tensor product is decomposable, for the shortest few chains one finds by the well-known tensor product rules for $\mathfrak{su}(2)$:

$$\begin{aligned} L = 2 : & \quad (1) + (0); \\ L = 3 : & \quad (\tfrac{3}{2}) + 2(\tfrac{1}{2}); \\ L = 4 : & \quad (2) + 3(1) + 2(0); \\ L = 5 : & \quad (\tfrac{5}{2}) + 4(\tfrac{3}{2}) + 5(\tfrac{1}{2}); \\ L = 6 : & \quad (3) + 5(2) + 9(1) + 5(0); \\ & \quad \dots \end{aligned} \quad (4.15)$$

Here (Q) denotes a finite irrep of angular momentum Q and dimension $2Q + 1$.

- Each multiplet has one common energy eigenvalue.

4.2 Spectrum of the Closed Chain

We would like to gain some experience with the spectrum of spin chains. In the following we will therefore investigate the spectrum of the finite closed XXX chain.

Conventional Strategy. How to obtain the spectrum of a finite chain in practice? A conventional strategy, which works for arbitrary quantum mechanical models with finitely many states, is as follows:

- Enumerate a basis of $\mathbb{V}^{\otimes L}$, e.g. $|\downarrow \dots \downarrow \downarrow\rangle, |\downarrow \dots \downarrow \uparrow\rangle, \dots$ amounting to 2^L states in total.
- Evaluate \mathcal{H} in this basis as a $2^L \times 2^L$ matrix. This uninspiring task of basic combinatorics leads to a sparse matrix of integer entries.
- Next solve the eigenvalue problem of the Hamiltonian matrix.

The problem is ideally suited for computer algebra:

- One can automatically evaluate the Hamiltonian as a matrix for fairly large L .
- An exact diagonalisation in terms of algebraic numbers is feasible only for small L .
- Numerical evaluation of the eigenvalues allows slightly larger values of L .
- The spectrum is a big mess.
- Eigenvalues appear in multiplets.

Short Chains. The spectrum of the closed chain of small length L takes a fairly simple form:

L	eigenvalue multiplets		
2	$(0) \times 0, \quad (0) \times 4;$		
3	$(\frac{3}{2}) \times 0, \quad 2(\frac{1}{2}) \times 3;$		
4	$(2) \times 0, \quad 2(1) \times 2, \quad (1) \times 4,$ $(0) \times 6, \quad (0) \times 2;$		
5	$(\frac{5}{2}) \times 0, \quad 2(\frac{3}{2}) \times \frac{1}{2}(5 + \sqrt{5}), \quad 2(\frac{3}{2}) \times \frac{1}{2}(5 - \sqrt{5}),$ $(\frac{1}{2}) \times 4, \quad 2(\frac{1}{2}) \times 4 + \sqrt{5}, \quad 2(\frac{1}{2}) \times 4 - \sqrt{5};$		
6	$(3) \times 0, \quad 2(2) \times 3, \quad 2(2) \times 1,$ $(2) \times 4, \quad 2(1) \times \frac{1}{2}(7 + \sqrt{17}), \quad 2(1) \times \frac{1}{2}(7 - \sqrt{17}),$ $2(1) \times 5, \quad (1) \times (5 + \sqrt{5}), \quad (1) \times (5 - \sqrt{5}),$ $(1) \times 2, \quad (0) \times (5 + \sqrt{13}), \quad (0) \times (5 - \sqrt{13}),$ $2(0) \times 4, \quad (0) \times 6;$		
		

(4.16)

Note that the $\mathfrak{su}(2)$ eigenvalue multiplets denoted by (Q) often appear with an extra multiplicity of 2 in which case they are denoted by $2(Q)$. The pairing is largely a consequence of parity symmetry. However, parity is not sufficient to explain all of the pairings. Such extra pairings can be related to integrability.

Spectrum in Mathematica. Let us present a concise implementation of the XXX Hamiltonian in *Mathematica*.

First, we need to find a way to represent spin chain states. An immediate thought would be to define them as vectors with 2^L components. A drawback of this approach is that one obtains rather abstract and obscure objects which grow exponentially fast with L and which are not so easy to act upon. An alternative and more symbolic approach is to “define” a set of abstract basis vectors and allow for linear combinations. For example, we can represent pure spin chain states by functions whose arguments denote the spin orientations

$$|\uparrow, \uparrow, \downarrow, \uparrow, \downarrow\rangle \rightarrow \text{State}[1, 1, 0, 1, 0]. \quad (4.17)$$

The function `State` is undefined by default, so it remains unevaluated and can be used to represent linear combinations, e.g.

$$10 \text{State}[1, 1, 0, 1, 0] - 5 \text{State}[1, 0, 1, 1, 0]. \quad (4.18)$$

Next we have to represent the Hamiltonian \mathcal{H} through some replacement operator

$$\text{Ham} : \sum * \text{State}[\dots] \rightarrow \sum * \text{State}[\dots]. \quad (4.19)$$

A homogeneous nearest neighbour Hamiltonian can be implemented by the following code:

$$\begin{aligned} \text{Ham}[X_] := \\ X /. \text{Psi_State} :> \text{Module}[\{k, L=\text{Length}[\text{Psi}]\}, \\ \text{Sum}[\text{HamAt}[\text{Psi}, k, \text{Mod}[k+1, L, 1]], \\ \{k, L\}]]; \end{aligned} \quad (4.20)$$

This function replaces (`/.`, `ReplaceAll`) every occurrence of `State` in the argument `X` with the homogeneous action of the kernel `HamAt`. Some notes:

- `Psi_State` symbolises any object `State[...]`, i.e. any object with head `State`.⁴
- The use of the replacement operator `:>` (`RuleDelayed`) as opposed to `->` (`Rule`) is essential because it evaluates the right hand side only after insertion of `Psi`.
- The above definition assumes that the argument `X` is a linear combination of `State` objects. If `X` is not a linear combination of `State` objects, `Ham` does whatever it does (replace objects). Lists, vectors, matrices, nested lists of linear combinations of `State` objects are permissible as arguments: `Ham` will act on each element individually.
- The construct `Module` defines a local variable `k`⁵ and a local variable `L` assigned with the length of the state `Psi`.

⁴Almost all objects in *Mathematica* (except variables and concrete numbers) are *headed lists*. They can be treated much like lists (which are in fact objects with head `List`).

⁵Sometimes using the same variable names as arguments of a `Sum` and elsewhere can lead to undesired interference (depending on the order of evaluation of sub-expressions). To avoid a potential interference it makes sense to make the summation variable local.

The Hamiltonian kernel for the XXX model can be defined as

$$\begin{aligned} \text{HamAt}[\text{Psi_State}, k_ , l_] &:= \\ \text{Psi} - \text{Permute}[\text{Psi}, \text{Cycles}[\{\{k, l\}\}]]; \end{aligned} \quad (4.21)$$

It uses some pre-defined combinatorial methods to implement the permutation of two sites in the symbol `Psi`.

We are now ready to act on states. In order to obtain the complete spectrum we have to enumerate a basis of $\mathbb{V}^{\otimes L}$. As a shortcut, we can employ the binary representation of integers $0, \dots, 2^L - 1$:

$$\begin{aligned} \text{Basis}[L_] &:= \\ \text{Table}[\text{State} @@ \text{IntegerDigits}[k, 2, L], & \\ \{k, 0, 2^L - 1\}]; \end{aligned} \quad (4.22)$$

Here the operator `@@` (`Apply`) replaces the head of the binary representation of `k` (which is `List`) with `State`. The variable `states` is now a list of pure basis states.

To evaluate the Hamiltonian on the states we can use the following construct:

$$\begin{aligned} \text{HamMat}[\text{states_}] &:= \\ \text{Module}[\{X = \text{Ham}[\text{states}]\}, & \\ \text{Coefficient}[X, \#] \& /@ \text{states}]; \end{aligned} \quad (4.23)$$

Some notes:

- `Ham[states]` evaluates `Ham` on every element of the list `states`. Usually, one would have to explicitly declare this behaviour for the function `Ham` by means of `SetAttributes[Ham, Listable]`. In our case, the definition via a replacement rule automatically implements this desired behaviour.
- The operator `&` (`Function`) represents a *pure function* (a function without a declaration) which returns `Coefficient[X, #]` where `#` is the argument passed to the function. In practice it extracts the coefficient of the argument within `X`.
- The operator `/@` (`Map`) evaluates the above pure function on all elements of the list `states`. This is the matrix representation of `Ham` in the basis `states`.⁶

To finally extract the eigenvalues, generate the Hamiltonian matrix via (remember to substitute or define `L` as a not too large positive integer)

$$\text{emat} = \text{HamMat}[\text{Basis}[L]]; \quad (4.24)$$

and use `Eigenvalues[emat]`, `Eigenvalues[N[emat]]` or `Eigenvalues[N[emat], 20]`.

Bethe Equations. Now, the Heisenberg spin chain is a very special model with many features reminiscent of integrability. Unfortunately, there is no universal notion of quantum integrability as in the finite-dimensional classical case (Liouville). In particular, it is unclear how to define the number of degrees of

⁶Potentially, one should `Transpose` the matrix.

freedom in a quantum theory. Nevertheless, there exist powerful methods for computing relevant observables. For example, the spectral problem can be transformed to a convenient set of equations. Let us first state the result, and postpone the derivation to later.

Consider a set of M algebraic equations (Bethe equations) for the M variables $u_k \in \mathbb{C}$ (Bethe roots)

$$\left(\frac{u_k + \frac{i}{2}}{u_k - \frac{i}{2}} \right)^L = \prod_{\substack{j=1 \\ j \neq k}}^M \frac{u_k - u_j + i}{u_k - u_j - i} \quad \text{for } k = 1, \dots, M. \quad (4.25)$$

The claim is that for every eigenstate multiplet with angular momentum $Q = L/2 - M$ of \mathcal{H} there is a solution of the above equations with $M \leq L/2$ distinct Bethe roots u_k .⁷ The energy eigenvalue of this state can be read off easily

$$E = \sum_{k=1}^M \left(\frac{i}{u_k + \frac{i}{2}} - \frac{i}{u_k - \frac{i}{2}} \right). \quad (4.26)$$

For example, we can consider the case $L = 6$, $M = 3$ which corresponds to a $\mathfrak{su}(2)$ singlet. A solutions is given by

$$u_{1,2} = \pm \sqrt{-\frac{5}{12} + \frac{\sqrt{13}}{6}}, \quad u_3 = 0, \quad E = 5 + \sqrt{13}. \quad (4.27)$$

This agrees precisely with an eigenstate of the Heisenberg Hamiltonian that we have identified earlier. The treatment of the spectral problem via Bethe equations has some benefits:

- We have transformed a problem of linear algebra directly to algebraic equations. We can thus skip combinatorics and characteristic polynomials.
- We can use the Bethe equations efficiently for approximations at large L and M . For example, the anti-ferromagnetic ground state can be approximated at large L in which case the Bethe equations turn into integral equations.

In the following sections we shall derive the above Bethe equations by means of the coordinate Bethe ansatz.

4.3 Coordinate Bethe Ansatz

The coordinate Bethe ansatz is based on the chain with infinite boundary conditions where asymptotically the spins are aligned down. It provides the complete solution for these boundary conditions in terms of eigenstates and energies. It is based on classifying states by the number M of up-spins. Due to $\mathfrak{su}(2)$ symmetry, the latter is a conserved quantity.

⁷There are some subtleties related to the $SU(2)$ symmetry for the XXX model, and one has to pay attention to Bethe roots at ∞ and $\pm \frac{i}{2}$.

Vacuum State. We start with a very simple state, the *ferromagnetic vacuum*

$$|0\rangle := |\downarrow\downarrow\downarrow\ldots\downarrow\rangle. \quad (4.28)$$

By construction this state has zero energy (locally as well as globally)

$$\mathcal{H}_{k,k+1}|0\rangle = \mathcal{I}_{k,k+1}|0\rangle - \mathcal{P}_{k,k+1}|0\rangle = |0\rangle - |0\rangle = 0. \quad (4.29)$$

Therefore $\mathcal{H}|0\rangle = 0$ and the ground state energy is zero

$$E = 0. \quad (4.30)$$

This solves the problem for $M = 0$. Here, the boundary conditions actually do not play a role.

Magnon States. Now flip one spin at site k

$$|k\rangle := |\downarrow\ldots\downarrow\overset{k}{\uparrow}\downarrow\ldots\downarrow\rangle. \quad (4.31)$$

These states enumerated by k form a closed sector under the Hamiltonian due to conservation of the z -component of spin \mathcal{Q}^z .

How to obtain eigenstates of \mathcal{H} ? Note that the Hamiltonian is homogeneous and commutes with a shift of the chain by one unit.⁸ We can thus look for simultaneous eigenstates of the Hamiltonian and the shift operator. Momentum eigenstates are plane waves⁹

$$|p\rangle := \sum_k e^{ipk} |k\rangle. \quad (4.32)$$

This state is called a *magnon state*. It can be viewed as a particle excitation¹⁰ of the above vacuum state.

Since there is a unique state with a given momentum p , it must already be an energy eigenstate. We can now act with \mathcal{H} on $|p\rangle$ and obtain (after a shift of summation variable to match the states on the r.h.s.)

$$\begin{aligned} \mathcal{H}|p\rangle &= \sum_k e^{ipk} \left(\overbrace{|k\rangle - |k-1\rangle}^{H_{k-1,k}} + \overbrace{|k\rangle - |k+1\rangle}^{H_{k,k+1}} \right) \\ &= \sum_k e^{ipk} (1 - e^{ip} + 1 - e^{-ip}) |k\rangle \\ &= e(p) |p\rangle \end{aligned} \quad (4.33)$$

with the *magnon dispersion relation*

$$e(p) = 2(1 - \cos p) = 4 \sin^2(\tfrac{1}{2}p). \quad (4.34)$$

⁸The lattice shift is a discrete version of the momentum generator.

⁹The notation is slightly ambiguous, but it should become clear from the context whether $|*\rangle$ refers to a position eigenstate $|k\rangle$ or a momentum eigenstate $|p\rangle$.

¹⁰Here the notion of particle is an object which carries an individual momentum p .

For a closed chain, the momentum would furthermore be quantised by the periodic boundary conditions to

$$p = \frac{2\pi n}{L}, \quad \text{where } n = 0, \dots, L-1. \quad (4.35)$$

For other boundary conditions on a finite chain, the momenta would be quantised in a similar fashion. For the infinite chain, however, p is a continuous parameter. Note that in all cases the momentum is defined only modulo 2π because the position k is sampled only at the discrete lattice positions. A shift by 2π corresponds to a change of Brillouin zone which leaves the eigenstate unchanged.

This solves the problem for $M = 1$. In what follows, we shall only consider the infinite boundary conditions.

Scattering Factor. We continue with states with two spin flips

$$|k < l\rangle := |\downarrow \dots \downarrow \overset{k}{\uparrow} \downarrow \dots \downarrow \overset{l}{\uparrow} \downarrow \dots \downarrow\rangle. \quad (4.36)$$

Here we make the assumption that $k < l$. Again, these states form a closed sector for the Hamiltonian, and we wish to construct eigenstates.

When the spin flips are well-separated we can treat the state as the combination of two individual magnons. The nearest neighbour Hamiltonian will hardly ever see both spin flips at the same time, therefore we can make an ansatz for eigenstates of the form

$$|p < q\rangle = \sum_{k < l = -\infty}^{+\infty} e^{ipk + iql} |k < l\rangle. \quad (4.37)$$

Some comments:

- This state has overall momentum $P = p + q$.
- The momenta of the individual spin flips are not literally Fourier coefficients because their wave functions do not extend over the whole chain, but are constrained by an ordering $k < l$ of the spin flips. Nevertheless we can use p and q as labels for a particular state.
- The notation $|p < q\rangle$ is not meant to imply that p is numerically less than q , but rather that the magnon with momentum p is *to the left of* the magnon with momentum q .

By construction, each of these states is almost an eigenstate with eigenvalue

$$E = e(p) + e(q). \quad (4.38)$$

Acting with the combination $\mathcal{H} - e(p) - e(q)$ on $|p < q\rangle$ yields

$$(e^{ip+iq} - 2e^{iq} + 1) \sum_{k=-\infty}^{+\infty} e^{i(p+q)k} |k < k+1\rangle. \quad (4.39)$$

Interestingly, only a contact term $\sum_k e^{i(p+q)k} |k < k+1\rangle$ remains and violates the eigenstate condition. Since this state is symmetric in p and q we can act on the

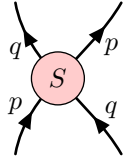
state $|q < p\rangle$ with the magnon momenta interchanged and obtain a proportional term

$$(e^{ip+iq} - 2e^{ip} + 1) \sum_{k=-\infty}^{+\infty} e^{i(p+q)k} |k < k+1\rangle. \quad (4.40)$$

We can now patch together the two partial wave functions and construct an exact eigenstate¹¹

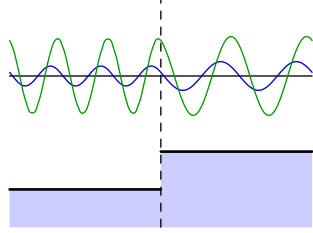
$$|p, q\rangle := |p < q\rangle + S(p, q)|q < p\rangle \quad (4.41)$$

with a *scattering factor* S

$$S(p, q) := -\frac{e^{ip+iq} - 2e^{iq} + 1}{e^{ip+iq} - 2e^{ip} + 1}. \quad (4.42)$$


The scattering factor is analogous to the scattering factor or scattering matrix in QM and QFT.¹²

The process of patching together two wave functions is analogous to the construction of quantum mechanical wave functions at a one-dimensional potential step.


(4.43)

In our context, the distance of the magnons is the relevant position variable and the potential step is at the minimum distance of one lattice site.

Factorised Scattering. Before considering closed chains, let us have a look at three-magnon states. There are $6 = 3!$ asymptotic regions for magnons which carry one momentum p_k each. A useful ansatz for an eigenstate is the so-called *Bethe ansatz*

$$\begin{aligned} |p_1, p_2, p_3\rangle = & |p_1 < p_2 < p_3\rangle + S_{12}S_{13}S_{23}|p_3 < p_2 < p_1\rangle \\ & + S_{12}|p_2 < p_1 < p_3\rangle + S_{13}S_{23}|p_3 < p_1 < p_2\rangle \\ & + S_{23}|p_1 < p_3 < p_2\rangle + S_{12}S_{13}|p_2 < p_3 < p_1\rangle. \end{aligned} \quad (4.44)$$

¹¹We pay no attention to the overall normalisation of the state. Therefore the state $|p, q\rangle$ is independent of the order of p and q (up to normalisation).

¹²The setup for these two objects is slightly different: The ordinary scattering factor in higher-dimensional problems of QM and QFT relates ingoing and outgoing states where each particle has a well-defined momentum in the distant past and distant future. The scattering factor of the Bethe ansatz relates two partial wave functions with different spatial ordering of the individual particles. The latter is something that works only with one spatial dimension. Therefore an ordinary scattering factor corresponds to a time-like process whereas the scattering factor in the Bethe ansatz corresponds to a space-like process.

In this combination, all pairwise contact terms of the Hamiltonian action vanish by construction due to the choice of appropriate pairwise scattering factors between any two partial wave functions.

Conventionally, one should anticipate a triple contact term

$$(\mathcal{H} - E)|p_1, p_2, p_3\rangle \sim \sum_k e^{iP_k} |k < k+1 < k+2\rangle. \quad (4.45)$$

Such a term would be cancelled by some combination of the full one-parameter family of states $|p_1 < p_2 < p_3\rangle$ with common energy E and momentum P .

However, due to a miracle this contact term is absent without further ado. This miracle is called integrability.¹³ It works analogously for any number of magnons as we shall discuss below. We only need the two-magnon scattering factor to construct arbitrary states.

In other words, scattering of more than two magnons factorises into a sequence of pairwise magnon scattering processes, for example:

$$\text{Diagram 1} = \text{Diagram 2} + \text{Diagram 3} \quad (4.46)$$

For pairwise scattering, conservation of total momentum and total energy ensures that the individual momenta are not deformed but merely exchanged. Therefore, in factorised scattering processes, the particle momenta are only ever permuted. Conversely, if the particle momenta are merely permuted by scattering, the above ansatz for the complete wave function is complete, and scattering factorises.

Factorised scattering means that there is no elementary scattering factor for three or more magnons. Such a factor would lead to a substantially different behaviour in that one would have to integrate over admissible momenta of the particles. This is an option for three or more particles because conservation of total momentum and total energy are not sufficient to guarantee the conservation of all individual momenta. Conservation of additional *local commuting* charges excludes deformations of the kinematical configuration, and therefore implies factorised scattering.

Solution of the Infinite Chain. We have found an explicit and exact solution for the eigenstates of the infinite chain with an arbitrary number of magnons

$$|0\rangle = |\downarrow \dots \downarrow\rangle, \quad E = 0,$$

¹³The absence of the contact term is also a consequence of the pairwise nature of the Hamiltonian. This is not in contradiction with the fact that most models with nearest neighbour Hamiltonians are non-integrable. Generically these models have a pairwise scattering *matrix* which is not consistent with the assumption of factorised scattering in which case the above ansatz has leftover pairwise contact terms.

$$\begin{aligned}
|p\rangle &= \sum_k e^{ipk} |\dots \overset{k}{\uparrow} \dots\rangle, & E &= e(p), \\
|p, q\rangle &= |p < q\rangle + S(p, q) |q < p\rangle, & E &= e(p) + e(q), \\
|p_k\rangle &= \sum_{\pi \in S_M} S_\pi |p_{\pi(1)} < \dots < p_{\pi(M)}\rangle, & E &= \sum_k e(p_k).
\end{aligned} \tag{4.47}$$

The momenta p_k are arbitrary numbers, therefore the spectrum is continuous. Please note:

- The ordering of the p_k does not matter up to normalisation: magnons are identical particles.
- The momenta p_k are defined modulo 2π : they move on a lattice.
- For two identical momenta we have

$$S(p, p) = -1. \tag{4.48}$$

This indicates that the particles obey Fermi statistics. Consequently, they are also subject to the exclusion principle

$$|p, p, \dots\rangle = 0, \tag{4.49}$$

which follows from the above form of eigenstates. The XXX model on the infinite chain is equivalent to *free fermions* on a one-dimensional lattice!

- Zero-momentum particles are special:

$$S(p, 0) = 1, \quad e(0) = 0. \tag{4.50}$$

They behave as free bosons which do not interact with any of the other particles. They represent the $\mathfrak{su}(2)$ ladder operators which allow to walk between the states of an $SU(2)$ multiplet.

- The momenta should typically be real for wave functions to be normalisable (in the ordinary sense of plane waves).
- Complex momenta correspond to wave functions which grow exponentially at $k \rightarrow +\infty$ or $k \rightarrow -\infty$ and make the wave function non-normalisable.

Nevertheless, particular combinations of complex momenta are permissible: Whenever $S(p, q) = 0, \infty$, some partial wave functions of a state $|p, q, \dots\rangle$ have a coefficient 0.¹⁴ Under suitable conditions, the exponentially growing regions of the wave function are eliminated by a zero coefficient.

$$\tag{4.51}$$

Such normalisable states are called *bound states*. They can be viewed as different types of particle excitations with one independent (real) momentum and a different dispersion relation. Bound states made from more than two magnons also exist.

¹⁴One has to arrange the overall normalisation such that none of the relevant scattering factors is ∞ .

4.4 Bethe Equations

We now know how to solve the infinite XXX chain, but we would like to understand the spectrum of finite chains. We can use the above results on magnon scattering to derive the Bethe equations which describe the spectrum of finite chains.

Closed Chains. Let us start with closed chains. We can compare states of the closed chain with periodic states of the infinite chain. In quantum mechanics, the appropriate notion of periodicity is a periodic wave function of the type

$$\langle k, \dots | \Psi \rangle = \langle k + L, \dots | \Psi \rangle. \quad (4.52)$$

A wave function for the closed chain can be constructed as follows:

- Take an eigenstate of the infinite chain and pick a range of L sites that is to be mapped to the closed chain. The wave function on the closed chain is taken to agree with those parts of the eigenstate on the infinite chain where all magnons reside within the range.
- Focus on the leftmost excitation and pay attention to how the wave function of the eigenstate evolves as this excitation is shifted from the first site within the range towards the right.
- Moving the excitation by L sites generates a factor of $e^{ip_k L}$ by construction.
- Along the way, it will move past all the other excitations and pick up a factor of $S(p_k, p_j)$ for each permutation.¹⁵
- The eigenstate is periodic if all the phase factors multiply to 1, in other words

$$\langle k_1, k_2, \dots, k_M | \Psi \rangle = \langle k_2, \dots, k_M, k_1 + M | \Psi \rangle. \quad (4.53)$$

This periodicity condition ensures that $\mathcal{H}_{L,1}$ behaves exactly like $\mathcal{H}_{L,L+1}$ implying that the wave function restricted to the closed chain yields an exact eigenstate.

This leads to the *Bethe equations* for a closed chain

$$e^{ip_k L} \prod_{\substack{j=1 \\ j \neq k}}^M S(p_k, p_j) = 1, \quad \text{for all } k = 1, \dots, M. \quad (4.54)$$

¹⁵The wave function changes rapidly at a single site, there is no interaction of the magnons at a distance. This is a crucial insight to make this construction exact.

Graphically, the Bethe equations can be represented as follows:

$$(4.55)$$

They amount to one equation for each unknown variable p_k . This effectively quantises the spectrum. A simple consistency requirement for the closed chain already leads to a discrete set of solutions.

The total energy and total momentum of a solution can be read off from the set of magnon momenta p_k

$$E = \sum_{k=1}^M e(p_k), \quad P = \sum_{k=1}^M p_k. \quad (4.56)$$

Note that one can derive a simple condition on P by multiplying all Bethe equations and using the fact that $S(p, q)S(q, p) = 1$, namely

$$e^{iPL} = 1. \quad (4.57)$$

This relationship corresponds to triviality of an overall shift by L sites where e^{iP} is the eigenvalue of the cyclic shift operator by a single site.

Rapidities. It is convenient to introduce a different set of so-called rapidity variables u_k instead of the momenta p_k

$$p_k = 2 \operatorname{arccot} 2u_k, \quad u_k = \frac{1}{2} \cot \frac{1}{2}p_k, \quad e^{ip_k} = \frac{u_k + \frac{i}{2}}{u_k - \frac{i}{2}}. \quad (4.58)$$

This transformation of variables eliminates the 2π -ambiguity of the p_k and typically leads to rational functions in the u_k . For instance, the scattering factor simplifies to a rational function¹⁶

$$S(u, v) = \frac{u - v - i}{u - v + i}. \quad (4.59)$$

The Bethe equations then take the rational form in terms of the so-called Bethe roots u_k which we introduced earlier

$$\left(\frac{u_k + \frac{i}{2}}{u_k - \frac{i}{2}} \right)^L = \prod_{\substack{j=1 \\ j \neq k}}^M \frac{u_k - u_j + i}{u_k - u_j - i} \quad \text{for } k = 1, \dots, M. \quad (4.60)$$

¹⁶This form of the scattering factor neatly shows that bound states are obtained for the simple condition $u_k = u_j \pm i$ where S is singular. Higher bound states correspond to so-called *Bethe strings* $u_k = u_0 + ik$.

Each solution of the Bethe equations corresponds to an eigenstate on the closed chain, whose momentum and energy eigenvalues can be extracted easily via

$$e^{iP} = \prod_{k=1}^M \frac{u_k + \frac{i}{2}}{u_k - \frac{i}{2}}, \quad E = \sum_{k=1}^M \left(\frac{i}{u_k + \frac{i}{2}} - \frac{i}{u_k - \frac{i}{2}} \right). \quad (4.61)$$

Let us mention some facts about admissible configurations of rapidities:

- The u_k are real or form complex conjugate pairs.¹⁷
- All u_k must be distinct except for the special value $u_k = \infty$ which can appear several times.
- The $\mathfrak{su}(2)$ ladder operators at $p_k = 0$ correspond to $u_k = \infty$.
- The pair of special values $u_k = \pm \frac{i}{2}$ where $p_k = \pm i\infty$ corresponds to a tightly bound state of two magnons with overall momentum π and energy 2. It makes appearance in some singular solutions. Apart from this special configuration, any two Bethe roots are never separated by exactly i on a finite chain.
- We should restrict to at most half filling $M \leq \frac{1}{2}L$; the other states with $M > \frac{1}{2}L$ are formally represented via a collection of $u_k = \infty$ added to a solution with $M \leq \frac{1}{2}L$.

Note that although the rational form of the Bethe equations has a very nice analytic form, the trigonometric form in terms of momenta is more useful towards finding solutions numerically because of better stability properties.

Open Chains. The spectral problem for an open chain can be solved in a similar fashion as the one of the closed chain. However, the treatment of the boundaries requires some new concepts. Consider an open chain with Hamiltonian

$$\mathcal{H} = \sum_{k=1}^{L-1} \mathcal{H}_{k,k+1}. \quad (4.62)$$

To quantify the effect of the boundaries, consider a semi-infinite chain starting at site $k = 1$. Act with $\mathcal{H} - e(p)$ on a one-magnon state $|+p\rangle$.

$$(\mathcal{H} - e(p))|+p\rangle = (1 - e^{+ip})|1\rangle. \quad (4.63)$$

As for the two-magnon state, there is a residual term located at the boundary. This term can be compensated by another partial eigenstate with equal energy $e(\bar{p}) = e(p)$, namely $\bar{p} = -p$.

$$(\mathcal{H} - e(p))|-p\rangle = (1 - e^{-ip})|1\rangle. \quad (4.64)$$

Now combine the states into an exact eigenstate^{18 19}

$$|p\rangle = e^{-ip} |+p\rangle + e^{+ip} K_L(-p)|-p\rangle \quad (4.65)$$

¹⁷Normalisability is not an issue for finite chains.

¹⁸The factors of $e^{\pm ip}$ were inserted to compensate for the plane wave factor at site $k = 1$.

¹⁹Up to normalisation, the exact eigenstates are invariant under flipping the sign of the momentum p because they are a superposition of ingoing and outgoing waves.

with the boundary scattering factor

$$K_L(-p) = -e^{-2ip} \frac{1 - e^{+ip}}{1 - e^{-ip}} = e^{-ip}. \quad (4.66)$$

Similarly, one can construct exact eigenstates for a semi-infinite chain ending at site $k = L$

$$|p\rangle = e^{-ipL} | +p\rangle + e^{+ipL} K_R(+p) | -p\rangle \quad (4.67)$$

with boundary scattering factor

$$K_R(+p) = e^{+ip}. \quad (4.68)$$

Compatibility of both boundaries leads to a set of Bethe equations for the open chain

$$\frac{e^{i(L-1)(+p_k)}}{e^{i(L-1)(-p_k)}} \frac{K_R(+p_k)}{K_L(-p_k)} \prod_{\substack{j=1 \\ j \neq k}}^M \frac{S(+p_k, p_j)}{S(-p_k, p_j)} = 1, \quad (4.69)$$

or in a graphical representation:

$$\frac{e^{+ip_k(L-1)}}{e^{-ip_k(L-1)}} K_L \dots S \dots S \dots S \dots S \dots K_R = 1. \quad (4.70)$$

Note that these equations are invariant under flipping the sign of any momentum $p_j \rightarrow -p_j$. Flipping the sign of p_k inverts the equation.

The Bethe equations in rational form read

$$\left(\frac{u_k + \frac{i}{2}}{u_k - \frac{i}{2}} \right)^{2L} = \prod_{\substack{j=1 \\ j \neq k}}^M \frac{u_k - u_j + i}{u_k - u_j - i} \frac{u_k + u_j + i}{u_k + u_j - i}. \quad (4.71)$$

One can also treat different open boundary conditions in this form which amount to some additional factors in the equations.

4.5 Generalisations

Bethe equations can be formulated for many quantum integrable systems. In particular, there are many generalisations of the above Heisenberg Hamiltonian. Curiously, the Bethe equations always take a rather simple and universal form. Even better, their structure directly reflects some properties of the group and representation theory of the underlying spins. In order to see this, let us explore some generalisations of the XXX model.

Bethe Equations for the XXZ Model. The XXX model is part of a larger XXZ family of integrable models which are solvable by the above Bethe ansatz.²⁰ Strictly speaking the XXZ model is the model defined above. However, we can add a few parameters while preserving the features of the original model²¹

$$\begin{aligned}\mathcal{H}_{k,k+1} = & \alpha_1(1 \otimes 1) + \alpha_2(\sigma^z \otimes 1) + \alpha_3(1 \otimes \sigma^z) + \alpha_4(\sigma^z \otimes \sigma^z) \\ & + \alpha_5(\sigma^x \otimes \sigma^x + \sigma^y \otimes \sigma^y) + i\alpha_6(\sigma^x \otimes \sigma^y - \sigma^y \otimes \sigma^x).\end{aligned}\quad (4.72)$$

The 6 free parameter have the following meaning:

- one overall shift of energies proportional to the length: $\delta\alpha_1$,
- one trivial deformation for closed chains: $\delta\alpha_2 = -\delta\alpha_3$,
- one shift proportional to \mathcal{Q}^z : $\delta\alpha_2 = +\delta\alpha_3$,
- one overall scaling of energies: $\delta\alpha_k = \alpha_k\delta\beta$,
- one quantum deformation parameter \hbar also known as $q = e^{i\hbar}$ and the anisotropy $\Delta = \frac{1}{2}(q + q^{-1})$,
- one magnetic flux parameter ρ .

The resulting Bethe equations for closed chains read

$$\left(\frac{\sin \hbar(u_k + \frac{i}{2})}{\sin \hbar(u_k - \frac{i}{2})} \right)^L e^{i\rho L} = \prod_{\substack{j=1 \\ j \neq k}}^M \frac{\sin \hbar(u_k - u_j + i)}{\sin \hbar(u_k - u_j - i)}. \quad (4.73)$$

These Bethe equations are called *trigonometric* as opposed to the *rational* Bethe equations for the XXX model.²² The total momentum and energy are given by

$$P = \sum_{k=1}^M p(u_k), \quad E = \gamma_1 L + \gamma_2 M + \gamma_3 \sum_{k=1}^M e(u_k) \quad (4.74)$$

with

$$e^{ip(u)} = \frac{\sin \hbar(u + \frac{i}{2})}{\sin \hbar(u - \frac{i}{2})}, \quad e(u) = p'(u). \quad (4.75)$$

Evidently, these equations reduce to the rational case in the limit $\hbar \rightarrow 0$.

XXX model with Higher Spin. We can also use a different Hilbert space for the spin chain, for example a spin $s = 1$ representation spanned by three states $|0\rangle$, $|1\rangle$ and $|2\rangle$ corresponding to spin up, spin zero and spin down. The so-called XXX₁

²⁰The latter is part of the even larger XYZ family, but its solution requires more advances techniques because there is no U(1) symmetry to preserve the number of magnons.

²¹This is in fact the most general nearest neighbour Hamiltonian which commutes with $\mathcal{Q}^z = \frac{1}{2} \sum_k \sigma_k^z$.

²²Both sets of Bethe equations can be written in either rational or trigonometric form with a suitable choice of variables, e.g. $z_k = \exp(i\hbar u_k)$ for XXZ. The distinguished set of variables, however, is where u_j appears only in the combination $u_j - u_k$. Using these variables the Bethe equations are rational and trigonometric for XXX and XXZ, respectively.

Hamiltonian has $SU(2)$ symmetry, in particular it preserves \mathcal{Q}^z . Therefore, the Hamiltonian kernel takes a block-diagonal form in the basis E

$$\mathcal{H}_{k,k+1} = \begin{pmatrix} * & & & & \\ & * & * & & \\ & * & * & & \\ & & & * & * & * \\ & & & * & * & * \\ & & & * & * & * \\ & & & & * & * \\ & & & & * & * \\ & & & & & * \end{pmatrix}, \quad E = \begin{pmatrix} |00\rangle \\ |10\rangle \\ |01\rangle \\ |20\rangle \\ |11\rangle \\ |02\rangle \\ |21\rangle \\ |12\rangle \\ |22\rangle \end{pmatrix}. \quad (4.76)$$

We do not reproduce the coefficients because they do not add a qualitative insight. The above Bethe ansatz works with small alterations:

- vacuum:

$$|0\rangle = |0 \dots 0\rangle. \quad (4.77)$$

- one-magnon states:

$$|p\rangle = \sum_k e^{ipk} |\dots \overset{k}{1} \dots\rangle. \quad (4.78)$$

- two-magnon states:

$$|p < q\rangle = \sum_{k < l} e^{ipk + iql} |\dots \overset{k}{1} \dots \overset{l}{1} \dots\rangle, \\ |p; 2\rangle = \sum_k e^{ipk} |\dots \overset{k}{2} \dots\rangle. \quad (4.79)$$

The action of the Hamiltonian on partial eigenstates now yields some additional terms

$$(\mathcal{H} - E)|p < q\rangle = \sum_k e^{i(p+q)k} (*|\dots \overset{k}{11} \dots\rangle + *|\dots \overset{k}{2} \dots\rangle), \\ (\mathcal{H} - E)|p; 2\rangle = \sum_k e^{ipk} (*|\dots \overset{k}{11} \dots\rangle + *|\dots \overset{k}{2} \dots\rangle). \quad (4.80)$$

The scattering ansatz needs to be supplemented in order to compensate them appropriately.

$$|p, q\rangle = |p < q\rangle + S|q < p\rangle + C|p + q; 2\rangle. \quad (4.81)$$

To construct the exact eigenstate we now have to solve two linear equations. The coefficient S is the scattering factor which is relevant for IR physics. The contact term C is important for the solution, but it merely describes the UV physics of the eigenstate.²³

The resulting Bethe equations for a closed chain read

$$\left(\frac{u_k + i}{u_k - i}\right)^L = \prod_{\substack{j=1 \\ j \neq k}}^M \frac{u_k - u_j + i}{u_k - u_j - i}, \quad e^{ip} = \frac{u + i}{u - i}, \quad e(u) = p'(u). \quad (4.82)$$

²³The term $|p + 2; 2\rangle$ should be viewed as a contribution when both magnons reside on a single site. We did not have to consider such terms before because for a spin- $1/2$ representation a single site can only be excited once.

Note that the Bethe equations are almost the same up to a different prefactor of i on the l.h.s. of the Bethe equations and likewise in the definition of the magnon momentum.

The generalisation to arbitrary spin s representations at each site is evident (and correct)

$$\left(\frac{u_k + i s}{u_k - i s}\right)^L = \prod_{\substack{j=1 \\ j \neq k}}^M \frac{u_k - u_j + i}{u_k - u_j - i}, \quad e^{ip} = \frac{u + i s}{u - i s}. \quad (4.83)$$

The corresponding model is called the XXX_s model.

Bethe Ansatz at Higher Rank. Generalisations of the XXX model to higher-rank groups exist. For example, consider a chain with $\text{SU}(N)$ symmetry and spins in the fundamental representation

$$\mathbb{V} = \mathbb{C}^N, \quad |1\rangle, \dots, |N\rangle \in \mathbb{V}. \quad (4.84)$$

An integrable nearest neighbour Hamiltonian is given by the kernel

$$\mathcal{H}_{k,k+1} = \mathcal{I}_{k,k+1} - \mathcal{P}_{k,k+1}. \quad (4.85)$$

More explicitly, this kernel acts as follows

$$\mathcal{H}|ab\rangle = |ab\rangle - |ba\rangle. \quad (4.86)$$

We can again perform the Bethe ansatz:

- vacuum:

$$|0\rangle^1 := |1 \dots 1\rangle. \quad (4.87)$$

- there are now $N - 1$ flavours of one-magnon states labelled by $a = 2, \dots, N$

$$|p, a\rangle^1 := \sum_k e^{ipk} |\dots \overset{k}{a} \dots\rangle. \quad (4.88)$$

- To accommodate for the various combinations of magnon flavours, we need a *scattering matrix*²⁴ instead of a scattering factor for the definition of two-magnon states

$$\begin{aligned} |(p, a), (q, b)\rangle^1 &= |(p, a) < (q, b)\rangle^1 \\ &+ \sum_{c,d=2}^N S_{ab}^{cd}(p, q) |(q, d) < (p, c)\rangle^1. \end{aligned} \quad (4.89)$$

The S-matrix may again be represented graphically as follows:



$$(4.90)$$

²⁴More precisely it is a tensor of rank 4, but when acting on two-magnon states it can be viewed as a matrix.

The scattering matrix is a new feature for models based on a higher-rank algebra.

- The matrix can be computed as before by matching all asymptotic regions. In our case, one finds

$$S_{ab}^{cd}(u, v) = \frac{(u - v)\delta_a^c \delta_b^d + i\delta_a^d \delta_b^c}{u - v - i}. \quad (4.91)$$

- It preserves the residual $SU(N - 1)$ of the magnons on the vacuum state.
- For $u \rightarrow \infty$ or $v \rightarrow \infty$ it is trivial

$$S_{ab}^{cd}(\infty, v) = S_{ab}^{cd}(u, \infty) = \delta_a^c \delta_b^d. \quad (4.92)$$

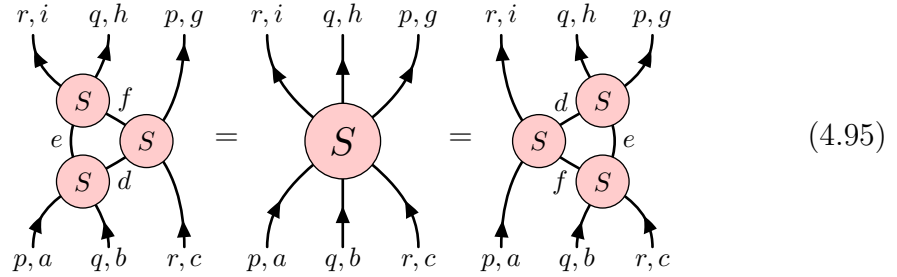
- For equal rapidities it reads

$$S_{ab}^{cd}(u, u) = -\delta_a^d \delta_b^c. \quad (4.93)$$

- It satisfies the *Yang–Baxter equation* which guarantees that states of factorised scattering can be defined consistently

$$S_{ab}^{de}(p, q) S_{dc}^{gf}(p, r) S_{ef}^{hi}(q, r) = S_{bc}^{ef}(q, r) S_{af}^{di}(p, r) S_{de}^{gh}(p, q). \quad (4.94)$$

The flow of indices is best explained using a figure:



An abbreviated version of the formal expression reads

$$S_{12} S_{13} S_{23} = S_{23} S_{13} S_{12}. \quad (4.96)$$

This equation is a central relation for all quantum integrable systems.

Nested Bethe Ansatz. The S-matrix now changes the flavour of the particles which are scattering. We thus cannot (easily) set up a consistency equation for periodic wave functions. We would like to “diagonalise” the S-matrix. However, there is no universal method to diagonalise a tensor, but this procedure has to be carefully designed for the problem in question:

- Step 1: Consider a new vacuum state

$$|0\rangle^2 = |2_1 2_2 \dots 2_M\rangle^1 := |(p_1, 2), \dots, (p_M, 2)\rangle^1. \quad (4.97)$$

The S-matrix is applied easily to this state because scattering is automatically a plain factor $S_{22}^{22}(p, q)$.

- Step 2: Introduce new types of excitations on the above vacuum

$$|(u, a)\rangle^2 := \sum_{k=1}^M \psi_k(u) |2_1 \dots 2_{k-1} a_k 2_{k+1} \dots 2_M\rangle^1. \quad (4.98)$$

There are now $N - 2$ types of excitations labelled by $a = 3, \dots, N$. The new wave function $\psi_k(u)$ is not a plane wave because the vacuum state $|0\rangle^2$ is not homogeneous. It must be carefully chosen to enable an easy construction of scattering states and thus it depends on all the underlying magnon momenta p_k . We refrain from presenting the details.

- Step 3: Constructing states with two new excitations leads to a new S-matrix S^2 with $(N - 2)^4$ components. This S-matrix has precisely the same form as the previous one but with fewer components.

This procedure is reminiscent of the Bethe ansatz. In terms of states and excitations, we have achieved the following:

$$\begin{array}{ccc}
\text{spins} & & \text{magnons} & & \text{excitations} \\
\begin{array}{c} |1\rangle \\ |2\rangle \\ |3\rangle \\ \vdots \\ |N\rangle \end{array} & \Rightarrow & \begin{array}{c} |2\rangle^1 : |1\rangle \rightarrow |2\rangle \\ |3\rangle^1 : |1\rangle \rightarrow |3\rangle \\ \vdots \\ |N\rangle^1 : |1\rangle \rightarrow |N\rangle \end{array} & \Rightarrow & \begin{array}{c} |3\rangle^2 : |2\rangle \rightarrow |3\rangle \\ \vdots \\ |N\rangle^2 : |2\rangle \rightarrow |N\rangle \end{array}
\end{array} \quad (4.99)$$

The Bethe ansatz singles out the vacuum state $|1\rangle$ and converts all other spin states to magnon excitations $|a\rangle^1 : |1\rangle \rightarrow |a\rangle$ with $a = 2, \dots, N$. The next step singles out one of the magnon excitations $|2\rangle^1 : |1\rangle \rightarrow |2\rangle$ and declares it as a new vacuum. The remaining magnons are obtained as new excitations $|a\rangle^2 : |2\rangle \rightarrow |a\rangle$ of the new vacuum with $a = 3, \dots, N$. The procedure, called the *nested Bethe ansatz* can be iterated $N - 1$ times in total. At the end we are left with

- the vacuum state $|1\rangle$,
- the magnon excitation $|2\rangle^1 : |1\rangle \rightarrow |2\rangle$,
- $N - 2$ higher excitations $|a\rangle^{a-1} : |a-1\rangle \rightarrow |a\rangle$ with $a = 3, \dots, N$.

Importantly, these interactions now all scatter diagonally, so the scattering matrix has been disintegrated into a collection of scattering factors $S^{a,b}(u^a, v^b)$

$$\begin{array}{c}
v^b, b \quad u^a, a \\
\swarrow \quad \searrow \\
\text{---} S \text{---} \\
\nwarrow \quad \nearrow \\
u^a, a \quad v^b, b
\end{array} \quad (4.100)$$

There is no mixing between the various flavours of excitations. It is in fact excluded by conservation of charges of the excitations.

For a given set of excitations, one can construct an eigenstate on the infinite chain. These arise as a sum over all admissible distributions of the excitations. In each

distribution we must stack the excitations on the vacuum sites as towers without gaps:

$$|4, 3, 1, 4, 1, 1, 2\rangle \longrightarrow \begin{array}{ccccccc} 4(u_1^4) & & & 4(u_2^4) & & & \\ 3(u_1^3) & 3(u_2^3) & & 3(u_3^3) & & & \\ 2(u_1^2) & 2(u_2^2) & & 2(u_3^2) & & 2(u_4^2) & \\ |1\rangle & |1\rangle & |1\rangle & |1\rangle & |1\rangle & |1\rangle & |1\rangle \end{array} \quad (4.101)$$

The relative phase factors between two distributions are determined by hopping rules: There is a factor for moving one excitation on top of another excitation from the left or from the right:

$$b(v^b) \xrightarrow{F^{a,b}(u^a, v^b)} b(v^b) \xleftarrow{F^{b,a}(v^b, u^a)} b(v^b) \quad (4.102)$$

$a(u^a)$

This factor $F^{a,b}(u^a, v^b)$ depends on the flavours of the excitations and on their rapidities. Note that moving two excitations past each other yields their scattering factor

$$S^{a,b}(u^a, v^b) = \frac{F^{a,b}(u^a, v^b)}{F^{b,a}(v^b, u^a)}. \quad (4.103)$$

Bethe Equations for Higher Rank. For $SU(N)$, the elements of the diagonalised scattering matrix simply read

$$\begin{aligned} S^{a,a}(u^a, v^a) &= \frac{u^a - v^a - \frac{i}{2}}{u^a - v^a + \frac{i}{2}}, \\ S^{a,a\pm 1}(u^a, v^{a\pm 1}) &= \frac{u^a - v^{a\pm 1} + \frac{i}{2}}{u^a - v^{a\pm 1} - \frac{i}{2}}, \\ S^{a,b}(u^a, v^b) &= 1 \quad \text{for } |a - b| > 1. \end{aligned} \quad (4.104)$$

It is straightforward to set up the Bethe equations for a closed chain. The Bethe equations for the level-1 magnons read

$$\left(\frac{u_k^1 + \frac{i}{2}}{u_k^1 - \frac{i}{2}} \right)^L = \prod_{\substack{j=1 \\ j \neq k}}^{M^1} \frac{u_k^1 - u_j^1 + \frac{i}{2}}{u_k^1 - u_j^1 - \frac{i}{2}} \prod_{j=1}^{M^2} \frac{u_k^1 - u_j^2 - \frac{i}{2}}{u_k^1 - u_j^2 + \frac{i}{2}}. \quad (4.105)$$

The Bethe equations for higher-level excitations take the form

$$1 = \prod_{j=1}^{M^{a-1}} \frac{u_k^a - u_j^{a-1} - \frac{i}{2}}{u_k^a - u_j^{a-1} + \frac{i}{2}} \prod_{\substack{j=1 \\ j \neq k}}^{M^a} \frac{u_k^a - u_j^a + \frac{i}{2}}{u_k^a - u_j^a - \frac{i}{2}} \prod_{j=1}^{M^{a+1}} \frac{u_k^a - u_j^{a+1} - \frac{i}{2}}{u_k^a - u_j^{a+1} + \frac{i}{2}}, \quad (4.106)$$

and the top-level equations read

$$1 = \prod_{j=1}^{M^{N-2}} \frac{u_k^{N-1} - u_j^{N-2} - \frac{i}{2}}{u_k^{N-1} - u_j^{N-2} + \frac{i}{2}} \prod_{\substack{j=1 \\ j \neq k}}^{M^{N-1}} \frac{u_k^{N-1} - u_j^{N-1} + \frac{i}{2}}{u_k^{N-1} - u_j^{N-1} - \frac{i}{2}}. \quad (4.107)$$

The total momentum and energy are expressed as

$$e^{iP} = \prod_{k=1}^{M^1} \frac{u_k^1 + \frac{i}{2}}{u_k^1 - \frac{i}{2}}, \quad E = \sum_{k=1}^{M^1} \left(\frac{\frac{i}{2}}{u_k^1 + \frac{i}{2}} - \frac{\frac{i}{2}}{u_k^1 - \frac{i}{2}} \right). \quad (4.108)$$

Inspecting these equations leads to the following generalisation to arbitrary simple Lie (super)algebras

- The interactions of the Bethe roots (r.h.s. of the Bethe equations) follow the symmetric Cartan matrix DA ²⁵ of the underlying group as

$$S^{a,b}(u^a, v^b) = \frac{u^a - v^b - \frac{i}{2}(DA)_{a,b}}{u^a - v^b + \frac{i}{2}(DA)_{a,b}}. \quad (4.109)$$

The latter is directly encoded into the Dynkin diagram of the corresponding algebra.

For example, for $A_{N-1} \simeq \text{SU}(N)$ the Cartan matrix reads

$$DA = \begin{pmatrix} +2 & -1 & & \\ -1 & \ddots & \ddots & \\ & \ddots & \ddots & -1 \\ & & -1 & +2 \end{pmatrix} \quad (4.110)$$

and the associated Dynkin diagram takes the form:

$$\begin{array}{ccccccc} \bigcirc & \text{---} & \bigcirc & \text{---} & \bigcirc & \text{---} & \cdots & \text{---} & \bigcirc & \text{---} & \bigcirc \\ 1 & & 2 & & 3 & & & & N-2 & & N-1 \end{array} \quad (4.111)$$

- The momentum, energy and propagation of the Bethe roots (l.h.s. of the Bethe equations) follow the Dynkin labels of the underlying spin representation.

These equations have all of the generalisations discussed above: trigonometric deformations, introduction of magnetic fluxes, open chains, higher representations. One can also make the spin chain inhomogeneous while preserving integrability. This can be achieved by a non-homogeneous (and typically non-local) Hamiltonian or by using site-dependent spin representations.

²⁵For the simply-laced groups A, D, E the Cartan matrix A is symmetric and $D = 1$. For the other groups $D = \text{diag}(\dots)$ makes the asymmetric Cartan matrix A symmetric in the product DA .

5 Long Chains

In this chapter we consider the spectrum of the closed Heisenberg spin chain in the limit of large length where combinatorics typically becomes cumbersome. We will use the Bethe equations to investigate the structure of states and their energies at the lower and upper end of the spectrum.

5.1 Magnon Spectrum

The ferromagnetic vacuum $|0\rangle$ (and its $SU(2)$ descendants) with $E = 0$ is the exact ground state for any length L . First, we consider states with a fixed number M of magnons in the limit of long chains $L \rightarrow \infty$ focusing on the states with the lowest energies.

Mode Numbers. Throughout this chapter we shall write the Bethe equations in logarithmic form

$$iL \log \frac{u_k + \frac{i}{2}}{u_k - \frac{i}{2}} - i \sum_{\substack{j=1 \\ j \neq k}}^M \log \frac{u_k - u_j + i}{u_k - u_j - i} + 2\pi n_k = 0. \quad (5.1)$$

For every Bethe equation the logarithm introduces an ambiguity of shifts by integer multiples of $2\pi i$. In order to fix it, we ordinarily assume that the logarithm function has its branch cut along the negative real axis and that the imaginary part ranges between $-\pi$ and $+\pi$. The integers n_k then become characteristic numbers of the solution, they will be called the *mode number* of the associated Bethe root.¹ They range between $-\frac{1}{2}L$ and $\frac{1}{2}L$.

Single Magnons. First, we consider single-magnon states which can be solved exactly. The Bethe equation for the single Bethe root u reduces to

$$iL \log \frac{u + \frac{i}{2}}{u - \frac{i}{2}} + 2\pi n = 0. \quad (5.2)$$

This is solved by

$$u = \frac{1}{2} \cot \frac{\pi n}{L}, \quad p = \frac{2\pi n}{L}, \quad e = 4 \sin^2 \frac{\pi n}{L}. \quad (5.3)$$

¹In the presence of complex Bethe roots the definition of mode numbers is somewhat fuzzy. This is because the arguments of logarithms may come close to the branch cut in which case a minor shift of the Bethe root can imply a shift of mode number by ± 1 whereas the physics is almost the same.

The lowest excitations are obtained for $|n| \ll L$, we shall thus assume that n remains finite while $L \rightarrow \infty$. Then we can approximate the above expressions by

$$u = \frac{L}{2\pi n}, \quad p = \frac{2\pi n}{L}, \quad e = \frac{4\pi^2 n^2}{L^2}. \quad (5.4)$$

We thus learn that the energies and momenta of the lowest states scale as

$$P \sim \frac{1}{L}, \quad E \sim \frac{1}{L^2}. \quad (5.5)$$

Several Magnons. Next we consider the case of several excitations at distinct mode numbers n_k . In this case one may expect the above locations of Bethe roots $u_k = L/2\pi n_k$ to remain valid at leading order with perturbations due to scattering. Indeed, the scattering phase is suppressed at large L due to the u_k being very large

$$-i \log \frac{u_k - u_j + i}{u_k - u_j - i} \approx -i \log \frac{L/2\pi n_k - L/2\pi n_j + i}{L/2\pi n_k - L/2\pi n_j - i} \approx 0. \quad (5.6)$$

The leading-order spectrum of momenta and energies follows immediately from the leading order positions.

So far we have assumed that the n_k are distinct. This would be in agreement with the earlier statement that magnons are fermions for which an exclusion principle should hold. Nevertheless, a valid solution can have several n_k taking the same values as long as the associated u_k do not coincide exactly. Let us therefore make an ansatz for the spacing of the u_k

$$u_k = \frac{L}{2\pi n} + \delta u_k. \quad (5.7)$$

Then the momentum term in the Bethe equation expands as

$$iL \log \left(\frac{u_k + \frac{i}{2}}{u_k - \frac{i}{2}} \right) = -2\pi n + \frac{4\pi^2 n^2}{L} \delta u_k + \mathcal{O}(\delta u_k^2/L^2). \quad (5.8)$$

Analogously, the scattering term of the Bethe equation should be approximately 1 implying $\delta u_k \gg 1$ and the expansion

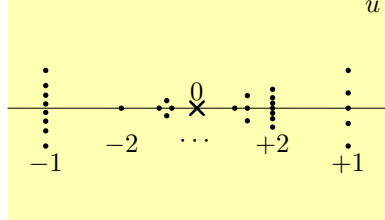
$$-i \log \frac{u_k - u_j + i}{u_k - u_j - i} = \frac{2}{\delta u_k - \delta u_j} + \mathcal{O}(1/\delta u_k^2). \quad (5.9)$$

Substituting both terms we find the equation

$$\frac{4\pi^2 n^2}{L} \delta u_k + \sum_{\substack{j=1 \\ j \neq k}}^M \frac{2}{\delta u_k - \delta u_j} = 0. \quad (5.10)$$

This equation has a purely imaginary solution proportional to the roots of the Hermite polynomials, and one can show that the Bethe roots scale as $\delta u_k \sim \sqrt{L/M}/n$. In particular, this type of correction to the Bethe roots does not alter the expressions for the magnon momenta and energies to leading order. A *stack* of M magnons at a common mode number n carries M times the momentum and energy of a single magnon at this mode number. In other words, one can consider the magnons as bosons in the limit $L \rightarrow \infty$ with M kept finite.

Magnon Spectrum. We have learned that we can have an arbitrary number of magnons at each given mode number. Since the scattering of magnons with different mode numbers is suppressed, the same holds for stacks of different mode numbers because their composite scattering phase is just a finite factor times the scattering phase of the individual magnons. A generic distribution of finitely many Bethe roots at finite mode numbers in the limit of long chains takes the form:


(5.11)

The magnon spectrum to leading order therefore takes a very simple form which depends only on the occupation numbers M_n of magnon stacks at mode number n

$$M = \sum_n M_n, \quad P = \sum_n M_n \frac{2\pi n}{L}, \quad E = \sum_n M_n \frac{4\pi^2 n^2}{L^2}. \quad (5.12)$$

This completes the leading order spectrum of finitely many magnons at finite mode numbers. To obtain more accurate expressions for reasonably large but finite L , one can compute correction terms in $1/L$. These *finite-size corrections* effectively scale as M/L .

5.2 Ferromagnetic Continuum

Based on the above considerations of magnons, we can also contemplate what happens if we take the number of magnons M to be large as we take the limit $L \rightarrow \infty$. These magnons have to be distributed over the mode numbers, and we can either choose to populate large mode numbers with finitely many magnons or finite mode numbers with a large number of magnons. As the energy of magnon states scales as $E \sim Mn^2$, the states with finite mode number and large stacks will have the lower energy, and we shall focus on these states.

We can convince ourselves that the above considerations remain valid as long as $1 \ll M \ll L$. In these cases, the correction terms to all expressions are substantially smaller than the leading terms, and our approximations remain valid. When we take $M \sim L$, however, most of the above approximations break down at the same time. This indicates that something interesting may happen.

Distribution of Bethe Roots. We have already seen that the Bethe roots scale as $u_k \sim L$ in the limit $u \rightarrow \infty$. Moreover, for $M_n \sim L$ we can estimate that the stacks of Bethe roots have length of order L and thus the separation of Bethe roots

should approach a finite value:

(5.13)

To describe the limit $L \rightarrow \infty$, we first rescale $u = \tilde{u}L$. The stacks of Bethe roots are then represented by a set $\mathcal{C} = \bigcup_k \mathcal{C}_k$ of contours \mathcal{C}_k in the complex plane and a density function ρ on \mathcal{C} describing the density of Bethe roots

$$u \rightarrow \tilde{u}L, \quad \sum_k \rightarrow L \int_{\mathcal{C}} d\tilde{u} \rho(\tilde{u}). \quad (5.14)$$

The limit of the Bethe roots is obtained by straight-forward expansion yielding a singular integral equation

$$\mathcal{P} \int_{\mathcal{C}} \frac{2 d\tilde{v} \rho(\tilde{v})}{\tilde{u} - \tilde{v}} - \frac{1}{\tilde{u}} + 2\pi n_k = 0 \quad \text{for } \tilde{u} \in \mathcal{C}_k. \quad (5.15)$$

Note that the integrand has a pole at $\tilde{u} = \tilde{v}$ and $\mathcal{P} \int$ denotes the principal value integral corresponding to the gap in the discrete sum. Similarly, the expressions for the number of magnons in each stack, momentum and energy read

$$M_k = L \int_{\mathcal{C}_k} d\tilde{u} \rho(\tilde{u}), \quad P = \int_{\mathcal{C}} \frac{d\tilde{u} \rho(\tilde{u})}{\tilde{u}}, \quad E = \frac{1}{L} \int_{\mathcal{C}} \frac{d\tilde{u} \rho(\tilde{u})}{\tilde{u}^2}. \quad (5.16)$$

Unlike the case of finitely many magnons, we can observe that now all magnons effectively interact with all others. There are useful mathematical methods to address the above kind of problem of an integral equation with singular kernel in the complex plane, also known as a Riemann–Hilbert problem.

Spectral Curve. We will not go into the details of the solution here, but merely show that the above problem is equivalent to the spectral curve of the Heisenberg magnet discussed previously: To that end, define the quasi-momentum function $q(\tilde{u})$ as

$$q(\tilde{u}) := \int_{\mathcal{C}} \frac{d\tilde{v} \rho(\tilde{v})}{\tilde{v} - \tilde{u}} + \frac{1}{2\tilde{u}}. \quad (5.17)$$

This function is analytic on the complex plane except for the pole at $\tilde{u} = 0$ and discontinuities at the contours \mathcal{C} . Furthermore, it behaves as $q(\tilde{u}) \sim 1/\tilde{u}$ at $\tilde{u} \rightarrow \infty$. The above Bethe equations written in terms of $q(\tilde{u})$ read

$$\lim_{\epsilon \rightarrow 0} [q(\tilde{u} + \epsilon) + q(\tilde{u} - \epsilon)] = 2\pi n_k \quad \text{for } \tilde{u} \in \mathcal{C}_k, \quad (5.18)$$

where the principal value integral $\mathcal{P} \int$ corresponds to the symmetrically regularised evaluation of the function $q(\tilde{u})$. The Bethe equations tell that the

analytic continuation of the function $q(\tilde{u})$ at the contours \mathcal{C} is given by $-q(\tilde{u})$ up to a shift of $2\pi n$. In other words, they ensure that the function $\pm q'(\tilde{u})$ describes an analytic function on a two-sheeted cover of the complex plane, and the contours \mathcal{C} correspond to the branch cuts. Altogether the above properties characterise the spectral curve of the classical Heisenberg magnet. Even more, the expressions for momentum and energy match up to some appropriate rescaling. This shows that the limit $L \rightarrow \infty$ of the Heisenberg spin chain in the ferromagnetic regime yields the Heisenberg magnet.

An interesting corollary of this relationship is that the Heisenberg spin chain can be viewed as a consistent quantisation of the classical Heisenberg magnet.² The parameter $1/L$ then serves as the quantum parameter \hbar . Quantum corrections in $\hbar \sim 1/L$ can be computed from the Bethe equations. For example, one finds that the filling numbers I_k of the spectral curve directly map to the excitation number M_k of the stacks of Bethe roots. Whereas the former are positive real numbers, the latter are quantised as integers. Another related effect which can be computed from the Bethe equations as well as from the spectral curve is the energy shift by introducing one additional magnon into the system.

Hamiltonian Framework. Finally, we would like to show in the Hamiltonian framework that the above continuum limit of the Heisenberg chain yields the Heisenberg magnet. We thus have to convert the quantum mechanical model to a classical one and perform the continuum limit.

The first step consists in taking the expectation value which should behave classically. A spin- $1/2$ state $|S\rangle$ can be prepared by a unit spin vector \vec{S} such that $\langle S|\vec{\sigma}|S\rangle = \vec{S}$.³ The expectation value of some operator \mathcal{X} acting on a spin- $1/2$ state can then be written as

$$\langle \mathcal{X} \rangle_S = \text{Tr} \left[\frac{1}{2} (1 + \vec{S} \cdot \vec{\sigma}) \mathcal{X} \right]. \quad (5.19)$$

We then apply the expectation value to the Hamiltonian kernel

$$\langle \mathcal{H}_{k,l} \rangle_S = \text{Tr}_{k,l} \left[\frac{1}{4} (1 + \vec{S}_k \cdot \vec{\sigma}_k) (1 + \vec{S}_l \cdot \vec{\sigma}_l) (\mathcal{I}_{k,l} - \mathcal{P}_{k,l}) \right] \quad (5.20)$$

$$= \frac{1}{4} \text{Tr} [1 + \vec{S}_k \cdot \vec{\sigma}] \text{Tr} [1 + \vec{S}_l \cdot \vec{\sigma}] \quad (5.21)$$

$$- \frac{1}{4} \text{Tr} [(1 + \vec{S}_k \cdot \vec{\sigma})(1 + \vec{S}_l \cdot \vec{\sigma})] \quad (5.22)$$

$$= \frac{1}{2} - \frac{1}{2} \vec{S}_k \cdot \vec{S}_l. \quad (5.23)$$

We thus find the Hamiltonian of the classical Heisenberg spin chain

$$H = \frac{1}{2} \sum_k (1 - \vec{S}_k \cdot \vec{S}_{k+1}), \quad (5.24)$$

which is a classical integrable model.

²Just as in other discrete quantisations of field theories, continuous translation symmetry is broken in the quantum theory. However the process of quantisation is hardly ever unique and there may be other quantisations of the field theory to preserve such symmetries.

³The classical limit can be achieved by taking the spin representation on each spin site very large in order to make the spin vector behave classically. This insight is useful because it can be applied to the Bethe equations.

Next we perform the continuum limit by putting the spin sites at a spacing ϵ in the coordinate x and taking the limit $\epsilon \rightarrow 0$. The spins S_k are then given by a smooth function $S(x)$ of the coordinate

$$\vec{S}_k = \vec{S}(k\epsilon), \quad (5.25)$$

which also implies that the spins on the chain change very slowly with the position k . The resulting continuum limit of the spin chain Hamiltonian reads

$$H = \frac{1}{\epsilon} \int dx \frac{1}{2} [1 - \vec{S} \cdot (\vec{S} + \epsilon \vec{S}' + \frac{1}{2} \epsilon^2 \vec{S}'' + \dots)] \quad (5.26)$$

$$= -\frac{1}{4} \epsilon \int dx \vec{S} \cdot \vec{S}'' + \dots \quad (5.27)$$

$$= \frac{1}{4} \epsilon \int dx \vec{S}'^2 + \dots \quad (5.28)$$

It agrees with the Hamiltonian of the Heisenberg magnet up to a rescaling. Note that also the commutator of spin operators $\vec{\sigma} \cdot \vec{S}_k$ yields the desired Poisson brackets in the limit.

5.3 Anti-Ferromagnetic Ground State

Next we would like to explore the states of highest energies. Upon flipping the sign of the Hamiltonian, this corresponds to the low-energy regime of the anti-ferromagnetic spin chain, i.e. the anti-ferromagnetic ground state and its excitations. Nevertheless, we shall keep the original sign assignment, and consider the high-energy limit of the ferromagnetic spin chain.

Entanglement. The state of lowest energy is achieved by aligning the spins. Perfect alignment can be achieved for an arbitrary length, and therefore the ferromagnetic ground state has a very simple form. To maximise the energy, two neighbouring spins should have opposite orientation. However, for any pair of spins, there are two such states $|\uparrow\downarrow\rangle$ and $|\downarrow\uparrow\rangle$ and neither of them is an eigenstate of the Hamiltonian kernel. The eigenstates are the entangled states

$$|\uparrow\downarrow\rangle + |\downarrow\uparrow\rangle \quad \text{and} \quad |\uparrow\downarrow\rangle - |\downarrow\uparrow\rangle. \quad (5.29)$$

The former belongs to the same SU(2) triplet as $|\uparrow\uparrow\rangle$ and $|\downarrow\downarrow\rangle$ and it has zero energy. The latter state is an SU(2) singlet and it has energy $E = 2$.

The goal is to entangle as many neighbouring pairs of spins to SU(2) singlets as possible. Unfortunately, three spins cannot be prepared in such a way that two pairs of them are in the desired entanglement. Similarly, a long state of alternating spins $|\dots\uparrow\downarrow\uparrow\downarrow\dots\rangle$ is not an eigenstate of the overall Hamiltonian. Any eigenstate involving such an alternating-spin state will also involve spin configurations such as $|\dots\uparrow\uparrow\downarrow\downarrow\dots\rangle$ or $|\dots\uparrow\downarrow\downarrow\uparrow\dots\rangle$. Consequently, the energy of the anti-ferromagnetic ground state must be less than $2L$. Due to the above considerations, it is virtually impossible to write the state in a closed form for reasonably large L . The Bethe equations, however, allow us to compute the exact energy in the limit $L \rightarrow \infty$.

Bethe Equations. We start again from the logarithmic form of the Bethe equations. We shall assume that all Bethe roots u_k are real in which case we can use the relationship

$$\log \frac{u+i}{u-i} = i\pi \operatorname{sign}(u) - 2i \arctan u. \quad (5.30)$$

Furthermore, we assume the Bethe roots to be ordered with the index k , then the Bethe equations take the form

$$2 \arctan(2u_k) - \frac{2}{L} \sum_{j=1}^M \arctan(u_k - u_j) + \frac{2\pi\tilde{n}_k}{L} = 0. \quad (5.31)$$

The shifted mode numbers $\tilde{n}_k = n_k + k - \frac{1}{2}M - \frac{1}{2} - \frac{1}{2}L \operatorname{sign}(u_k)$ receive contributions from the sign functions and they are integers or half-integers.

The sets of permissible mode numbers n_k obey an interesting statistics in the high energy regime: As usual, they range between $-L/2$ and $+L/2$. The mode number $n_k = 0$ is special, the Bethe equation is always solved by $u_k = \infty$ corresponding to an $SU(2)$ descendant, and it can be occupied several times. All the other mode numbers n_k should be occupied at most once.⁴ Moreover, the neighbours $n_k \pm 1$ of occupied mode numbers should not be occupied. Clearly, not all the states of the Heisenberg chain are of this form because we have restricted to real Bethe roots.⁵

We can now consider the anti-ferromagnetic ground state, i.e. the state of highest energy. The Bethe roots of this state turn out to be all real, so we can access it with the above statistics. We know that we can occupy at most every other mode number, so the maximum number of Bethe roots is $M = \frac{1}{2}L$.⁶ We should not occupy the mode number $n_k = 0$ because it corresponds to $SU(2)$ descendants and because it does not contribute to the energy. Then the only admissible configuration with real Bethe roots is to occupy all odd integers n_k .⁷

$$\begin{array}{cccccccccccccccc} -1 & -3 & -5 & -7 & -9 & -11 & \pm 13 & +11 & +9 & +7 & +5 & +3 & +1 \\ \bullet & \circ & \bullet & \circ & \bullet & \circ & \bullet & \circ & \bullet & \circ & \bullet & \circ & \bullet \end{array} \quad (5.32)$$

The anti-ferromagnetic ground state is thus given by the configuration

$$M = \frac{1}{2}L \quad \text{and} \quad n_k = L\theta_{2k>M} - 2k + 1. \quad (5.33)$$

Consequently, the shifted mode numbers read $\tilde{n}_k = \frac{1}{2}M - k + \frac{1}{2}$.

⁴As in the low-energy spectrum, multiple excitations of a mode number lead to complex Bethe roots. In this regime, complex Bethe roots are typically treated as compounds with spacing $\Delta u \approx i$ (closely related to Bethe strings). The compounds are treated as independent particles with real momenta obeying a somewhat more complicated statistics. We will not need them for the highest-energy state.

⁵The enumeration of states can be continued to complex Bethe roots, where the assignment of the mode numbers becomes somewhat fuzzy.

⁶We assume L to be even; we shall comment on the case of odd L later.

⁷Note that there are many other states with $M = \frac{1}{2}L$, but these have complex Bethe roots or Bethe roots at $u_k = \infty$.

Integral Equations. Now we are ready to address the limit of very long chains, $L \rightarrow \infty$, for which we would like to determine the leading behaviour of the energy. In this limit the Bethe roots approach each other and eventually form a continuum. For the leading behaviour, it is sufficient to describe the continuum by its density $\rho(u)$ of Bethe roots and the corresponding counting function $k(u)$ as follows

$$\rho(u) = \frac{1}{L} \frac{dk}{du}, \quad k(u) = L \int_{-\infty}^u dv \rho(v). \quad (5.34)$$

The resulting Bethe equation can be written immediately by converting the sum to an integral and by substituting $k(u)$

$$0 = 2 \arctan(2u) - 2 \int_{-\infty}^{+\infty} dv \rho(v) \arctan(u - v) - 2\pi \int_{-\infty}^u dv \rho(v) + \frac{1}{2}\pi. \quad (5.35)$$

This integral equation describes the anti-ferromagnetic ground state. The inverse trigonometric functions make it difficult to solve, but we can differentiate w.r.t. u to convert them to rational functions

$$\frac{4}{1+4u^2} - \int \frac{2 dv \rho(v)}{1+(u-v)^2} - 2\pi\rho(u) = 0. \quad (5.36)$$

An important feature of this integral equation is that the integral kernel is of difference form, and hence the equation can be solved by Fourier transformation

$$\rho(u) = \int \frac{d\theta}{2\pi} e^{iu\theta} R(\theta), \quad R(\theta) = \int du e^{-iu\theta} \rho(u). \quad (5.37)$$

Noting the relevant Fourier integral

$$\int \frac{du}{2\pi} \frac{2e^{-iu\theta}}{1+u^2} = e^{-|\theta|}, \quad (5.38)$$

the transformed equation takes a simple form which is readily solved

$$e^{-|\theta|/2} - e^{-|\theta|} R(\theta) - R(\theta) = 0, \quad R(\theta) = \frac{1}{2 \cosh(\frac{1}{2}\theta)}. \quad (5.39)$$

The Fourier transformation of the solution yields the desired density and upon integration the counting function

$$\rho(u) = \frac{1}{2 \cosh(\pi u)}, \quad k(u) = \frac{L}{4} + \frac{L}{\pi} \arctan \tanh(\tfrac{1}{2}\pi u). \quad (5.40)$$

Ground State Properties. We can now compute the characteristic quantities of the anti-ferromagnetic ground state such as energy, momentum and angular momentum. The energy is best computed in Fourier space

$$E = L \int \frac{4 du \rho(u)}{1+4u^2} = L \int d\theta e^{-|\theta|/2} R(\theta) = 2L \ln 2 < 2L. \quad (5.41)$$

By construction the state is parity-invariant, hence its total momentum should be either $P = 0$ or $P = \pi$. Considering the occupied mode numbers n_k one can deduce

$$P = \begin{cases} 0 & \text{for } L \text{ even,} \\ \pi & \text{for } L \text{ odd.} \end{cases} \quad (5.42)$$

Finally, the angular momentum $Q = L/2 - M$ is determined by the number of magnons because there are no Bethe roots at $u_k = \infty$. The state is half-filled and therefore the angular momentum is zero

$$Q = \frac{1}{2}L - M = 0. \quad (5.43)$$

Noting that $M = k(\infty) = LR(0)$, we can also verify from the solution that the z -component of angular momentum vanishes

$$Q_z = M - \frac{1}{2}L = k(\infty) - \frac{1}{2}L = L(R(0) - \frac{1}{2}) = 0 + \mathcal{O}(L^0). \quad (5.44)$$

5.4 Spinons

Next, we shall consider excitations of the anti-ferromagnetic ground state. Sticking to our conventions, the anti-ferromagnetic ground state is the state of highest energy. Therefore, excited states have a lower energy and the excitations carry negative energy. Besides this oddity due to conventions, the so-called *spinon* excitations have some other counter-intuitive features which we shall discuss following their derivation.

Bethe Equations. Excitations of the anti-ferromagnetic ground state correspond to gaps in the sequence of mode numbers. An elementary excitation is a gap of *two* unoccupied mode numbers rather than one. We thus shift all the mode numbers n_k above a certain k by -1 . We shall trace only the changes in the equations and charges due to this gap. The integral equation receives one additional term due to the gap

$$0 = 2 \arctan(2u) - 2 \int_{-\infty}^{+\infty} dv \rho(v) \arctan(u - v) \quad (5.45)$$

$$- 2\pi \int_{-\infty}^u dv \rho(v) + \frac{1}{4}\pi - \frac{\pi}{2L} \text{sign}(u - u_0). \quad (5.46)$$

Note that the modification term is of order $1/L$,⁸ let us consider the variation $\delta\rho$ of the density ρ due to its introduction. As before, we differentiate w.r.t. u and find

$$- \int_{-\infty}^{+\infty} \frac{2 dv \delta\rho(v)}{1 + (u - v)^2} - 2\pi\delta\rho(u) - \frac{2\pi}{L} \delta(u - u_0) = 0. \quad (5.47)$$

⁸This is not the only relevant term of order $1/L$ in the expansion of the equation. However, all correction terms except for the one written above appear in the equation for the ground state as well, and here we want to focus on the changes due to the gap.

Again we can easily find the solution by Fourier transformation

$$\delta R(\theta) = -\frac{1}{L} \frac{e^{|\theta|/2 - iu_0\theta}}{2 \cosh(\frac{1}{2}\theta)}. \quad (5.48)$$

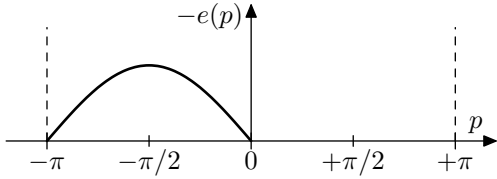
Spinon Properties. The resulting energy shift due to the excitation reads

$$e(u_0) = -\int \frac{d\theta e^{-iu_0\theta}}{2 \cosh(\frac{1}{2}\theta)} = -\frac{\pi}{\cosh(\pi u_0)}. \quad (5.49)$$

The determination of the momentum shift due to the excitation requires some care and extra assumptions.⁹ One finds

$$\begin{aligned} p(u_0) &= L \int du \delta\rho(u) [\pi - 2 \arctan(2u)] \\ &= 2 \arctan \tanh(\tfrac{1}{2}\pi u_0) - \tfrac{1}{2}\pi. \end{aligned} \quad (5.50)$$

When expressing the energy as a function of the momentum, we find the neat dispersion relation

$$e(p) = -\pi \sin(-p). \quad (5.51)$$


A curiosity of the spinon excitation is that the momentum covers only *half* of the Brillouin zone (with boundaries excluded)¹⁰

$$-\pi < p(u_0) < 0. \quad (5.52)$$

A related curiosity is that the shift of angular momentum induced by the excitation is one *half* unit

$$\delta Q_z = L(\delta R(0) - \tfrac{1}{2}) = -\tfrac{1}{2}. \quad (5.53)$$

The latter result appears to be evidently wrong. In analogy to the magnons, one would think that an excitation corresponds to a spin flip. Flipping a spin can only change the overall z -component of the angular momentum by an integer. Paradoxically, the calculation shows that the spinon carries only half a unit of spin. How can this be?

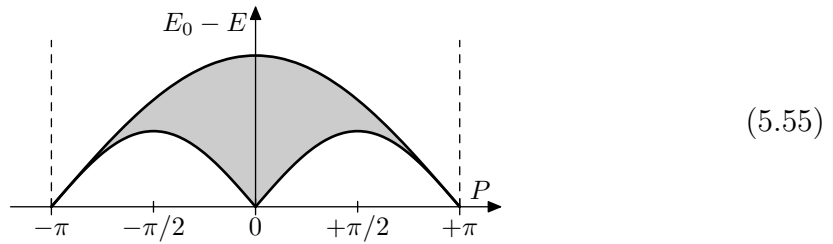
⁹The momentum p_k of each discrete magnon has an ambiguity of 2π which is the same as the ambiguity of the total momentum P . However, we consider a continuous distribution of magnons whose ambiguity is not universal.

¹⁰Whether this is the left or right half of the Brillouin zone will turn out to be merely a matter of convention.

Physical Spinon States. A spinon is not an elementary spin flip, it is a collective excitation of the anti-ferromagnetic ground state. These excitations carry spin $s = 1/2$, hence there is actually a doublet of excitations for each given momentum. Importantly, a spinon cannot exist on its own, it must be accompanied by another spinon in a physical state. Together the two spinons shift the z -component of the angular momentum by ± 1 or 0. Moreover, their overall momentum and energy read

$$P = p_1 + p_2, \quad E = e(p_1) + e(p_2). \quad (5.54)$$

Importantly, the sum of the two spinon momenta now covers the full Brillouin zone symmetrically (for $L \equiv 2 \pmod{4}$):¹¹



This constraint can be understood well by considering the set of occupied mode numbers: If we remove one magnon, this leaves behind a gap of three consecutive numbers. However, the above spinon excitation was constructed as an elementary gap of merely two consecutive numbers. One elementary gap changes the distribution of numbers at either end of the sequence between odd and even numbers. Due to parity considerations, a second gap is unavoidable for a consistent behaviour at both ends.¹² A physical state therefore must always have an even number of elementary gaps whose positions can be chosen arbitrarily, e.g. for $L = 26$ and gaps at $-4/-5$ and $+10/+11$:

$$\begin{array}{cccccccccccccccccccccccccccc} -1 & -3 & & -6 & -8 & -10 & -12 & +12 & & +9 & +7 & +5 & +3 & +1 \\ \bullet & \circ & \bullet & \circ & \circ & \bullet & \circ & \bullet & \circ & \bullet & \circ & \bullet & \circ & \circ & \bullet & \circ & \bullet & \circ & \bullet & \circ & \bullet & \circ & \bullet & \circ & \bullet \end{array} \quad (5.56)$$

Each elementary gap corresponds to one spinon. In this picture, longer gaps correspond to a collection of spinons at nearby momenta.

The important conclusion to draw is that the elementary excitations of the anti-ferromagnetic vacuum is the spin- $1/2$ spinon with an individual momentum. This picture is consistent under the constraint that the number of spinons must be even on a chain of even length.

Odd Length. The picture is slightly different for chains of odd length. In this case, there is no perfect sequence of mode numbers connecting both ends. Here, there must be an *odd* number of elementary gaps. The anti-ferromagnetic vacuum

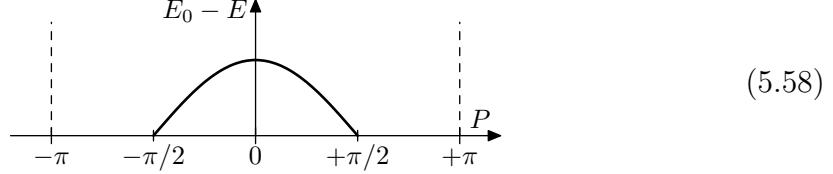
¹¹The three bounding curves are obtained by setting $p_1 = 0$, $p_1 = -\pi$ or $p_1 = p_2$.

¹²A sequence ending with an even number should be viewed as another elementary gap right at the end.

itself is not a proper physical state, it needs to be accompanied by at least one spinon, e.g. for $L = 25$ and a gap at $-4/-5$

$$\begin{array}{cccccccccccccccc} -1 & -3 & & -6 & -8 & -10 & -12 & +11 & +9 & +7 & +5 & +3 & +1 \\ \bullet & \circ & \bullet & \circ & \circ & \bullet & \circ & \bullet & \circ & \bullet & \circ & \bullet & \circ & \bullet & \circ & \bullet & \circ & \bullet \end{array} \quad (5.57)$$

The spectrum of one-magnon states takes the form (for $L \equiv 1 \pmod{4}$):



In order to maximise the energy, the momentum of the spinon should be close to $p = 0$ or $p = -\pi$. This means that there are two doublets of anti-ferromagnetic ground states of energy slightly away from the vacuum energy $E = 2L \ln 2$. The momentum of the anti-ferromagnetic vacuum state without any spinon can be inferred from the chain of mode numbers as

$$P \equiv \frac{1}{2}\pi L \pmod{2\pi}. \quad (5.59)$$

The momenta of the two doublets of anti-ferromagnetic ground states at odd length are therefore $P \approx \pm \frac{1}{2}\pi$.

Spinon Scattering. So far we have computed the properties of an individual spinon, but we have not yet considered the permissible distributions of spinon momenta on a closed chain. The spinons can be considered honest excitations of a ground state in direct analogy to the magnons on top of the ferromagnetic vacuum. Therefore, their admissible momenta can be determined by a suitable set of Bethe equations. In order to set it up, one needs the scattering matrix of spinons. We will not derive it but merely state the final result

$$\begin{aligned} \mathcal{S}(u_k, u_j) = & \frac{\Gamma\left(1 - \frac{i}{2}(u_k - u_j)\right) \Gamma\left(\frac{1}{2} + \frac{i}{2}(u_k - u_j)\right)}{\Gamma\left(1 + \frac{i}{2}(u_k - u_j)\right) \Gamma\left(\frac{1}{2} - \frac{i}{2}(u_k - u_j)\right)} \\ & \cdot \left[\frac{u_k - u_j}{u_k - u_j + i} \mathcal{I} + \frac{i}{u_k - u_j + i} \mathcal{P} \right]. \end{aligned} \quad (5.60)$$

Here the rapidity parameters u_k are related to the particle momenta p_k by the inverse of the above relationship

$$u_k = \frac{2}{\pi} \operatorname{artanh} \tan\left(\frac{1}{2}p_k + \frac{1}{4}\pi\right). \quad (5.61)$$

Note that the spinon scattering matrix is the same as the scattering matrix of the coordinate Bethe ansatz for a chain with $\mathrm{SU}(3)$ symmetry up to the prefactor.

5.5 Spectrum Overview

We finish this chapter with an overview of the spectrum at large length L . The ferromagnetic ground state has zero energy (by construction), zero momentum and maximum spin

$$E = 0, \quad P = 0, \quad Q = \frac{1}{2}L. \quad (5.62)$$

The spectrum of finitely many magnon excitations of the ferromagnetic vacuum takes the form

$$E = \sum_n M_n \frac{4\pi^2 n^2}{L^2}, \quad P = \sum_n M_n \frac{2\pi n}{L}, \quad Q = \frac{1}{2}L - \sum_n M_n. \quad (5.63)$$

When the number of magnons becomes very large and scales as $M \sim L$, one finds trajectories of states with the following scaling behaviour

$$E \sim \frac{1}{L}, \quad -\pi < P \leq \pi, \quad Q \sim L, \quad (5.64)$$

which are described by the classical Heisenberg magnet. In fact the classical solutions serve as accumulation points of quantum states. The spectrum of quantum excitations around these is reminiscent of the above magnon spectrum.

The top of the spectrum is described by the anti-ferromagnetic ground state(s)

$$E = E_0 = 2L \ln 2, \quad P \equiv \frac{\pi}{2} L, \quad Q = 0. \quad (5.65)$$

The spectrum of spinon excitations below the anti-ferromagnetic ground state(s) for small momenta takes the form

$$E_0 - E = \sum_k \frac{2\pi^2 |n_k|}{L}, \quad P = \pi \mathbb{Z} + \sum_k \frac{2\pi n_k}{L}, \quad Q \leq \sum_k \frac{1}{2}. \quad (5.66)$$

For larger spinon momenta one finds a spectrum of the form

$$E_0 - E \sim 1, \quad -\pi < P \leq \pi, \quad Q \sim 1. \quad (5.67)$$

Note that the latter spinons probe the whole of the Brillouin zone, whereas the stacks of magnons remain at very small momenta. In other words, the above regions near the anti-ferromagnetic ground state preserve the discreteness of the spin chain, whereas the regions near the ferromagnetic ground state are described well by a continuum model.

For intermediate energies $1/L \ll E \ll 2L \ln 2$ the Bethe equations provide the exact quantum spectrum of the model, but not too much insight into the qualitative distribution of the vast majority of the 2^L eigenstates.

6 Quantum Integrability

Next we would like to discuss a formalism to deal with a large class of quantum integrable systems. One of the main tools, the quantum analog of the inverse scattering method, is based on this formalism.

6.1 R-Matrix Formalism

In the nested Bethe ansatz we have started with an $SU(N)$ fundamental spin chain, and reduced it at various levels $k = 1, \dots, N - 1$ to excitations with $SU(N - k)$ residual symmetry. An interesting observation is that in every step we obtained a scattering matrix of the same form

$$S_{ab}^{cd}(u, v) = \frac{(u - v)\delta_a^c \delta_b^d + i\delta_a^d \delta_b^c}{u - v - i}, \quad (6.1)$$

where the indices $a, b, c, d = k + 1, \dots, N$ could take $N - k$ values. Furthermore we obtained the same S-matrix for the scattering of spinons with two spin degrees of freedom up to an overall functional factor.

Since nothing much changed in each step of the nested Bethe ansatz, we can take a step backwards from the first level and consider the so-called *R-matrix*

$$R_{ab}^{cd}(u, v) = \frac{(u - v)\delta_a^c \delta_b^d + i\delta_a^d \delta_b^c}{u - v + i}, \quad (6.2)$$

where $a, b, c, d = 1, \dots, N$. This matrix enjoys the full $SU(N)$ symmetry of the spin chain as well as a couple of features to be discussed below which make it ideally suited for the construction and investigation of quantum integrable models. It differs from the above scattering matrices by an overall functional prefactor of $(u - v - i)/(u - v + i)$ which will be largely inconsequential but convenient for our purposes.

R-Matrix Notations. Before we discuss the properties of R-matrices which come to use in the construction of integrable systems we shall introduce some notation for combining R-matrices which is very helpful for working out identities.

The R-matrix is a linear operator acting on the tensor square of the vector space $\mathbb{V} = \mathbb{C}^N$

$$\mathcal{R} : \mathbb{V} \otimes \mathbb{V} \rightarrow \mathbb{V} \otimes \mathbb{V}. \quad (6.3)$$

Moreover, it depends on one complex parameter associated to each of the two vector spaces, $\mathcal{R} = \mathcal{R}(u, v)$. Here it makes sense to also allow the point at infinity

$u, v = \infty$ as a parameter value. In fact, the R-matrix depends only on the difference of these parameters $\mathcal{R}(u, v) = \mathcal{R}(u - v)$, but we will hardly make use of this feature.

More concretely, the R-matrix takes the form

$$\mathcal{R}(u, v) = \frac{(u - v)\mathcal{I} + i\mathcal{P}}{u - v + i}, \quad (6.4)$$

where \mathcal{I} and \mathcal{P} denote the identity and permutation operators acting on $\mathbb{V} \otimes \mathbb{V}$. Note that the vector space \mathbb{V} is a representation space of the Lie group $\text{SU}(N)$, and the R-matrix is symmetric under the canonical action of $\text{SU}(N)$ on the tensor product $\mathbb{V} \otimes \mathbb{V}$.

Introducing a basis $\{E^a\}$ for the vector space \mathbb{V} and a dual basis $\{E_a\}$ for \mathbb{V}^* we can decompose the R-matrix into components \mathcal{R}_{ab}^{cd} ,

$$\mathcal{R} = (E^a \otimes E^b) R_{ab}^{cd} (E_c \otimes E_d). \quad (6.5)$$

In that sense, the R-matrix is actually a tensor of rank 4 with N^4 components (most of which are zero).¹ The components read

$$R_{ab}^{cd}(u, v) = \frac{(u - v)\delta_a^c \delta_b^d + i\delta_a^d \delta_b^c}{u - v + i}. \quad (6.6)$$

They are formulated in terms of Kronecker symbols δ_b^a which are invariant under $\text{SU}(N)$ by construction.

Let us now introduce an abbreviated symbolic and a graphical notation to deal with operators acting on tensor products of vector spaces \mathbb{V} such as the R-matrix. In order to distinguish the vector spaces within the tensor product, each space receives a label \mathbb{V}_k .

In the symbolic notation, some operator $\mathcal{X}_{k,\dots,m}$ acts linearly on a tensor product of spaces

$$\mathcal{X}_{k,\dots,m} : \mathbb{V}_k \otimes \dots \otimes \mathbb{V}_m \rightarrow \mathbb{V}_k \otimes \dots \otimes \mathbb{V}_m. \quad (6.7)$$

This operator can also act on a tensor product with additional vector spaces, in which case it is assumed to act on the latter as the identity. For example, $\mathcal{X}_{23} := \mathcal{I}_1 \otimes \mathcal{X}_{23}$ when acting on $\mathbb{V}_1 \otimes \mathbb{V}_2 \otimes \mathbb{V}_3$ and $\mathcal{X}_{23} := \mathcal{I}_1 \otimes \mathcal{X}_{23} \otimes \mathcal{I}_4$ when acting on $\mathbb{V}_1 \otimes \mathbb{V}_2 \otimes \mathbb{V}_3 \otimes \mathbb{V}_4$.

The R-matrix acts on a pair of spaces $\mathbb{V}_k, \mathbb{V}_l$ with associated parameters u_k, u_l . A useful shorthand notation is

$$\mathcal{R}_{k,l} := \mathcal{R}_{k,l}(u_k, u_l) : \mathbb{V}_k \otimes \mathbb{V}_l \rightarrow \mathbb{V}_k \otimes \mathbb{V}_l. \quad (6.8)$$

The short notation is sufficient because the parameters are linked tightly to the spaces.

¹The term “matrix” refers to the fact that the R-matrix is a linear operator and can thus be written as a matrix. Often, R-matrices are written in $N^2 \times N^2$ matrix notation where the two ingoing and two outgoing indices are (implicitly) combined into a composite index.

In the graphical notation an operator is represented by some blob which has one ingoing and one outgoing leg for each vector space it acts upon. The R-matrix therefore has the following graphical representation:

$$\text{Diagram of } \mathcal{R} = \frac{u-v}{u-v+i} \text{ (crossing)} + \frac{i}{u-v+i} \text{ (parallel lines)} \quad (6.9)$$

Each vector space has an associated parameter which is displayed next to the corresponding legs. The lines without operator blobs represent Kronecker symbols δ_b^a which are combined into identity or permutation operators, respectively.

Note that the R-matrix flips the ordering of the two legs in the graphical notation, whereas in the symbolic notation the ordering of the constituent vector spaces remains formally unchanged. It makes sense to consider the R-matrix as an operator which encodes the permutation of two vector spaces. Therefore, within a tangle of lines, one would expect to find an R-matrix at every intersection of two lines.

The above notations allow to conveniently combine operators acting on tensor products of vector spaces. For instance we can write or draw²

$$\mathcal{R}_{13}\mathcal{R}_{23} = \text{Diagram of two R-matrices} \quad (6.10)$$

In components these expressions represent the combination

$$R_{ag}^{df}(u, w)R_{bc}^{eg}(v, w). \quad (6.11)$$

Note that the parameter w associated to \mathbb{V}_3 becomes an argument to both involved R-matrices.

Properties of R-Matrices. The defining property of R-matrices is the Yang–Baxter equation

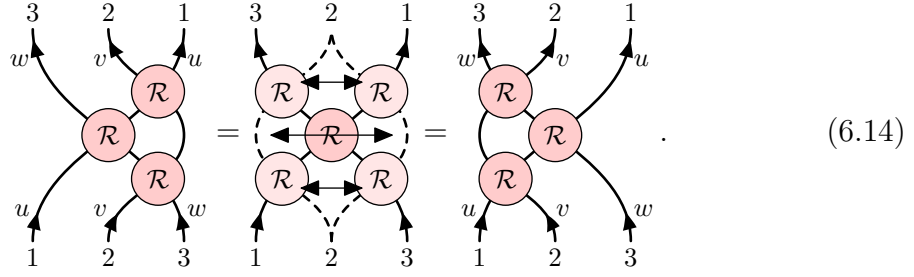
$$\mathcal{R}_{12}(u, v)\mathcal{R}_{13}(u, w)\mathcal{R}_{23}(v, w) = \mathcal{R}_{23}(v, w)\mathcal{R}_{13}(u, w)\mathcal{R}_{12}(u, v). \quad (6.12)$$

In the context of the scattering matrix, this property is a prerequisite for factorised scattering. More concisely, the YBE can be written as

$$\mathcal{R}_{12}\mathcal{R}_{13}\mathcal{R}_{23} = \mathcal{R}_{23}\mathcal{R}_{13}\mathcal{R}_{12}. \quad (6.13)$$

²There is some ambiguity in associating the flow of arrows to the order of multiplication of operators, and whether the latter is naturally from right to left or left to right. At the end of the day both choices are equivalent, but one has to stick to one convention. We shall assume the operators to be ordered from right to left along the flow of arrows.

The graphical representation of the YBE takes an inspiring form



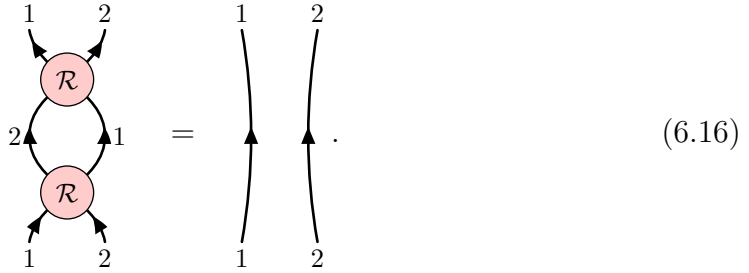
$$(6.14)$$

When considering a tangle of lines with the appropriate R-matrices at each intersection, the YBE allows us to shift one strand past an intersection of two other strands. As the figures show, the order of the R-matrices is inverted by such an operation.

Another important property is that \mathcal{R}_{21} is the inverse of \mathcal{R}_{12}

$$\mathcal{R}_{21}\mathcal{R}_{12} = \mathcal{I}. \quad (6.15)$$

The graphical representation for the above property tells us that we can remove a double crossing of two strands and pull them straight



$$(6.16)$$

Note that for $\mathcal{R}_{12} = \mathcal{R}_{12}(u, v)$ the operator \mathcal{R}_{21} is defined as

$$\mathcal{R}_{21} := \mathcal{R}_{21}(v, u) = \mathcal{P}_{12}\mathcal{R}_{12}(v, u)\mathcal{P}_{12} = \frac{(u - v)\mathcal{I} - i\mathcal{P}}{u - v - i}. \quad (6.17)$$

The combination of the above two rules leads to an interesting structure

$$\mathcal{R}_{12}\mathcal{R}_{13}\mathcal{R}_{23} = \mathcal{R}_{23}\mathcal{R}_{13}\mathcal{R}_{12}, \quad \mathcal{R}_{12}\mathcal{R}_{21} = \mathcal{I}. \quad (6.18)$$

These are in fact the defining relations of the permutation group, where $\mathcal{R}_{k,l}$ represents a pairwise permutation between two elements labelled k and l . This feature allows to use R-matrices as the pairwise scattering matrix for a factorised scattering problem because for every permutation there is a unique combination of pairwise R-matrices up to identities. For a tangle of lines, the above identities imply that only the permutation between the ingoing and outgoing vector spaces matters. In other words, lines can be deformed at will as long as at every crossing an R-matrix is inserted.

In addition, there are two properties related to special points which will be useful for the construction of integrable systems.

When both parameters are the same, $u = v$, the R-matrix becomes the permutation

$$\mathcal{R}(u, u) = \mathcal{P}, \quad \begin{array}{c} \begin{array}{ccc} 2 & & 1 \\ & \swarrow & \searrow \\ & \mathcal{R} & \\ & \swarrow & \searrow \\ 1 & & 2 \end{array} \end{array} = \begin{array}{c} \begin{array}{ccc} 2 & & 1 \\ & \uparrow & \downarrow \\ & & \\ & \downarrow & \uparrow \\ 1 & & 2 \end{array} \end{array}. \quad (6.19)$$

In the scattering context, this identity implies identical particles.

For the class of rational R-matrices the points $u = \infty$ or $v = \infty$ are also special. Here the R-matrix trivialises to the identity

$$\mathcal{R}(u, \infty) = \mathcal{R}(\infty, v) = \mathcal{I}, \quad (6.20)$$

or graphically

$$\begin{array}{c} \begin{array}{ccc} 2 & & 1 \\ & \swarrow & \searrow \\ & \mathcal{R} & \\ & \swarrow & \searrow \\ \infty & & \infty \\ u & & u \\ 1 & & 2 \end{array} \end{array} = \begin{array}{c} \begin{array}{ccc} 2 & & 1 \\ & \swarrow & \searrow \\ & \mathcal{R} & \\ & \swarrow & \searrow \\ \infty & & \infty \\ v & & v \\ 1 & & 2 \end{array} \end{array} = \begin{array}{c} \begin{array}{ccc} 2 & & 1 \\ & \swarrow & \searrow \\ & & \\ & \swarrow & \searrow \\ 1 & & 2 \end{array} \end{array}. \quad (6.21)$$

In the scattering context, this identity relates a magnon at zero momentum to a symmetry of the system.

R-Matrix Generalisations. Note that the above R-matrix is one of the simplest ones that exist; there are many much more elaborate generalisations. Let us summarise a few of them briefly which share most of the above properties:

- The space \mathbb{V} can be replaced by different representation spaces potentially of a different Lie group.
- The above R-matrix has no parameters beyond those associated to the two vector spaces. Most R-matrices allow for several globally defined deformation parameters. These deformation parameters may alter or spoil the properties associated to the special point $u, v = \infty$.
- Our R-matrix was defined on the tensor square of the space \mathbb{V} . R-matrices can also be defined for tensor products of inequivalent spaces $\mathbb{V}_k, \mathbb{V}_k$. In this case many of the discussed properties only hold when introducing one R-matrix for each pair of admissible spaces. Alternatively, one could consider the direct sum of all admissible vector spaces with a single R-matrix acting on the tensor square.
- We considered the case where every vector space has one associated parameter. Generalisations of this concept involve several (or no) parameters associated to a vector space.
- The R-matrix considered above depends on the difference of its two parameters. Most known examples obey such a difference form. There are, however, notable exceptions where the R-matrix is not of difference form (even after taking into account reparametrisations discussed below).

- One can apply a map $u \mapsto f(u)$ to the parameters of \mathcal{R} without spoiling most of the properties discussed above (the location of the special points evidently changes). For example, our S-matrix was initially given in terms of momenta p, q instead of rapidities u, v . The difference property, however, singles out a preferred choice of parameters.
- For most purposes, the overall normalisation of the R-matrix does not matter. For instance, one often considers polynomial R-matrices where the denominator of our R-matrix was removed. Such extra factors modify some of the above relations slightly. For instance, $\mathcal{R}_{21}\mathcal{R}_{12}$ will equal the identity merely up to some overall factor.

6.2 Charges

In the following we shall construct a class of quantum operators acting on the spin chain based on the above R-matrix.

Monodromy and Transfer Matrices. In classical field theory, we introduced the Lax connection as a formulation of integrability. For spin chains, however, space is discrete and states are quantum. Therefore, a Lax connection is not applicable; it is replaced by the *Lax operator*. The Lax operator can be understood as the parallel transport of the Lax connection past one site of the spin chain which is the minimum meaningful distance in this model. Moreover, the Lax operator is a matrix-valued quantum operator, rather than a matrix-valued function of phase space. As such it acts on two spaces, the state of the spin site as well as the auxiliary space of the matrix. Lax matrices satisfy a number of properties related to integrability which are practically the same as those of R-matrices introduced above. Therefore we shall always refer to Lax operators as R-matrices.³

Next let us now consider the spin chain as a whole. We assume that the chain has closed boundary conditions. Using the above analogy with classical field theory, the monodromy matrix $\mathcal{T}(u)$ for the spin chain (which describes half of the Lax pair) is pieced together from an R-matrix for each site

$$\mathcal{T}_a(u) = \mathcal{R}_{a,L}\mathcal{R}_{a,L-1}\dots\mathcal{R}_{a,2}\mathcal{R}_{a,1}. \quad (6.22)$$

In graphical notation the monodromy matrix reads

$$a \xrightarrow{u} \text{oval } \mathcal{T}(u) \xrightarrow{u} a = a \xrightarrow{u} \text{circle } \mathcal{R} \xrightarrow{\text{circle } \mathcal{R}} \text{circle } \mathcal{R} \xrightarrow{\text{circle } \mathcal{R}} \text{circle } \mathcal{R} \xrightarrow{u} a. \quad (6.23)$$

The monodromy matrix $\mathcal{T}_a(u)$ is a matrix of operators which act on the Hilbert space of the quantum spin chain. Note that the parameter $u = u_a$ is associated to

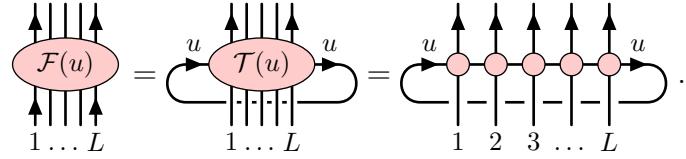
³An inconsequential prefactor for R-matrices is often chosen to eliminate the denominator and make the Lax operator a polynomial in u . Moreover, the parameter v corresponding to the spin chain sites is typically fixed to some value.

the auxiliary space \mathbb{V}_a on which the matrix acts (i.e. the space of the classical Lax pair). The parameters v_k associated to the spin sites are fixed to some values. Since we are interested in *homogeneous* spin chain models we choose all parameters to be equal, conveniently $v_k = 0$.⁴

It is now straight-forward to construct charges in involution as the trace of the monodromy matrix

$$\mathcal{F}(u) = \text{tr}_a \mathcal{T}_a(u). \quad (6.24)$$

This so-called transfer matrix $\mathcal{F}(u)$ can be written graphically as⁵

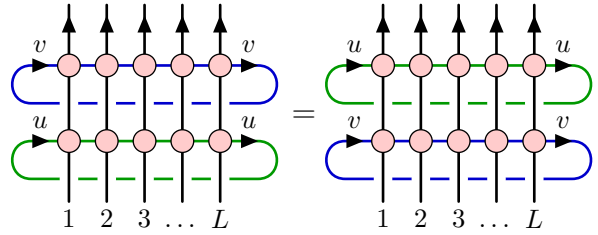


$$\mathcal{F}(u) = \text{tr}_a \mathcal{T}_a(u) = \text{tr}_a \left(\begin{array}{c} \text{---} u \text{---} \\ \text{---} \end{array} \right) = \text{tr}_a \left(\begin{array}{c} \text{---} u \text{---} \\ \text{---} \end{array} \right). \quad (6.25)$$

Two transfer matrices commute at arbitrary spectral parameters u, v

$$[\mathcal{F}(u), \mathcal{F}(v)] = 0. \quad (6.26)$$

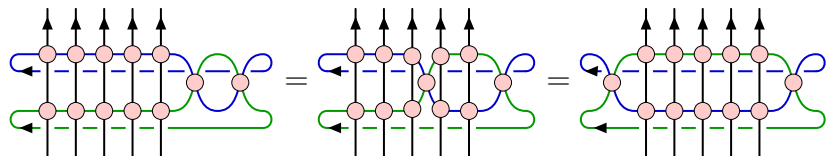
To see this is quite evident in graphical notation where we need to show the following equality



$$\begin{array}{c} \text{---} v \text{---} \\ \text{---} u \text{---} \end{array} = \begin{array}{c} \text{---} u \text{---} \\ \text{---} v \text{---} \end{array}. \quad (6.27)$$

We have already learned that we can deform the lines and move them past others lines and intersections. This allows to move the upper loop past the lower loop and thus switch their ordering.

A symbolic proof is also straight-forward, but requires several steps which are not as easy to spot in a long sequence of symbols. The first step is to let the two loops overlap somewhere by inserting an R-matrix and its inverse. The next step consists in pulling the upper loop below the lower loop past all intersections along the spin chain. In a final step the R-matrix and its inverse are removed by pulling the loops apart. These three steps look as follows



$$\begin{array}{c} \text{---} v \text{---} \\ \text{---} u \text{---} \end{array} = \begin{array}{c} \text{---} v \text{---} \\ \text{---} u \text{---} \end{array} = \begin{array}{c} \text{---} u \text{---} \\ \text{---} v \text{---} \end{array}. \quad (6.28)$$

⁴An *inhomogeneous* spin chain with $v_k \neq v_l$ is integrable as well and can be treated with minor modifications.

⁵Since the chain is periodic, the lines should be drawn on the surface of a cylinder. The loop can thus be closed without introducing further crossings.

Local Charges. Next we have to define a suitable Hamiltonian for the system. This should be constructed out of the transfer matrix $\mathcal{F}(u)$ such that it automatically commutes with the transfer matrices $\mathcal{F}(v)$ at arbitrary values v . We shall see that the expansion around the point $u = 0$ (which coincides with the values of the parameters v_k associated to the spin sites) is perfectly suited for this purpose.

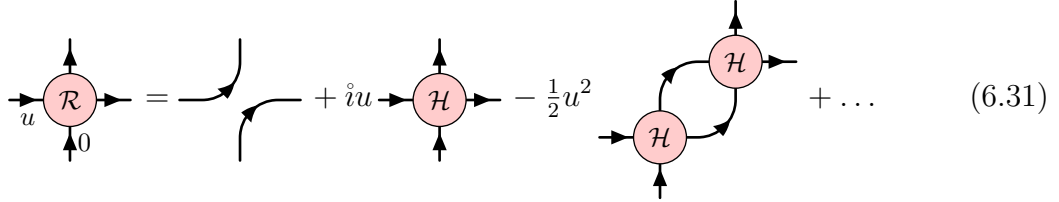
Let us therefore expand the R-matrix around the point $u = 0$ with fixed $u_k = 0$. We find

$$\mathcal{R}_{a,k}(u, 0) = \mathcal{P}_{a,k} + iu\mathcal{P}_{a,k}\mathcal{H}_{a,k} - \frac{1}{2}u^2\mathcal{P}_{a,k}\mathcal{H}_{a,k}^2 + \dots \quad (6.29)$$

with the Hamiltonian kernel of the Heisenberg XXX model or its generalisation to the $SU(N)$ fundamental spin chain

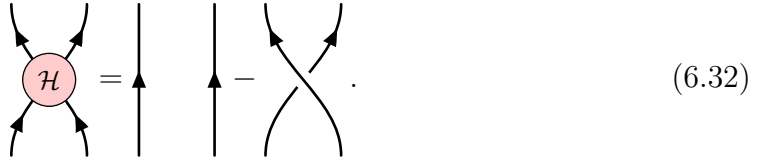
$$\mathcal{H}_{k,l} = \mathcal{I}_{k,l} - \mathcal{P}_{k,l}. \quad (6.30)$$

In a graphical notation the expansion can be written as



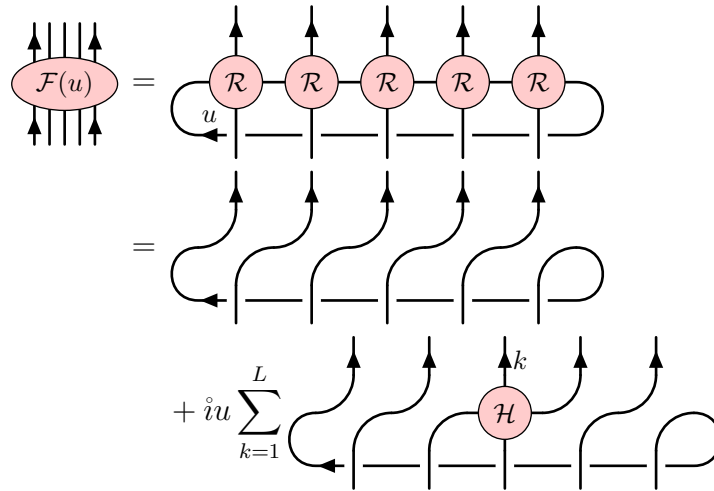
$$\mathcal{R}(u) = \text{crossing} + iu\mathcal{H} - \frac{1}{2}u^2 \text{H-loop} + \dots \quad (6.31)$$

with the Hamiltonian kernel taking the form⁶



$$\mathcal{H} = \text{parallel lines} - \text{crossing} \quad (6.32)$$

Now we can expand the transfer matrix $\mathcal{F}(u)$ around the point $u = 0$. Up to second order we find



$$\mathcal{F}(u) = \text{chain of } \mathcal{R} = \text{chain of } \mathcal{R} + iu \sum_{k=1}^L \text{chain of } \mathcal{R} \text{ with } \mathcal{H} \text{ at } k$$

⁶We use a different convention to for the R-matrix and kernels of local operators: The R-matrix is located at the intersection of two crossing lines, whereas the Hamiltonian joins two lines which do not cross. This implies a different ordering for the external legs.

$$\begin{aligned}
& -u^2 \sum_{\substack{k < l=1 \\ |k-l| > 1}}^L \text{Diagram 1} \\
& -u^2 \sum_{k=1}^L \text{Diagram 2} \\
& -\frac{1}{2}u^2 \sum_{k=1}^L \text{Diagram 3} \\
& + \dots
\end{aligned} \tag{6.33}$$

Diagram 1: A chain of four vertical lines. The second and fourth lines have a red circle labeled \mathcal{H} with an upward arrow labeled k and l respectively. Curved lines connect the first to second, second to third, and third to fourth lines, with arrows indicating a cyclic shift.

Diagram 2: A chain of four vertical lines. The second and third lines have a red circle labeled \mathcal{H} with upward arrows labeled k and $k+1$ respectively. Curved lines connect the first to second, second to third, and third to fourth lines, with arrows indicating a cyclic shift.

Diagram 3: A chain of four vertical lines. The second line has a red circle labeled \mathcal{H}^2 with an upward arrow labeled k . Curved lines connect the first to second, second to third, and third to fourth lines, with arrows indicating a cyclic shift.

Let us discuss the arising terms one at a time:

The leading term describes a cyclic shift \mathcal{U} of the closed chain

$$\text{Diagram 4} = \text{Diagram 5} \tag{6.34}$$

Diagram 4: A red oval labeled \mathcal{U} with four vertical lines passing through it, each with an upward arrow.

Diagram 5: Four curved lines representing a cyclic shift, with arrows indicating the direction of the shift.

Also the sub-leading terms are cyclic shift operations for most of the legs, so it makes sense to factor out the operator \mathcal{U} .

We denote the term at linear order in u by $-iu\mathcal{U}\mathcal{H}$. The operator \mathcal{H} is in fact the Hamiltonian given by a homogeneous sum of Hamiltonian kernels around the closed chain

$$\text{Diagram 6} = \sum_{k=1}^L \text{Diagram 7} \tag{6.35}$$

Diagram 6: A red oval labeled \mathcal{H} with four vertical lines passing through it, each with an upward arrow.

Diagram 7: A diagram showing a vertical line with an upward arrow, followed by a red circle labeled \mathcal{H} with two curved lines passing through it, labeled k and $k+1$ with upward arrows, followed by another vertical line with an upward arrow.

The term on the next line contains two insertions of the Hamiltonian kernels at arbitrary non-overlapping positions of the spin chain. All of these terms are generated by the square of the Hamiltonian $-\frac{1}{2}u^2\mathcal{U}\mathcal{H}^2$. However, one has to pay attention to the terms where two kernels overlap: The terms where two kernels are inserted at the same location is covered precisely by the last line. The second but last line describes terms where the insertions are shifted by one site. Those terms arise in \mathcal{H}^2 , but only with half of the coefficient. Conversely, there are further terms in \mathcal{H}^2 where the order of insertions is flipped. We summarise these additional and missing terms in the operator

$$\text{Diagram 8} = \sum_{k=1}^L \text{Diagram 9} \tag{6.36}$$

Diagram 8: A red oval labeled \mathcal{F}_3 with four vertical lines passing through it, each with an upward arrow.

Diagram 9: A diagram showing a vertical line with an upward arrow labeled $k-1$, followed by a red circle labeled \mathcal{F}_3 with two curved lines passing through it, labeled k and $k+1$ with upward arrows, followed by another vertical line with an upward arrow.

It is a local operator with kernel that acts on next-to-nearest neighbours

$$\mathcal{F}_3 = \frac{i}{2} \mathcal{H} \mathcal{H} - \frac{i}{2} \mathcal{H} \mathcal{H} . \quad (6.37)$$

In formulas we can write this kernel as

$$\mathcal{F}_{3;k,l,m} = \frac{i}{2} [\mathcal{H}_{l,m}, \mathcal{H}_{k,l}]. \quad (6.38)$$

Altogether we find that the expansion is written nicely as an exponential

$$\mathcal{F}(u) = \mathcal{U} \exp(iu\mathcal{H} + iu^2\mathcal{F}_3 + \dots). \quad (6.39)$$

The operators \mathcal{F}_r in the exponent have the relevant property of being *local*. In fact, their kernels extend over an extended range of r sites. In particular, the first operator \mathcal{F}_2 in this tower is the Hamiltonian $\mathcal{F}_2 = \mathcal{H}$. Commutativity of the transfer matrices $\mathcal{F}(u)$ and $\mathcal{F}(v)$ at arbitrary values u, v leads to the involution property

$$[\mathcal{F}_r, \mathcal{F}_s] = 0. \quad (6.40)$$

We have thus constructed a tower of commuting local operators.

Locality of the integrable charges is a crucial feature for at least two reasons:

- For a Hilbert space of dimension N there always exist $N - 1$ commuting independent operators which also commute with a given Hamiltonian: In a basis where the Hamiltonian is diagonal, these are the remaining independent diagonal matrices. Since this construction does not rely on any special properties of the physical system, it can hardly be useful. In order to be useful, quantum integrability must require further properties for the commuting charges such as locality.
- In the magnon scattering picture, local charges act on the magnons individually provided that the latter are sufficiently well separated. For a state of m magnons, m local commuting charges are needed to guarantee that the momenta are individually conserved. Since the local charges do not distinguish the ordering of magnons along the chain, there are $m!$ partial eigenstates with degenerate charge eigenvalues. These are related by the factorised scattering matrix.

Multi-Local Charges. Another point of interest is $u = \infty$. Here the R-matrix has the following expansion

$$\mathcal{R}_{a,k}(u, 0) = \mathcal{I}_{a,k} + iu^{-1}\mathcal{Q}_{a,k} - \frac{1}{2}u^{-2}\mathcal{Q}_{a,k}^2 + \dots, \quad (6.41)$$

with the operator

$$\mathcal{Q}_{a,k} = \mathcal{P}_{a,k} - \mathcal{I}_{a,k}. \quad (6.42)$$

The expansion in terms of figures reads

$$\begin{array}{c} \uparrow \\ \textcircled{\mathcal{R}} \\ \uparrow 0 \end{array} \begin{array}{c} \leftarrow \\ \rightarrow \end{array} = \begin{array}{c} \uparrow \\ | \\ \rightarrow \end{array} + \frac{i}{u} \begin{array}{c} \uparrow \\ \textcircled{\mathcal{Q}} \\ \uparrow \end{array} \begin{array}{c} \leftarrow \\ \rightarrow \end{array} - \frac{1}{2u^2} \begin{array}{c} \uparrow \\ \textcircled{\mathcal{Q}^2} \\ \uparrow \end{array} \begin{array}{c} \leftarrow \\ \rightarrow \end{array} + \dots \quad (6.43)$$

and the operator \mathcal{Q} takes the form⁷

$$\begin{array}{c} \uparrow \\ \text{---} \circ \text{---} \\ \uparrow \end{array} Q = \begin{array}{c} \uparrow \\ \text{---} \curvearrowright \\ \uparrow \end{array} - \begin{array}{c} \uparrow \\ \text{---} | \text{---} \\ \uparrow \end{array} . \quad (6.44)$$

We now expand the monodromy matrix $\mathcal{T}_a(u)$ to second order

$$\begin{aligned}
& \text{Diagram 1: } \text{Oval } \mathcal{T}(u) \text{ with } u \text{ on left and right, and } L \text{ vertical lines with arrows.} \\
& = \text{Diagram 2: } \text{Five circles } \mathcal{R} \text{ in a row, each with } u \text{ on left and right, and } L \text{ vertical lines with arrows.} \\
& = \text{Diagram 3: } \text{Five vertical lines with arrows, connected by horizontal lines.} \\
& + \frac{i}{u} \sum_{k=1}^L \text{Diagram 4: } \text{Five vertical lines with arrows, a circle } \mathcal{Q} \text{ on the fourth line with arrow } k, \text{ and } L \text{ vertical lines with arrows.} \\
& - \frac{1}{u^2} \sum_{k < l=1}^L \text{Diagram 5: } \text{Five vertical lines with arrows, circles } \mathcal{Q} \text{ on the second and fourth lines with arrows } k \text{ and } l, \text{ and } L \text{ vertical lines with arrows.} \\
& - \frac{1}{2u^2} \sum_{k=1}^L \text{Diagram 6: } \text{Five vertical lines with arrows, a circle } \mathcal{Q}^2 \text{ on the fourth line with arrow } k, \text{ and } L \text{ vertical lines with arrows.} \\
& + \dots
\end{aligned} \tag{6.45}$$

Let us again discuss the terms that arise: The leading term is merely the identity operator.

At first order we find an operator Q_a which is the sum over the insertions of $Q_{a,k}$ at every site k of the spin chain

$$\text{Diagram 1} = \sum_{k=1}^L \text{Diagram 2} \quad (6.46)$$

It turns out that $\mathcal{Q}_{a,k}$ can be viewed as a fundamental representation of $U(N)$ acting on site k of the chain. Consequently, \mathcal{Q}_a is the tensor product representation of $U(N)$ on the whole chain.

⁷Here we use the same convention as with the R-matrix that \mathcal{Q} resides at the intersection of two lines.

At the next order we find again two insertions of $\mathcal{Q}_{a,k}$. These terms arise from $-\frac{1}{2}u^{-2}\mathcal{Q}_a^2$ which lets \mathcal{T}_a take the form of an exponential. As before, the coefficients of the terms differ by a factor of 2, and an equal number of terms with a different ordering is missing. We summarise them in an operator $\hat{\mathcal{Q}}_a$

$$\begin{aligned} \text{Diagram of } \hat{\mathcal{Q}}_a &= \frac{i}{2} \sum_{k < l=1}^L \text{Diagram 1} - \frac{i}{2} \sum_{k < l=1}^L \text{Diagram 2} \end{aligned} \quad (6.47)$$

This operator turns out to be the generator of an extended symmetry to be discussed further below.

Altogether we find for the expansion of the monodromy

$$\mathcal{T}_a(u) = \exp(iu^{-1}\mathcal{Q}_a + iu^{-2}\hat{\mathcal{Q}}_a + \dots). \quad (6.48)$$

From the above discussion it should be evident that the expansion of $\mathcal{T}(u)$ around $u = \infty$ yields a tower of *multi-local* charges. These act at several sites of the spin chain at the same time. The form of the expansion is very special, and related to the fact that the R-matrix reduces to the identity matrix at the point $u = \infty$. At generic points u , the monodromy matrix expands into a set of operators which act non-locally on the spin chain without apparent order.

6.3 Other Types of Bethe Ansätze

The Bethe equations describe the spectrum of quantum spin chains, but there are several ways in which they can be derived and formulated. The various approaches lead to different perspectives, which may be particularly helpful in addressing specific kinds of problems. In the following we present the main few approaches.

Algebraic Bethe Ansatz. We can apply the R-matrix formalism to construct eigenstates of the closed spin chain. This method is not only closer to the quantum field theory formalism, but it also largely based in algebra.

Let us first investigate the monodromy matrix for the Heisenberg XXX spin chain with $N = 2$. The monodromy matrix \mathcal{T} is a 2×2 matrix acting on the auxiliary spin site (as well as a big matrix acting on the space of the spin chain)

$$\mathcal{T}(u) = \begin{pmatrix} \mathcal{A}(u) & \mathcal{B}(u) \\ \mathcal{C}(u) & \mathcal{D}(u) \end{pmatrix}. \quad (6.49)$$

The components $\mathcal{A}, \mathcal{B}, \mathcal{C}, \mathcal{D}$ are operators acting on the spin chain which obey certain commutation relations. These can be summarised in the so-called

RTT-relations⁸

$$\mathcal{R}_{ab}(u, v) \mathcal{T}_a(u) \mathcal{T}_b(v) = \mathcal{T}_a(v) \mathcal{T}_b(u) \mathcal{R}_{ab}(u, v). \quad (6.50)$$

In the graphical notation they read

They follow straight-forwardly from repeated application of the Yang–Baxter equations.⁹

We know that our R-matrix is invariant under $SU(2)$, in particular, it preserves the number of up and down spins. Consequently, a spin flip in the auxiliary space must be compensated by an opposite spin flip on the spin chain. The components \mathcal{A} and \mathcal{D} do not change the number of up and down spins, whereas \mathcal{B} and \mathcal{C} increase and decrease the number of up spins by one unit, respectively.

Recalling that we treated a spin flip as a magnon particle, the above discussion is reminiscent of the framework of quantum field theory where \mathcal{B} and \mathcal{C} take the roles of creation and annihilation operators, respectively, whereas \mathcal{A} and \mathcal{D} serve as charges. The RTT relations provide the commutation relations which are of the same kind as the commutation relations for (free) particles, but somewhat more involved.

To construct eigenstates we start again with a ferromagnetic vacuum state

$$|0\rangle = |\downarrow\downarrow\ldots\downarrow\rangle. \quad (6.52)$$

This state is evidently annihilated by $\mathcal{C}(u)$ for any u . Excited states are generated by acting with several $\mathcal{B}(u)$'s on the vacuum.

$$|u_1, \dots, u_M\rangle = \mathcal{B}(u_1) \dots \mathcal{B}(u_M) |0\rangle. \quad (6.53)$$

This state has M up spins, and therefore it is an M -magnon state. The u_k correspond to the magnon rapidities which are related to the momenta by the relation $u_k = \frac{1}{2} \cot(\frac{1}{2} p_k)$ we used earlier to introduce the rapidity variables. The operator $\mathcal{B}(u_k)$ places a magnon with momentum p_k on top of the existing magnon. This is done precisely in accordance with the rules to assemble multi-magnon states described above. All of this construction is neatly encoded into the R-matrix. Altogether, the above construction of eigenstates is reminiscent of the inverse scattering method and it is called the *quantum inverse scattering method*.

⁸The name originates from a notation where the monodromy matrix is assigned the letter T.

⁹The RTT-relations imply that the monodromy matrix $\mathcal{T}(u)$ is an R-matrix as well. This R-matrix is slightly more general than the one we discussed above: It acts on two inequivalent spaces, the auxiliary spin site and the Hilbert space of the spin chain. The spin chain space supplies not just one parameter v , but rather one parameter v_k for each spin site. We merely *decided* to set all these parameters to zero $v_k = 0$.

So far we have not specified boundary conditions because the monodromy matrix simply end at the first and the last sites. For a closed chain the latter should be related as any other pair of adjacent sites. This is achieved by the trace within the transfer matrix $\mathcal{F}(u)$. We are thus interested in its eigenvalues which includes the energy spectrum of the closed chain. Let us therefore act with

$$\mathcal{F}(u) = \mathcal{A}(u) + \mathcal{D}(u) \quad (6.54)$$

on a state $|u_1, \dots, u_M\rangle$. This operation can be performed by means of the RTT algebra of the components $\mathcal{A}, \mathcal{B}, \mathcal{D}$. Not too surprisingly, the state is an eigenstate of $\mathcal{F}(u)$ precisely if the magnon rapidities u_k satisfy the closed chain Bethe equations

$$\left(\frac{u_k + \frac{i}{2}}{u_k - \frac{i}{2}} \right)^L = \prod_{\substack{j=1 \\ j \neq k}}^M \frac{u_k - u_j + i}{u_k - u_j - i} \quad \text{for } k = 1, \dots, M. \quad (6.55)$$

Interestingly, we can now compute the eigenvalue $F(u)$ of $\mathcal{F}(u)$ with full dependence on u

$$F(u) = \prod_{k=1}^M \frac{u - u_k - \frac{i}{2}}{u - u_k + \frac{i}{2}} + \left(\frac{u}{u + i} \right)^L \prod_{k=1}^M \frac{u - u_k + \frac{3i}{2}}{u - u_k + \frac{i}{2}}. \quad (6.56)$$

The two terms roughly correspond to action of the operators $\mathcal{A}(u)$ and $\mathcal{D}(u)$ up to a bunch of extra contributions which cancel between the two terms when the Bethe equations hold.

Above, we have derived a relationship between the expansion of $\mathcal{F}(u)$ at $u = 0$ and some local charges including the Hamiltonian

$$\mathcal{F}(u) = \mathcal{U} \exp(iu\mathcal{H} + iu^2\mathcal{F}_3 + \dots). \quad (6.57)$$

The same relationship evidently holds for the eigenvalues. We thus find¹⁰

$$\begin{aligned} F(u) &= U \exp(iuE + iu^2F_3 + \dots), \\ U &= \prod_{k=1}^M \frac{-u_k - \frac{i}{2}}{-u_k + \frac{i}{2}}, \\ E &= \sum_{k=1}^M \left(\frac{i}{u_k + \frac{i}{2}} - \frac{i}{u_k - \frac{i}{2}} \right), \\ F_3 &= \sum_{k=1}^M \left(\frac{i}{2(u_k + \frac{i}{2})^2} - \frac{i}{2(u_k - \frac{i}{2})^2} \right). \end{aligned} \quad (6.58)$$

A benefit of this so-called *algebraic Bethe ansatz* is that it is readily generalised to bigger symmetry algebras. Let us sketch how to apply the algebraic

¹⁰All of the *local* charge eigenvalues originate from the first term only because the second term is suppressed by u^L . At sufficiently large order this term also contributes, but the corresponding charges can hardly be called local because they extend over whole length of the spin chain.

Bethe ansatz to the $SU(N)$ fundamental spin chain. We first decompose the monodromy matrix as follows

$$\mathcal{T} = \begin{pmatrix} \mathcal{A}^1 & \mathcal{B}^1 & * & * \\ \mathcal{C}^1 & \mathcal{A}^2 & \ddots & * \\ * & \ddots & \ddots & \mathcal{B}^{N-1} \\ * & * & \mathcal{C}^{N-1} & \mathcal{A}^N \end{pmatrix}. \quad (6.59)$$

The operators \mathcal{B}^r and \mathcal{C}^r serve as creation and annihilation operators of $N - 1$ kinds. They correspond one-to-one to the various excitations of the nested Bethe ansatz. The operators \mathcal{A}^r on the diagonal leave the numbers of all kinds of excitations invariant.¹¹ We will not need the other operators explicitly because they can be written as combinations of the above elementary building blocks. A generic state is then written as

$$|u_k^r, u_l^s, \dots\rangle = \mathcal{B}^r(u_k^r) \mathcal{B}^s(u_l^s) \dots |0\rangle. \quad (6.60)$$

where the vacuum is again the state with all spins aligned such that it is annihilated by all \mathcal{C}^r .

Analytic Bethe Ansatz. Let us reconsider the eigenvalue of the transfer matrix from the algebraic Bethe ansatz

$$F(u) = \prod_{k=1}^M \frac{u - u_k - \frac{i}{2}}{u - u_k + \frac{i}{2}} + \left(\frac{u}{u + i} \right)^L \prod_{k=1}^M \frac{u - u_k + \frac{3i}{2}}{u - u_k + \frac{i}{2}}. \quad (6.61)$$

Compare this to the definition of the transfer matrix

$$\mathcal{F}(u) = \text{tr}_a \mathcal{R}_{a,L} \mathcal{R}_{a,L-1} \dots \mathcal{R}_{a,2} \mathcal{R}_{a,1}, \quad \mathcal{R}_{a,k} = \frac{u \mathcal{I}_{a,k} + i \mathcal{P}_{a,k}}{u + i}. \quad (6.62)$$

One immediately observes that $\mathcal{F}(u)$ is a rational function with an L -fold pole at $u = -i$, no other poles and $\mathcal{F}(\infty) = 2\mathcal{I}$. The eigenvalue $F(u)$ has the same properties, but additional apparent poles at $u = u_k - \frac{i}{2}$. How do these observations fit together? Did something go wrong?

Let us therefore investigate the residue of $F(u)$ at the dynamical pole $u = u_k - \frac{i}{2}$

$$\begin{aligned} & F(u_k - \frac{i}{2} + \epsilon) \\ & \sim -\frac{i}{\epsilon} \prod_{\substack{j=1 \\ j \neq k}}^M \frac{u_k - u_j - i}{u_k - u_j} + \frac{i}{\epsilon} \left(\frac{u_k - \frac{i}{2}}{u_k + \frac{i}{2}} \right)^L \prod_{\substack{j=1 \\ j \neq k}}^M \frac{u_k - u_j + i}{u_k - u_j} \\ & \sim -\frac{i}{\epsilon} \prod_{\substack{j=1 \\ j \neq k}}^M \frac{u_k - u_j - i}{u_k - u_j} \left(1 - \left(\frac{u_k - \frac{i}{2}}{u_k + \frac{i}{2}} \right)^L \prod_{\substack{j=1 \\ j \neq k}}^M \frac{u_k - u_j + i}{u_k - u_j - i} \right). \end{aligned} \quad (6.63)$$

¹¹In the context of Lie algebra the above operators correspond to *Chevalley-Serre generators* and *simple roots* of the algebra.

This shows that the residue is zero whenever the Bethe equations are satisfied, and there are no unwanted dynamical poles.

We can use the above observations to formulate the *analytic Bethe ansatz*: Suppose we are given the above form of the transfer matrix eigenvalue function $F(u)$ with unknown Bethe roots u_k . The u_k are then constrained by the requirement that $F(u)$ has no poles other than an L -fold pole at $u = -i$. In other words, $F(u)$ must be an analytic function except at $u = -i$.

Baxter Equation. Recall the eigenvalue of the transfer matrix and introduce the slightly modified but more symmetric function $T(u) := (u + \frac{i}{2})^L F(u - \frac{i}{2})$

$$T(u) = (u + \frac{i}{2})^L \prod_{k=1}^M \frac{u - u_k - i}{u - u_k} + (u - \frac{i}{2})^L \prod_{k=1}^M \frac{u - u_k + i}{u - u_k}. \quad (6.64)$$

This function is polynomial of degree L with leading term $2u^L$. Furthermore, introduce the so-called Baxter Q -function $Q(u) = \prod_{k=1}^M (u - u_k)$. The above expression takes the form

$$T(u)Q(u) = (u + \frac{i}{2})^L Q(u - i) + (u - \frac{i}{2})^L Q(u + i). \quad (6.65)$$

On the one hand, the equation defines $T(u)$ as a function of $Q(u)$. On the other hand, it takes the form of a difference equation for $Q(u)$ which is known as the *Baxter equation*.

An important insight is: With the further assumption that $T(u)$ and $Q(u)$ are unknown *polynomials*, the Baxter equation becomes equivalent to the Bethe equations! Some comments

- The roots of the polynomial $Q(u)$ are the Bethe roots.
- $T(u)$ describes the transfer matrix for a given set of Bethe roots encoded into $Q(u)$.
- For any given $T(u)$, there are two solutions of the Baxter equation because the difference equation is of second order.
- The difference equation can be viewed as a quantisation of a differential equation describing classical physics.
- The Baxter equation generalises to many other integrable systems. In particular it can be formulated for models where the coordinate Bethe ansatz does not apply, such as the Heisenberg XYZ chain. In the latter example, the functions T and Q are not polynomials but rather elliptic functions with two periodicities on the complex plane.

T-System. We defined the transfer matrix as a trace of a monodromy matrix with an auxiliary space transforming in the fundamental representation of $SU(N)$. The concept of transfer matrices can be generalised easily to auxiliary spaces transforming in higher representations. The higher transfer matrices all commute with each other at arbitrary parameters.

The eigenvalue of the spin-1 transfer matrix for the Heisenberg XXX spin chain reads

$$T_1(u) = (u+i)^L \prod_{k=1}^M \frac{u-u_k - \frac{3i}{2}}{u-u_k + \frac{i}{2}} + (u-i)^L \prod_{k=1}^M \frac{u-u_k + \frac{3i}{2}}{u-u_k - \frac{i}{2}} + u^L \prod_{k=1}^M \frac{u-u_k - \frac{3i}{2}}{u-u_k + \frac{i}{2}} \frac{u-u_k + \frac{3i}{2}}{u-u_k - \frac{i}{2}}. \quad (6.66)$$

We have written the eigenvalue as a polynomial in analogy to $T_{1/2}(u) := T(u)$ vs. the original rational function $F(u)$.

These transfer matrices do not necessarily carry additional information, they merely reshuffle the available information. For instance there is a simple relationship between $T_{1/2}$ and T_1

$$T_{1/2}(u + \frac{i}{2})T_{1/2}(u - \frac{i}{2}) = u^L T_1(u) + (u+i)^L (u-i)^L. \quad (6.67)$$

This identity neatly reflects the $SU(2)$ multiplication rule $(\frac{1}{2}) \otimes (\frac{1}{2}) = (1) \oplus (0)$. The relationship can be understood as follows: We first act with two monodromy matrices with fundamental auxiliary sites on the state. To turn them into transfer matrices, we should take a trace on each auxiliary space (l.h.s.). However, we may also project the tensor product to the spin-1 and spin-0 components first (r.h.s.).¹² The shift of the parameters u by $\pm \frac{i}{2}$ is a quantum effect. It is related to the fact that the tensor product only splits up when the parameters differ by i .

A generalisation of the above identity corresponding to $(\frac{1}{2}n) \otimes (\frac{1}{2}) = (\frac{1}{2}(n+1)) \oplus (\frac{1}{2}(n-1))$ reads

$$T_{n/2}(u + \frac{i}{2})T_{1/2}(u - \frac{i}{2}n) = (u - \frac{i}{2}(n-1))^L T_{(n+1)/2}(u) + (u - \frac{i}{2}(n+1))^L T_{(n-1)/2}(u + i). \quad (6.68)$$

This identity allows to recursively construct transfer matrix eigenvalues for representations with arbitrary spin

$$T_{n/2}(u) = \sum_{r=0}^n (u + \frac{i}{2}(n-2r))^L \prod_{k=1}^M \frac{u-u_k + \frac{i}{2}(n+1)}{u-u_k + \frac{i}{2}(n+1-2r)} \frac{u-u_k - \frac{i}{2}(n+1)}{u-u_k + \frac{i}{2}(n-1-2r)}. \quad (6.69)$$

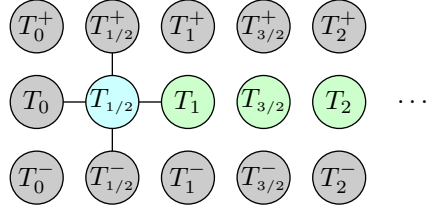
In particular for spin-0 we should set $T_0(u) = u^L$.

¹²Note that the product of two transfer matrices with rearranged connections due to the projections essentially winds twice around the closed chain. Therefore T_1 can be viewed as the analog of $F_2 = \text{tr } L^2$ which takes two loops around the chain before closing (with suitable modifications for the quantum case).

There are many similar identities that relate the various transfer matrix eigenvalues. A very useful generalisation is the defining relation of the *T-system*¹³

$$T_{n/2}(u + \frac{i}{2})T_{n/2}(u - \frac{i}{2}) = T_{(n+1)/2}(u)T_{(n-1)/2}(u) + T_{n/2}^+(u)T_{n/2}^-(u). \quad (6.70)$$

This equation has the form of a difference equation reminiscent of the Hirota equation. It is defined on a lattice of points given by three rows T_s^+ , T_s and T_s^- .



$$(6.71)$$

In our case the top and bottom rows as well as the first site of the middle row are given by fixed boundary values

$$T_{n/2}^\pm(u) = (u \pm \frac{i}{2}(n+1))^L, \quad T_0(u) = u^L. \quad (6.72)$$

The middle row contains the dynamical information on the system. Requiring that all the $T_s(u)$ are polynomials is equivalent to the Bethe equation and determines the spectrum of the closed Heisenberg XXX spin chain.

The benefit of the T-system equation is that it generalises to much more complicated systems such as integrable quantum field theories and the so-called thermodynamic Bethe ansatz. To that end one has to set up a suitable lattice of functions¹⁴ and specify appropriate boundary conditions. The drawback of this approach is that the T-system consists of infinitely many functions to be solved simultaneously.

¹³A reformulation of the T-system is the so-called *Y-system*. It uses a different set of variable functions Y to eliminate some unphysical degrees of freedom, but has a very similar form otherwise.

¹⁴The lattice is closely related to the symmetry algebra: The vertical direction corresponds to the Dynkin diagram; in our case there is just a single row (after removing the boundaries) corresponding to the single node of the Dynkin diagram for $SU(2)$. The horizontal direction corresponds to a reduced n -fold symmetric product of the fundamental representation corresponding to one node of the Dynkin diagram; in our case this is the representation with spin $(n/2)$.

7 Quantum Algebra

Integrability can be viewed a hidden extended symmetry of a model. In the following we will discuss several symmetry groups and concepts that come to play in this context.

7.1 Lie Algebra

Continuous symmetries in physics are often described by Lie algebras. Here we introduce some elements of Lie theory that come to use in integrable systems.

Lie Algebras. We assume familiarity with the concepts of Lie algebra. Nevertheless, let us give a summary of the most important features:

- A Lie algebra is a vector space \mathfrak{g} equipped with Lie brackets

$$[\cdot, \cdot] : \mathfrak{g} \times \mathfrak{g} \rightarrow \mathfrak{g}. \quad (7.1)$$

Lie brackets are bi-linear, anti-symmetric and satisfy the Jacobi identities.

- We will assume the algebras to be complex¹ and simple. Integrability is largely related to infinite-dimensional algebras which in turn are based on finite-dimensional algebras.
- A representation of a Lie algebra on a vector space \mathbb{V} is a linear map

$$\rho : \mathfrak{g} \rightarrow \text{End}(\mathbb{V}), \quad (7.2)$$

which preserves the Lie brackets as commutators on $\text{End}(\mathbb{V})$

$$[\rho(x), \rho(y)] = \rho([x, y]). \quad (7.3)$$

- We will often use a basis J^a , $a = 1, \dots, \dim(\mathfrak{g})$, for the space \mathfrak{g} .
- The Lie brackets are encoded by the structure constants f_c^{ab}

$$[J^a, J^b] = f_c^{ab} J^c. \quad (7.4)$$

- We usually have an invariant symmetric quadratic form²

$$T = c_{ab} J^a \otimes J^b, \quad (7.5)$$

which is the inverse of the Cartan–Killing form

$$K(x, y) = \text{tr } \rho_{\text{ad}}(x) \rho_{\text{ad}}(y), \quad c^{ab} \sim K(J^a, J^b). \quad (7.6)$$

¹Real algebras are equally suitable, but require additional care.

²Invariance is the statement $[J^a, T] = 0$, where the Lie bracket with a tensor product is defined as $[x, y \otimes z] := [x, y] \otimes z + y \otimes [x, z]$.

Loop Algebras. The algebras of integrability for field theories are typically based on infinite-dimensional loop algebras. The *loop algebra* $\mathfrak{g}[u, u^{-1}]$ ³ is an infinite-dimensional Lie algebra:

- It is based on some finite-dimensional Lie algebra \mathfrak{g} .
- It is spanned by the elements $J_n^a := u^n \otimes J^a$ with $a = 1, \dots, \dim(\mathfrak{g})$ and $n \in \mathbb{Z}$.⁴ The integer n can be called the *level* of the element.
- The Lie brackets of the loop algebra are defined in terms of the Lie brackets of \mathfrak{g} as

$$[J_m^a, J_n^b] = f_c^{ab} J_{m+n}^c. \quad (7.7)$$

Evidently, the Lie brackets satisfy the Jacobi identity.

- The subalgebra at level $n = 0$ is the original Lie algebra \mathfrak{g} .⁵
- There is a tower of quadratic invariant forms

$$T_n = \sum_{k=-\infty}^{\infty} c_{ab} J_k^a \otimes J_{n-k}^b. \quad (7.8)$$

Another relevant class of algebras are polynomial or half loop algebras. These are loop algebras restricted to positive or negative levels n , with the zeroth level either included or not. For positive levels, the algebras are denoted by $\mathfrak{g}[u]$ or $u\mathfrak{g}[u]$ depending on whether the zeroth level is included or not.

For integrable systems the class of *evaluation representations* is very important. For a given representation ρ of a finite-dimensional Lie algebra \mathfrak{g} on the space \mathbb{V} it is straight-forward to construct a corresponding one-parameter family of representations ρ_u of a (half) loop algebra

$$\rho_u(J_n^a) := u^n \rho(J^a). \quad (7.9)$$

The constant $u \in \mathbb{C}$ of the representation ρ_u is called the *evaluation parameter*.

A useful feature is that the evaluation representation has the same dimension as the underlying representation of the finite-dimensional Lie algebra. In particular, it can be finite. Moreover, the tensor product $\rho_{u,v} = \rho_u \otimes 1 + 1 \otimes \rho_v$ of two evaluation representations ρ_u, ρ_v is irreducible unless the evaluation parameters match, $u = v$. This has strong implications on invariant objects.

Affine Kac–Moody Algebras. Finally, let us mention the *affine Kac–Moody algebra* $\hat{\mathfrak{g}}$. This is the loop algebra $\mathfrak{g}[u, u^{-1}]$ extended by a *central element* C which arises in the Lie brackets

$$[J_m^a, J_n^b] = f_c^{ab} J_{m+n}^c + m\delta_{m+n,0} c^{ab} C. \quad (7.10)$$

³Here, we will not make a thorough distinction between polynomial algebras, their completion and formal power series.

⁴A loop algebra is formally defined by maps from the circle S^1 (“loop”) to \mathfrak{g} . To see the relationship, set $u = \exp(i\varphi)$ and perform a Fourier expansion in φ .

⁵A useful fact to keep in mind is that the original Lie algebra can be embedded into the loop algebra in many ways: Given a \mathbb{Z} -grading (generated by some element of the Cartan algebra), one can identify the level with (a multiple of) this grading and obtain the same Lie algebra.

Sometimes a *derivation* element D is also included in the affine algebra

$$[D, J_n^a] = nJ_n^a. \quad (7.11)$$

It serves as the conjugate of the central element C . It appears in the quadratic invariant form \hat{T} of $\hat{\mathfrak{g}}$ as $\hat{T} = T_0 - B \otimes C - C \otimes B$ and makes it invertible.

For our purposes, it makes sense to define a different derivation^{6 7}

$$[D, J_n^a] = nJ_{n-1}^a. \quad (7.12)$$

The relevant quadratic invariant form for this algebra is $\hat{T} = T_{-1} - B \otimes C - C \otimes B$.

Evaluation representations also exist for affine algebras, where they have vanishing central element eigenvalue. The presence of a derivation changes the situation: it acts on the evaluation parameter as a derivative. Then only the family of evaluation representations forms a representation of the enlarged algebra. This representation can be viewed as a one-dimensional *field* where the derivation acts as the momentum generator. The enlarged algebra thus covers spacetime symmetries of a 2-dimensional field theory.

Loop algebras are subalgebras of the affine Kac–Moody algebras where the central element has been projected out (and where the derivation has been dropped). In the following we will mostly consider loop algebras keeping in mind that the discussions could be extended to affine Kac–Moody algebras with minor adjustments.

7.2 Classical Integrability

In classical integrability we have derived a classical r -matrix satisfying the classical Yang–Baxter equation. A classical r -matrix fits well into the framework of *Lie bialgebras*.

Lie Bialgebra. A Lie bialgebra is a Lie algebra \mathfrak{g} whose dual \mathfrak{g}^* is also a Lie algebra such that the two Lie brackets are compatible.

It is convenient to formulate the above statements purely in terms of \mathfrak{g} without reference to the dual \mathfrak{g}^* . To that end, let us discuss the dual of a Lie bracket: Define an operation $\mu^* : \mathfrak{g}^* \rightarrow \mathfrak{g}^* \otimes \mathfrak{g}^*$ such that for all $x, y \in \mathfrak{g}$ and $c \in \mathfrak{g}^*$

$$c([x, y]) = \mu^*(c)(x \otimes y). \quad (7.13)$$

Conversely, the dual of the dual Lie bracket, the so-called *Lie cobracket* δ , is defined as a linear map

$$\delta : \mathfrak{g} \rightarrow \mathfrak{g} \otimes \mathfrak{g}. \quad (7.14)$$

⁶One can transform between the two forms of the derivation by an exponential map $z = \exp(u)$ such that $zdz/dz = d/du$.

⁷In fact, the derivation could be extended to a Virasoro algebra, but we need merely one additional element serving as the conjugate to C .

The cobracket must return an anti-symmetric element of the tensor product of two Lie algebras. It must also satisfy the dual of the Jacobi identity for all $c \in \mathfrak{g}$

$$(1 + \mathcal{P}_{12}\mathcal{P}_{23} + \mathcal{P}_{23}\mathcal{P}_{12})(\delta \otimes 1)(\delta(c)) = 0. \quad (7.15)$$

Compatibility between the algebra and the coalgebra is the statement

$$\delta([x, y]) = [x, \delta(y)] + [\delta(x), y], \quad (7.16)$$

where the Lie bracket on the tensor product is defined as

$$[x, y \otimes z] := [x, y] \otimes z + y \otimes [x, z], \quad (7.17)$$

and similarly for the other combination. The role of the cobracket will become clearer in the context of quantum algebras to be discussed below.

Classical r-Matrix. The classical r-matrix in the algebraic context is an element $r \in \mathfrak{g} \otimes \mathfrak{g}$ such that

$$\delta(x) = [r, x]. \quad (7.18)$$

Anti-symmetry of δ requires that the symmetric part $r + \mathcal{P}(r)$ is an invariant element of $\mathfrak{g} \otimes \mathfrak{g}$ (essentially proportional the invariant quadratic form). Furthermore, the dual Jacobi identity and the compatibility condition requires that the combination

$$[[r, r]] := [r_{12}, r_{13}] + [r_{12}, r_{23}] + [r_{13}, r_{23}] \quad (7.19)$$

is an invariant element of $\mathfrak{g}^{\otimes 3}$.

- A Lie bialgebra with r-matrix is called *coboundary*.
- A *coboundary* Lie bialgebra is called *quasi-triangular* if the classical Yang–Baxter equation holds

$$[[r, r]] = 0. \quad (7.20)$$

- A *quasi-triangular* Lie bialgebra is called *triangular* if the r-matrix is anti-symmetric

$$r = -\mathcal{P}(r). \quad (7.21)$$

Example. Earlier we have discussed a classical r-matrix of the form⁸

$$r(u, v) = \frac{c_{ab} \mathbf{J}^a \otimes \mathbf{J}^b}{u - v} = \frac{T}{u - v}. \quad (7.22)$$

We can recast it into an element of a loop algebra⁹

$$r = \frac{c_{ab} \mathbf{J}^a \otimes \mathbf{J}^b}{u - v} \in \mathfrak{g}[u, u^{-1}] \otimes \mathfrak{g}[v, v^{-1}]. \quad (7.23)$$

⁸More precisely, we discussed a representation $(\rho \otimes \rho)(r)$ of this r-matrix. In order to match with the below forms of the r-matrix as elements of loop algebras one employs evaluation representations $(\rho_u \otimes \rho_v)(r)$.

⁹More precisely, r is an element of a completion of the two loop algebras because it involves elements of arbitrarily high level.

It makes sense to expand this expression into levels by means of a formal power series. Assuming that $|u| \gg |v|$ we find

$$r = \sum_{n=0}^{\infty} \frac{v^n}{u^{n+1}} T = \sum_{n=0}^{\infty} c_{ab} J_{-n-1}^a \otimes J_n^b. \quad (7.24)$$

This r-matrix satisfies the classical Yang–Baxter equation $[[r, r]] = 0$. Note, however, that it is not anti-symmetric as the above rational form suggests.¹⁰ Nevertheless, the symmetric part of r is invariant as desired

$$r + \mathcal{P}(r) = \sum_{n=-\infty}^{\infty} c_{ab} J_{-n-1}^a \otimes J_n^b = T_{-1}. \quad (7.25)$$

Therefore this r-matrix describes a quasi-triangular Lie bialgebra.


Alternatively, we can perform an expansion with $|u| \ll |v|$

$$\tilde{r} = - \sum_{n=0}^{\infty} \frac{u^n}{v^{n+1}} T = - \sum_{k=0}^{\infty} c_{ab} J_n^a \otimes J_{-n-1}^b. \quad (7.26)$$


Likewise, this r-matrix satisfies the classical Yang–Baxter equation, and we find the symmetric part $r + \mathcal{P}(r) = -T_{-1}$.

It is tempting to take the linear combination $r' = r + \tilde{r}$ to remove the symmetric part of r' . Unfortunately, this r-matrix *does not* satisfy the classical Yang–Baxter equation $[[r + \tilde{r}, r + \tilde{r}]] \neq 0$ essentially because the latter is a non-linear relationship and therefore may change under linear combinations.


Classification and Construction. Solutions to the classical Yang–Baxter equation have been studied to some extent. In particular, the solutions of difference form for simple Lie algebras have been classified by Belavin and Drinfeld. There are essentially three classes depending on the location of poles in the complex plane:



rational



trigonometric



elliptic

(7.27)

- rational solutions with a single pole,
- trigonometric solutions with a one-dimensional lattice of poles,
- elliptic solutions with a two-dimensional lattice of poles.

For quantum integrable systems these three cases correspond to the Heisenberg XXX, XXZ and XYZ models, respectively.

¹⁰The crucial point is that the quadratic invariant T_{-1} is zero almost everywhere, but it is not identically zero. In accordance with Fourier transformations, it could be viewed as a delta function $T_{-1} \sim T\delta(x - y)$.

Towards a construction of r-matrices, a useful observation in the (first version of the) above example is that the r-matrix belongs to the space

$$r \in u^{-1}\mathfrak{g}[u^{-1}] \otimes \mathfrak{g}[v]. \quad (7.28)$$

Importantly, the space on the left is the conjugate of the space on the right with respect to the quadratic form T_{-1} . Therefore r as a matrix has a triangular form.

There is a construction which leads to r-matrices of a similar form. Starting with a conventional Lie bialgebra \mathfrak{g} , one can construct the *classical double algebra* $\mathfrak{dg} = \mathfrak{g} \oplus \mathfrak{g}^*$. Interestingly, the double algebra has a natural quasi-triangular structure. It also has the structure of a *Manin triple* $(\mathfrak{dg}, \mathfrak{g}, \mathfrak{g}^*)$. In our example, the starting point is the half loop algebra $\mathfrak{g}[u]$. Its dual is $\mathfrak{g}[u]^* = u^{-1}\mathfrak{g}[u^{-1}]$ and the double algebra is the complete loop algebra $\mathfrak{dg}[u] = \mathfrak{g}[u, u^{-1}]$.

7.3 Quantum Algebras

The symmetries of integrable quantum models are typically encoded into so-called *quantum algebras* based on loop and affine Lie algebras. Next we present some basic elements of quantum algebra.

Enveloping Algebra. In quantum physics one typically considers neither Lie groups G nor Lie algebras \mathfrak{g} , but rather their enveloping algebra $U(\mathfrak{g})$.

Towards defining enveloping algebras, consider first the tensor algebra $T(\mathfrak{g})$ of a Lie algebra \mathfrak{g} . The elements of this algebra are polynomials in the elements of \mathfrak{g} which are assumed not to commute within monomials. Multiplication within the tensor algebra is defined by concatenation of monomials. The tensor algebra merely inherits the vector space \mathfrak{g} of the Lie algebra, but not its algebraic structure.

The enveloping algebra $U(\mathfrak{g})$ is obtained by identifying commutators of elements of \mathfrak{g} with the corresponding Lie bracket

$$J^a J^b - J^b J^a = [J^a, J^b] = f_c^{ab} J^c. \quad (7.29)$$

Alternatively one can define the enveloping algebra as a quotient of the tensor algebra by the ideal spanned by the commutation relations

$$U[\mathfrak{g}] = T[\mathfrak{g}] / \text{span}(J^a J^b - J^b J^a - f_c^{ab} J^c). \quad (7.30)$$

This identification implies that monomials of J^a can be reordered arbitrarily at the cost of shorter polynomials. A basis of $U(\mathfrak{g})$ is therefore formed by orderless monomials in the J^a .¹¹

In the context of quantum physics, an enveloping algebra has several advantages over plain Lie groups and algebras:

¹¹The ordering of the letters matters for the algebraic structure, but not for enumerating a basis for the space of the algebra.

- It incorporates the Lie algebra $\mathfrak{g} = \text{span}(J^a)$ as the single-letter words and via the commutation relations.
- It incorporates operator products $J^a J^b$ which are essential for quantum mechanics.
- It incorporates the Lie group (formally) via the exponential map $G = \{\exp(x), x \in \mathfrak{g}\}$.
- Tensor products of representations are naturally defined.
- It allows for non-trivial deformations which come to use in integrable systems.

Hopf Algebra. The enveloping algebra has a natural *Hopf algebra* structure. A Hopf algebra is a bi-unital bi-associative bialgebra with an antipode map. Let us summarise the various properties of a Hopf algebra A over a field \mathbb{K} :

- The product μ and coproduct Δ are \mathbb{K} -linear (co)associative maps

$$\mu : A \otimes A \rightarrow A, \quad \Delta : A \rightarrow A \otimes A, \quad (7.31)$$

which are compatible in the following sense (for $X, Y \in A$)

$$\Delta(\mu(X \otimes Y)) = (\mu_{13} \otimes \mu_{24})(\Delta(X) \otimes \Delta(Y)). \quad (7.32)$$

Note that the compatibility relation ensures that tensor product representations are consistently defined via the coproduct

$$\rho_{12}(X) := (\rho_1 \otimes \rho_2)(\Delta(X)). \quad (7.33)$$

- The unit ϵ and counit η formalise the existence of a unit element $1 = \epsilon(1)$

$$\epsilon : \mathbb{K} \rightarrow A, \quad \eta : A \rightarrow \mathbb{K}. \quad (7.34)$$

They must satisfy the usual compatibility relations (for $x \in \mathbb{K}, Y \in A$)

$$\mu(\epsilon(x) \otimes Y) = xY, \quad \eta_1(\Delta(X)) = X. \quad (7.35)$$

- The antipode Σ is a linear map on the algebra

$$\Sigma : A \rightarrow A, \quad (7.36)$$

which satisfies

$$\mu(\Sigma_1(\Delta(X))) = \epsilon(\eta(X)). \quad (7.37)$$

If an antipode exists for a bialgebra, it is unique. Furthermore, the antipode is an anti-homomorphism of the algebra and of the coalgebra

$$\mu(\Sigma(X) \otimes \Sigma(Y)) = \Sigma(\mu(Y \otimes X)), \quad (7.38)$$

$$\Delta(\Sigma(X)) = (\Sigma \otimes \Sigma)(\tilde{\Delta}(X)). \quad (7.39)$$

Here $\tilde{\Delta}$ denotes the opposite coproduct with the two tensor factors interchanged.

Example. We illustrate the meaning of the maps using the example of the enveloping algebra $U[\mathfrak{g}]$. The product is defined by concatenation of monomials

$$\mu(X \otimes Y) := XY. \quad (7.40)$$

Note that the algebraic relations of \mathfrak{g} are implemented by identifications among the elements.

The coproduct is defined trivially to reproduce the usual tensor product representations of Lie algebra elements J^a and Lie group elements $\exp(x_a J^a)$

$$\Delta(1) = 1 \otimes 1, \quad \Delta(J^a) = J^a \otimes 1 + 1 \otimes J^a. \quad (7.41)$$

Coproducts of polynomials X are defined by means of the compatibility relation. Note that the iterated coproduct defines the action of symmetry generators on a spin chain, e.g.¹²

$$\Delta^{L-1}(1) = 1, \quad \Delta^{L-1}(J^a) = \sum_{k=1}^L J_k^a. \quad (7.42)$$

The unit and counit are defined as

$$\epsilon(1) = 1, \quad \eta(1) = 1, \quad \eta(J^a) = 0. \quad (7.43)$$

They implement the natural operations involving the unit element, and are hardly used in practice.

Finally, the antipode acts as

$$\Sigma(1) = 1, \quad \Sigma(J^a) = -J^a. \quad (7.44)$$

Since the antipode acts as the negative on the Lie algebra, it acts as the inverse on the Lie group. In that sense, it should be viewed as a generalisation of the inversion operation. In plain enveloping algebras it acts as an involution, but in more general situations Σ^2 differs from the identity map.

Universal R-Matrix. The framework of Hopf algebras can be extended to incorporate the R-matrix of quantum integrable systems. We introduce the so-called *universal R-matrix* \mathcal{R} which is an invertible algebraic element

$$\mathcal{R} \in A \otimes A. \quad (7.45)$$

The R-matrices which we have encountered so far should be viewed as representations $(\rho_1 \otimes \rho_2)(\mathcal{R})$ of the universal R-matrix.

The universal R-matrix relates the coproduct with the opposite coproduct

$$\mathcal{R}\Delta(X) = \tilde{\Delta}(X)\mathcal{R}. \quad (7.46)$$

¹²An iterated coproduct acts on any one of the intermediate tensor factors. The result does not depend on the choice of tensor factors because the coproduct is coassociative.

In other words, even though the coproduct is not strictly cocommutative, it is cocommutative up to conjugation by \mathcal{R} . This property is called *quasi-cocommutativity*. On the level of representations, the relation tells us that the tensor product of two representations $\rho_1 \otimes \rho_2$ is equivalent to the opposite one $\rho_2 \otimes \rho_1$.

The second important property called *quasi-triangularity* is

$$\Delta_1(\mathcal{R}) = \mathcal{R}_{13}\mathcal{R}_{23}, \quad \Delta_2(\mathcal{R}) = \mathcal{R}_{13}\mathcal{R}_{12}. \quad (7.47)$$

Among other useful features, it implies the Yang–Baxter equation

$$\mathcal{R}_{12}(\mathcal{R}_{13}\mathcal{R}_{23}) = \mathcal{R}_{12}\Delta_1(\mathcal{R}) = \tilde{\Delta}_1(\mathcal{R})\mathcal{R}_{12} = (\mathcal{R}_{23}\mathcal{R}_{13})\mathcal{R}_{12}. \quad (7.48)$$

This means that every R-matrix derived as a representation of the universal R-matrix satisfies the Yang–Baxter equation.

7.4 Yangian Algebra

We will now be more concrete about an algebra which is relevant to the Heisenberg XXX spin chain and generalisations, the so-called *Yangian algebra*. A noteworthy deformation is the *quantum affine algebra* which is relevant to XXZ-like spin chains.

Algebra. The Yangian algebra $Y(\mathfrak{g})$ of a finite-dimensional simple Lie algebra \mathfrak{g} is the algebra of polynomials in the elements J^a and \hat{J}^a with $a = 1, \dots, \dim \mathfrak{g}$. The elements J^a and \hat{J}^a are called level-zero and level-one generators, respectively.

The following identifications of polynomials apply

$$[J^a, J^b] = f_c^{ab} J^c. \quad (7.49)$$

In other words, the J^a generate the Lie algebra \mathfrak{g} . Furthermore,

$$[J^a, \hat{J}^b] = f_c^{ab} \hat{J}^c. \quad (7.50)$$

In other words, the \hat{J}^a transform in the adjoint representation of \mathfrak{g} . Finally, the so-called *Serre relation* must hold

$$[[J^a, \hat{J}^b], \hat{J}^c] + 2 \text{ cyclic} = \frac{1}{6} \hbar^2 f_d^{ag} f_e^{bh} f_f^{ci} f_{ghi} \{J^d, J^e, J^f\}. \quad (7.51)$$

The term on the r.h.s. is the totally symmetric product of three terms.

When the generators J^a and \hat{J}^a are identified with the generators J_0^a and J_1^a of the half loop algebra $\mathfrak{g}[u]$, the Serre relation is a deformation of the Jacobi identity for $J^a, \hat{J}^b, \hat{J}^c$. Without the deformation term on the r.h.s., the Jacobi identity makes sure that iterated commutators of the generators J_1^a yield the higher-level generators J_n^a and nothing else. The Yangian algebra $Y(\mathfrak{g})$ therefore is a

deformation of the enveloping algebra $U(\mathfrak{g}[u])$. The constant \hbar is the parameter of the deformation.¹³

The Yangian is a Hopf algebra. The coproduct for the Yangian generators is defined as

$$\begin{aligned}\Delta(1) &= 1 \otimes 1, \\ \Delta(J^a) &= J^a \otimes 1 + 1 \otimes J^a, \\ \Delta(\hat{J}^a) &= \hat{J}^a \otimes 1 + 1 \otimes \hat{J}^a + \hbar f_{bc}^a J^b \otimes J^c.\end{aligned}\tag{7.52}$$

The latter term is a deformation of the trivial coalgebra structure on the enveloping algebra. It is precisely compatible with the deformation of the algebra by means of the Serre relation. Furthermore, the antipode reads

$$\Sigma(J^a) = -J^a, \quad \Sigma(\hat{J}^a) = -\hat{J}^a + \frac{1}{2}\hbar f_{bc}^a f_d^{bc} J^d.\tag{7.53}$$

Interestingly, the square of the antipode is not the identity, but for the level-one generator \hat{J} it generates a shift by a level-zero generator J

$$\Sigma^2(\hat{J}^a) = \hat{J}^a - \hbar f_{bc}^a f_d^{bc} J^d.\tag{7.54}$$

This can be viewed as an indication for the presence of a quantum deformation.

Evaluation Representations. The Yangian algebra is a deformation of the enveloping algebra of a half loop algebra. Therefore it is conceivable that evaluation representations lift to the Yangian algebra. For some representation ρ of \mathfrak{g} , there may exist a one-parameter family of representations ρ_u of $Y(\mathfrak{g})$:

$$\rho_u(1) = 1, \quad \rho_u(J^a) = \rho(J^a), \quad \rho_u(\hat{J}^a) = u \rho(J^a).\tag{7.55}$$

Note that the deformation can invalidate evaluation representations. In particular, the r.h.s. of the Serre relation must be zero for a valid representation. Interestingly this condition is an identity formulated in terms of ρ of \mathfrak{g} alone. For $\mathfrak{su}(N)$ this poses no restrictions, but for example for the adjoint representations of $\mathfrak{so}(N)$ or \mathfrak{e}_8 the term is not zero. In the latter case, the sum of an adjoint and singlet representation can form a proper Yangian representation.

Spin Chains. To define the Yangian action on a homogeneous spin chain we pick the evaluation representation ρ_0 with homogeneous evaluation parameter $u = 0$ for every site

$$\rho_0(1) = 1, \quad \rho_0(J^a) = \rho(J^a), \quad \rho_0(\hat{J}^a) = 0.\tag{7.56}$$

The tensor product representation on the spin chain therefore reads

$$\rho_{\text{ch}} = (\rho_0 \otimes \dots \otimes \rho_0) \circ \Delta^{L-1}.\tag{7.57}$$

¹³In fact, Yangian algebras with arbitrary parameter $\hbar \neq 0$ are equivalent. We are free to fix the parameter to any value. A conventional choice is $\pm i/2$.

For the level-zero and level-one generators the iterated coproduct amounts to

$$\begin{aligned}\Delta^{L-1}(J^a) &= \sum_{k=1}^L J_k^a. \\ \Delta^{L-1}(\widehat{J}^a) &= \sum_{k=1}^L \widehat{J}_k^a + \hbar f_{bc}^a \sum_{k<l=1}^L J_k^b J_l^c.\end{aligned}\tag{7.58}$$

The representations therefore read

$$\rho_{\text{ch}}(J^a) = \sum_{k=1}^L \rho_k(J^a), \quad \rho_{\text{ch}}(\widehat{J}^a) = \hbar f_{bc}^a \sum_{k<l=1}^L \rho_k(J^b) \rho_l(J^c).\tag{7.59}$$

Note that these two combinations agree precisely with the multi-local charges \mathcal{Q} and $\widehat{\mathcal{Q}}$ in the expansion of the monodromy matrix $\mathcal{T}(u)$ at $u \rightarrow \infty$

$$\mathcal{T}(u) = \exp(iu^{-1}\mathcal{Q} + iu^{-2}\widehat{\mathcal{Q}} + \dots).\tag{7.60}$$

Let us discuss how the spin chain Hamiltonian interacts with the Yangian algebra

$$\mathcal{H} = \sum_k \mathcal{H}_{k,k+1}.\tag{7.61}$$

Our Hamiltonian was constructed such that it is manifestly symmetric under some Lie algebra \mathfrak{g} , e.g. $\mathfrak{su}(N)$

$$[\rho_{\text{ch}}(J^a), \mathcal{H}] = 0.\tag{7.62}$$

This follows immediately from the action on the Hamiltonian kernel $\mathcal{H}_{k,k+1}$

$$[(\rho_0 \otimes \rho_0) \circ \Delta(J^a), \mathcal{H}_{12}] = 0.\tag{7.63}$$

The situation is different for the level-one generators where one finds

$$[(\rho_0 \otimes \rho_0) \circ \Delta(\widehat{J}^a), \mathcal{H}_{12}] = \mathcal{X}_2^a - \mathcal{X}_1^a\tag{7.64}$$

with some operator \mathcal{X}_k^a acting on a single site. The action on the complete Hamiltonian turns out to be a telescoping sum

$$[\rho_{\text{ch}}(\widehat{J}^a), \mathcal{H}] = \sum_k (\mathcal{X}_{k+1}^a - \mathcal{X}_k^a).\tag{7.65}$$

Now we have to pay attention to boundary conditions. For a closed chain with Hamiltonian

$$\mathcal{H} = \sum_{k=1}^L \mathcal{H}_{k,k+1} = \mathcal{H}_{1,L} + \sum_{k=1}^{L-1} \mathcal{H}_{k,k+1}\tag{7.66}$$

one finds

$$[\rho_{\text{ch}}(\widehat{J}^a), \mathcal{H}] = \mathcal{X}_L^a - \mathcal{X}_1^a + \sum_{k=1}^{L-1} (\mathcal{X}_{k+1}^a - \mathcal{X}_k^a) = 2\mathcal{X}_L - 2\mathcal{X}_1.\tag{7.67}$$

Therefore Yangian *symmetry* is broken by periodic boundary conditions. The spectrum of the spin chain Hamiltonian does not organise itself according to representations of the Yangian algebra.¹⁴ Nevertheless, the Yangian is a useful algebra for the construction of eigenstates as we shall see. It also makes sense to consider it as a symmetry of the bulk Hamiltonian up to boundary terms.

Magnon States. In the action of the Yangian on magnon states one can nicely observe the relationship between the momentum p , rapidity u and evaluation representations ρ_u .

For a spin chain with $\mathfrak{su}(N)$ fundamental spins, the residual symmetry of the magnon picture is $\mathfrak{u}(N-1)$. For the Heisenberg XXX chain we have the z-components of J^a and \hat{J}^a at our disposal¹⁵

$$J_{\text{reg}}^z = \frac{1}{2} \sum_k (\sigma_k^z + 1), \quad \hat{J}^z = \hbar \sum_{k < l} (\sigma_k^- \sigma_l^+ - \sigma_k^+ \sigma_l^-). \quad (7.68)$$

Here the level-zero generator was regularised such that it can act on an infinite spin chain. Its action on the vacuum is normalised to zero, and it measures the number of flipped spins, i.e. the magnon number

$$J_{\text{reg}}^z |p_1, \dots, p_M\rangle = M |p_1, \dots, p_M\rangle. \quad (7.69)$$

For the level-one generator acting on a single magnon we obtain

$$\hat{J}^z |p\rangle = \hbar \sum_{k < l} (e^{ipk} |l\rangle - e^{ipl} |k\rangle). \quad (7.70)$$

Reorganising the sums and ignoring any boundary terms on the infinite chain we find

$$\hat{J}^z |p\rangle = \hbar \sum_{l=1}^{\infty} (e^{-ipl} - e^{ipl}) \sum_k e^{ipk} |k\rangle = u J_{\text{reg}}^z |p\rangle. \quad (7.71)$$

Let us perform the geometric series such that the eigenvalue u equals

$$u = \hbar \sum_{l=1}^{\infty} (e^{-ipl} - e^{ipl}) = \frac{\hbar}{1 - e^{-ip}} - \frac{\hbar}{1 - e^{ip}} = -i\hbar \cot(\frac{1}{2}p). \quad (7.72)$$

By setting $\hbar = i/2$ we recover the relationship $u = \frac{1}{2} \cot(\frac{1}{2}p)$ between momentum p and rapidity u . This implies that a single magnon state transforms in an evaluation representation of the residual Yangian algebra $Y(\mathfrak{su}(N-1))$ with rapidity u as the evaluation parameter. One can convince oneself that many-magnon partial eigenstates transform in tensor product representations with individual evaluation parameters determined by their momenta.

¹⁴Since the Yangian algebra is very large, its representations are typically large, too. If the Yangian was a symmetry, the degeneracies of eigenvalues would be very pronounced, up to the point that all eigenvalues are degenerate.

¹⁵We implicitly assume that the generators are in some representation, here the spin- $1/2$ representation.

R-Matrix. The S-matrix acts on two-magnon partial eigenstates and it interchanges the order of constituent magnons. This implies that the Yangian action on the spin chain acts differently on the ingoing and outgoing two-magnon states. Symmetry of the S-matrix or the analogous R-matrix means

$$\Delta(X)\mathcal{R} = \mathcal{R}\tilde{\Delta}(X) \quad \text{for any } X \in Y(\mathfrak{g}). \quad (7.73)$$

Here $\tilde{\Delta}$ is the opposite coproduct which takes into account that the ordering of magnons has flipped. Concretely, for $X = J^a, \hat{J}^a$

$$\begin{aligned} \Delta(J^a) &= J^a \otimes 1 + 1 \otimes J^a, \\ \Delta(\hat{J}^a) &= u(J^a \otimes 1) + v(1 \otimes J^a) + \hbar f_{bc}^a J^b \otimes J^c, \\ \tilde{\Delta}(\hat{J}^a) &= u(J^a \otimes 1) + v(1 \otimes J^a) - \hbar f_{bc}^a J^b \otimes J^c. \end{aligned} \quad (7.74)$$

Evidently, the coalgebra is not cocommutative, but the relation $\tilde{\Delta}(X) = \mathcal{R}^{-1}\Delta(X)\mathcal{R}$ implies that the opposite coproduct is equivalent to the ordinary coproduct. This feature is called *quasi-cocommutativity*.

The relation for $X = J^a$ and fundamental spins of $\mathfrak{su}(N)$ implies that \mathcal{R} must be of the form

$$\mathcal{R} = R_1\mathcal{I} + R_2\mathcal{P} \quad (7.75)$$

with two unconstrained functions $R_{1,2}$. This follows from the fact that \mathcal{I} and \mathcal{P} are the only $\mathfrak{su}(N)$ invariant operators. For the level-one generator $X = \hat{J}^a$ we obtain additional constraints implying $-2\hbar R_1 = (u - v)R_2$. Therefore the R-matrix must be proportional to

$$\mathcal{R} \sim (u - v)\mathcal{I} + 2\hbar\mathcal{P} \quad (7.76)$$

matching our earlier results for $\hbar = i/2$.

Classical Limit. Let us make a brief digression to the classical r-matrix which should clearly be related to the R-matrix. Here one takes a classical limit of the R-matrix where $u, v \rightarrow \infty$ and u/v remains finite. One finds the classical r-matrix as the leading correction term

$$\mathcal{R} \simeq 1 \otimes 1 + ir, \quad r = \frac{\mathcal{P} - \mathcal{I}}{u - v}. \quad (7.77)$$

Moreover, the cobracket of the Lie algebra can be obtained as the leading anti-symmetric part of the coproduct.

Tensor Products. The R/S-matrix acts on the tensor product of two representations. Let us investigate the latter.

In $\mathfrak{su}(N)$ the tensor product of two fundamental representations decomposes according to

$$\begin{aligned} \square \otimes \square &= \square\square \oplus \begin{smallmatrix} \square \\ \square \end{smallmatrix}, \\ \text{fund} \otimes \text{fund} &= \text{sym} \oplus \text{anti-sym}, \\ \left(\frac{1}{2}\right) \otimes \left(\frac{1}{2}\right) &= (1) \oplus (0) \quad \text{for } \mathfrak{su}(2). \end{aligned} \quad (7.78)$$

Since the Yangian algebra enhances the $\mathfrak{su}(N)$ Lie algebra, there is more: Consider three states in $\mathfrak{su}(2)$

$$\begin{aligned} |0\rangle &:= |\downarrow\downarrow\rangle \in \square\square, \\ |s\rangle &:= |\uparrow\downarrow\rangle + |\downarrow\uparrow\rangle \in \square\square, \\ |a\rangle &:= |\uparrow\downarrow\rangle - |\downarrow\uparrow\rangle \in \boxminus. \end{aligned} \quad (7.79)$$

Act with raising and lowering operators J^\pm, \hat{J}^\pm using $\rho := (\rho_u \otimes \rho_v) \circ \Delta$

$$\begin{aligned} \Delta(J^+)|0\rangle &= |\uparrow\downarrow\rangle + |\downarrow\uparrow\rangle = |s\rangle, \\ \Delta(\hat{J}^+)|0\rangle &= u|\uparrow\downarrow\rangle + v|\downarrow\uparrow\rangle + \frac{i}{2}|\uparrow\downarrow\rangle - \frac{i}{2}|\downarrow\uparrow\rangle \\ &= \frac{1}{2}(u+v)|s\rangle + \frac{1}{2}(v-u-i)|a\rangle, \\ \Delta(J^-)|a\rangle &= 0, \\ \Delta(\hat{J}^-)|a\rangle &= (v-u+i)|0\rangle. \end{aligned} \quad (7.80)$$

These relations among others can be summarised in the following diagram:

$$(7.81)$$

The representation $\rho = \rho_u \otimes \rho_v$ has an unconventional structure from the point of view of finite-dimensional simple Lie algebras. The different cases are summarised in the following table:

	reducible	irreducible	
decomposable	indecomposable		
never in $Y[\mathfrak{g}]$	for $u - v = \pm i$	$u - v \neq \pm i$	
(only in \mathfrak{g})		(\mathcal{R} almost always fixed)	(7.82)

Fusion. Note that the configuration $u - v = \pm i$ has appeared in several contexts:

- tensor product representations,
- poles and zeros of R/S-matrices,
- bound states of magnons,
- numerator and denominator of the Bethe equations.

These occurrences are all related: Given the structure of the Yangian action at $u - v = \pm i$, namely

$$\Delta(X) \sim \begin{pmatrix} * & * \\ 0 & * \end{pmatrix} \quad \text{but} \quad \tilde{\Delta}(X) \sim \begin{pmatrix} * & 0 \\ * & * \end{pmatrix}, \quad (7.83)$$

one can convince oneself that $\mathcal{R}\Delta(X) = \tilde{\Delta}(X)\mathcal{R}$ implies that \mathcal{R} cannot have maximum rank at $u - v = \pm i$. Hence there must be zeros.

For an S-matrix one would like to implement the relation $S_{21} = S_{12}^{-1}$ strictly. This implies the existence of poles at these locations to compensate for the zeros in S_{21} .

Poles in the S-matrix indicate the presence of bound states. Two particles in a suitable configuration can form a bound state whose propagator manifests as a pole

The diagram shows a four-point vertex labeled \mathcal{R} on the left. This is equal to a summation over 'bound states' of two three-point vertices on the right. Each three-point vertex is represented by a small pink circle with three external lines. The equation is labeled (7.84).

The S-matrix for scattering with bound states can be obtained as a product of scattering processes with the constituents

The diagram shows a four-point vertex labeled \mathcal{R} on the left. This is equal to a product of two three-point vertices on the right. Each three-point vertex is represented by a small pink circle with three external lines. The equation is labeled (7.85).

For the R-matrix there is an analogous relation called *quasi-triangularity*

$$\Delta_1(\mathcal{R}) = \mathcal{R}_{13}\mathcal{R}_{23}, \quad \Delta_2(\mathcal{R}) = \mathcal{R}_{13}\mathcal{R}_{12}. \quad (7.86)$$

These relation in fact imply the Yang–Baxter equation. They can also be used to determine the R-matrix for higher representations.

The poles of the S-matrix can be used to recursively construct the spectrum of all bound state particles and their symmetries. This is called the bootstrap:

- Start with the S-matrix of some particles.
- Find all poles of all available S-matrices.
- Compute the S-matrices for these bound states from quasi-triangularity.
- Repeat the previous steps with the enlarged set of bound states.
- Stop when all poles of all S-matrices have been accounted for.

Note that $\mathcal{R} = (u - v)\mathcal{I} + i\mathcal{P}$ has zeros at $u - v = \pm i$, i.e. $\mathcal{R} = \pm i(\mathcal{I} \pm \mathcal{P})$ becomes a projector. Therefore the R-matrix is sometimes (ab)used to project to sub-representations. For example, the first R-matrix in the following combination projects the space 12 to a symmetric combination

$$\mathcal{R}_{12}(u + \frac{i}{2}, u - \frac{i}{2})\mathcal{R}_{13}(u + \frac{i}{2}, v)\mathcal{R}_{23}(u + \frac{i}{2}, v). \quad (7.87)$$

8 Integrable Statistical Mechanics

The R-matrix formalism opens up applications of integrability to specific models of statistical mechanics in 2 (discrete) dimensions. In the following we will sketch some basic concepts of these models and their solution.

8.1 Models of Statistical Mechanics

As for quantum mechanics, there exists a forest of models some of which have been studied extensively while others have been invented. Let us present a few of these models which are relevant to the integrable context.

Ising Model. The Ising model is one of the most basic models of statistical mechanics. It can be viewed as the statistical mechanics analog of the Heisenberg spin chain:

- it is based on two discrete spin values,
- interactions are typically between nearest neighbours,
- it describes magnetism,

The main distinction is that it is a statistical mechanics model rather than a quantum mechanical one.

Consider a lattice of spins. The spin σ_k at lattice site k can take two values, $+$ or $-$. A state of the model is an assignment of spins σ_k on all lattice sites.¹

The energy of a state is given by a sum over all nearest neighbour pairs

$$E(\sigma) = -\lambda \sum_{(kl)} \sigma_k \sigma_l - h \sum_k \sigma_k. \quad (8.1)$$

The latter term describes the effect of a magnetic field which introduces a bias for the spin orientations. On the one hand one can now determine the minimum-energy configuration; for sufficiently large negative λ (compared to h) this would be an anti-ferromagnetic state with alternating spins, otherwise a ferromagnetic state with all spins aligned (in the direction of the magnetic field).

The fundamental object in statistical mechanics is the partition function

$$Z(\beta; \lambda, h) = \sum_{\sigma} \exp(-\beta E(\sigma)), \quad (8.2)$$

¹The quantum mechanical model would assign a (complex) number to each state.

where β denotes the inverse temperature. In the one-dimensional case, the problem has been solved by Ising. The two-dimensional case was solved by Onsager based on the equivalence to lattice fermions. These two cases are particularly simple because they represent integrable models.

Let us briefly sketch the solution of the one-dimensional model by means of a transfer matrix. The contribution to Z of a pair of spins can be summarised in a 2×2 matrix V

$$V = \begin{pmatrix} e^{+\beta\lambda+\beta h} & e^{-\beta\lambda} \\ e^{-\beta\lambda} & e^{+\beta\lambda-\beta h} \end{pmatrix}. \quad (8.3)$$

Products of this matrix summarise the contribution from consecutive spins. Matrix multiplication takes care of the summation over intermediate spins. For a closed chain of L sites one therefore finds simply

$$Z = \text{tr } V^L. \quad (8.4)$$

This expression can be evaluated by means of the eigenvalues of the above matrix.

This method is somewhat reminiscent of the methods used for integrable spin chains and we will see more of this at work later. Let us mention a relationship to a spin chain Hamiltonian here

$$\mathcal{H} = -\lambda \sum_k \sigma_k^z \sigma_{k+1}^z - h \sum_k \sigma_k^z. \quad (8.5)$$

This is part of the XXZ family of spin chain Hamiltonians. It is a singular case because spin transport along the chain is frozen out. We can write the partition function as a trace over the space of states

$$Z = \text{Tr} \exp(-\beta \mathcal{H}). \quad (8.6)$$

Note that the partition function tells us something about the complete spectrum of states rather than individual states.

Ice Model. The ice model is a model of the crystal structure of ice. Evidently, ice consists of water molecules H–O–H. These are arranged such that every oxygen atom is surrounded by 4 further oxygen atoms. On each of these links there is one hydrogen atom which is associated to either of the two oxygen atoms. Therefore there are two hydrogen atoms per oxygen atom in average.

However, the structure of ice is slightly more elaborate: The potential for the hydrogen atoms has two minima, it can reside in one of two spots along the line connecting the two adjacent oxygen atoms. On the other hand, the interactions between the atoms prefer configurations where two hydrogen atoms are close to each oxygen atom.

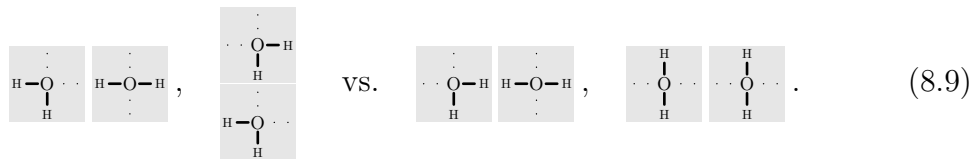


There are many configurations satisfying these criteria. To understand the entropy of ice, one has to count such configurations.

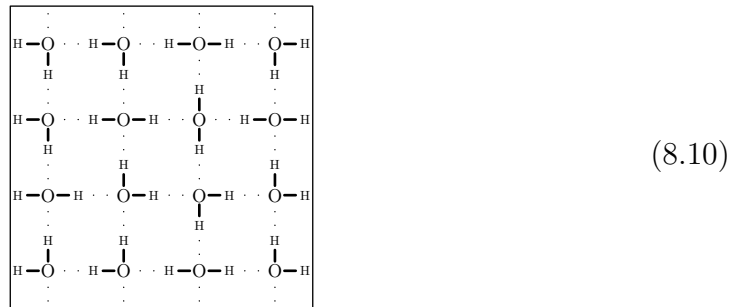
The model is a prototype of the class of *vertex models*. In distinction to the Ising model,² the fundamental building block is a vertex which can be in one of several configurations.



Adjacent vertices have to satisfy certain compatibility conditions. In our case, each link between two atoms has to be singly occupied. Two allowed and two disallowed junctions are



The structure of ice is three-dimensional. For a realistic model one would have to use a tetrahedral structure as the adjacency information. As a more abstract model, one can use a two-dimensional square lattice.



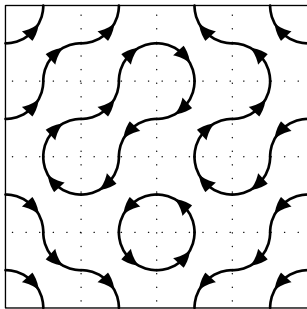
As one can see, many different configurations of this type are conceivable.

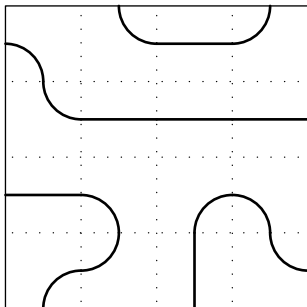
Lattice Path Models. A seemingly different class of models are *lattice path models*. Here one starts with a lattice. Paths are drawn on this lattice according to a particular set of rules, e.g. paths may or may not

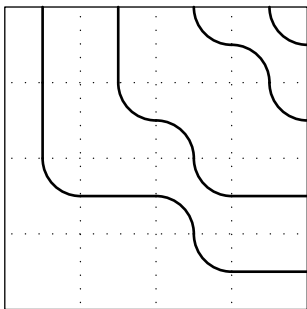
- form loops,
- be allowed to cross,
- be allowed to have straight segments or certain types of curves,
- be directed,
- fill all available space,
-

²Evidently, the Ising model with interactions between nearest neighbours can be represented as a vertex model. The above construction in terms of the matrix V provides such an implementation.

Examples of states in three different lattice path models are:

CPL:  (8.11)

FPL:  (8.12)

DLP:  (8.13)

Alternating Sign Matrices. An old problem of combinatorics is *alternating sign matrices*. On each row and on each column these matrices

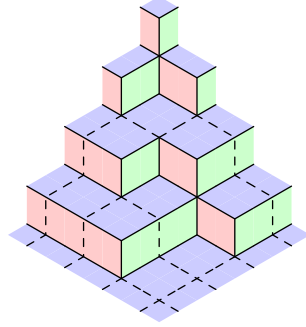
- have an alternating sequence of +1's and −1's
- which starts and ends with +1 and
- is diluted by an arbitrary number of 0's.

An example of a 4×4 alternating sign matrix is

$$\begin{pmatrix} 0 & 0 & + & 0 \\ 0 & + & - & + \\ + & 0 & 0 & 0 \\ 0 & 0 & + & 0 \end{pmatrix}. \quad (8.14)$$

The number of alternating sign matrices is a rapidly increasing sequence starting as 1, 2, 7, 42, 429, . . .

Box Storage Models. A final class of models is concerned with stacking boxes in the corner of a room, e.g.:



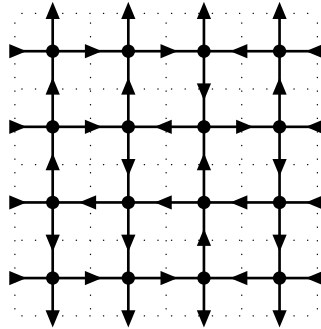
(8.15)

The stack of boxes must not decrease when moving closer towards the corner of the room. Here one may or may not restrict the increase of height by one box per unit step.

Note that this model is evidently equivalent to a rhombus (lozenge) tiling problem. The latter is equivalent to the dimer problem on the honeycomb lattice which is relevant to graphene. One can also relate the model with maximum step size to one of the lattice path models (DLP) where the latter represents the height contours of the former.

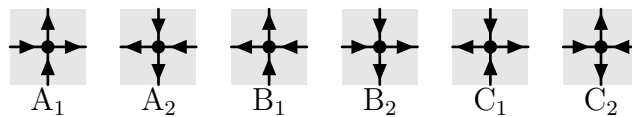
Six-Vertex Model. Most of the above models are particular formulations of the six-vertex model:

- The six-vertex model is a vertex model consisting of 6 types of vertices.
- Each vertex has 4 neighbours.
- Two neighbouring vertices are joined by a directed line.
- At each vertex there must be precisely two ingoing and two outgoing lines.



(8.16)

The 6 vertices are usually denoted by $ABC_{1,2}$:



(8.17)

By decomposing the space of the above models into a lattice of cells, we find that all of them are vertex models and there exists the following dictionary for the

vertices:

model	A ₁	A ₂	B ₁	B ₂	C ₁	C ₂
6-vertex						
ice						
FPLo						
FPLe						
CPL						
DLP						
ASM	0	0	0	0	-	+
box						

(8.18)

Note that the correspondence is not direct for two of the lattice path models. The model denoted by FPL requires separate dictionaries for the even and odd cells of the lattice, respectively. The model denoted by CPL in fact has 8 vertices, and two pairs of vertices (with the same outer links, but different internal connections) are encoded by two single vertices in the 6-vertex model. We will see later how this situation can be interpreted.

A generalisation of the 6-vertex model is the 8-vertex model which has two additional vertices with four ingoing or four outgoing lines:

$$\begin{array}{cccccccc}
 \begin{array}{c} \uparrow \\ \bullet \\ \downarrow \\ \uparrow \\ \bullet \\ \downarrow \end{array} & \begin{array}{c} \downarrow \\ \bullet \\ \uparrow \\ \downarrow \\ \bullet \\ \uparrow \end{array} & \begin{array}{c} \uparrow \\ \bullet \\ \downarrow \\ \uparrow \\ \bullet \\ \downarrow \end{array} & \begin{array}{c} \downarrow \\ \bullet \\ \uparrow \\ \downarrow \\ \bullet \\ \uparrow \end{array} & \begin{array}{c} \downarrow \\ \bullet \\ \uparrow \\ \downarrow \\ \bullet \\ \uparrow \end{array} & \begin{array}{c} \downarrow \\ \bullet \\ \uparrow \\ \downarrow \\ \bullet \\ \uparrow \end{array} & \begin{array}{c} \downarrow \\ \bullet \\ \uparrow \\ \downarrow \\ \bullet \\ \uparrow \end{array} & \begin{array}{c} \downarrow \\ \bullet \\ \uparrow \\ \downarrow \\ \bullet \\ \uparrow \end{array} \\
 A_1 & A_2 & B_1 & B_2 & C_1 & C_2 & D_1 & D_2
 \end{array}
 \quad (8.19)$$

It is more general in the sense that it has sources and sinks for the flow which violate the conservation of the flow of arrows. Many vertex models with more vertices have been considered. Often they are denoted by the number of vertices, e.g. a nineteen-vertex model.

8.2 Integrability

Boltzmann Weights. For combinatorial models, it is usually sufficient to count the number of permissible configurations. In statistical mechanics one may in addition want to compute the partition function at a given inverse temperature β . In that case, each of the 6 vertices is attributed a certain energy e_v . The partition function is given by

$$Z = \sum_{v(k)} \exp(-\beta E), \quad E = \sum_k e_{v(k)}. \quad (8.20)$$

The partition function can also be written as a sum of products of *Boltzmann weights* $\exp(-\beta e_{v(k)})$ for the vertices

$$Z = \sum_{v(k)} \prod_k P_{v(k)}, \quad P_v = \exp(-\beta e_v). \quad (8.21)$$

The Boltzmann weights of the 6 vertices ABC_{12} are denoted by a_{12} , b_{12} , c_{12} , respectively. The configuration of the above sample state of the 6 vertex model contributes the term $a_1^2 a_2^2 b_1^3 b_2^3 c_1^5 c_2^1$ to the partition function.

It makes sense to collect the Boltzmann weights into a matrix \mathcal{R}

[illegible]

In order to compute the partition function for a lattice of size $L \times K$, all we have to do is to multiply these matrices appropriately in a big lattice matrix \mathcal{M} . This is described conveniently in the graphical notation we introduced earlier:

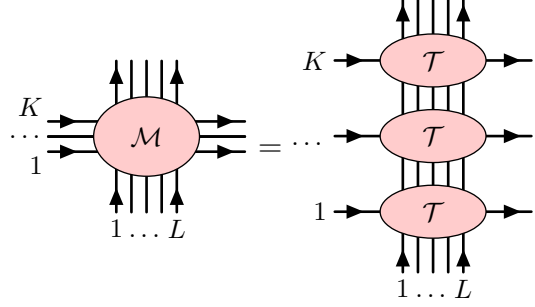
The diagram shows a large pink oval labeled \mathcal{M} on the left, representing a multi-input multi-output (MIMO) system. It has K horizontal input arrows on the left and L horizontal output arrows on the right. Above the oval are L vertical input arrows, and below it are K vertical output arrows. This is followed by an equals sign and a grid of smaller pink circles, each labeled \mathcal{R} . The grid has K rows and L columns. The top row of \mathcal{R} blocks has a horizontal input arrow labeled K on the left and a horizontal output arrow on the right. The bottom row has a horizontal input arrow labeled 1 on the left and a horizontal output arrow on the right. The first column of \mathcal{R} blocks has a vertical input arrow labeled 1 at the bottom and a vertical output arrow at the top. The last column has a vertical input arrow labeled L at the bottom and a vertical output arrow at the top. Ellipses (\dots) are placed between the \mathcal{M} block and the grid, and between the first and last columns of the grid, indicating the continuation of the structure.

The lattice matrix essentially describes the partition function. The matrix \mathcal{R} sums over all possible vertices with corresponding Boltzmann weight. Matrix multiplication then takes care that only matching adjacent vertices are selected.

In order to compute the lattice matrix it is convenient to decompose the lattice matrix \mathcal{M} into row matrices \mathcal{T}_j as

$$\mathcal{M} = \mathcal{T}_K \mathcal{T}_{K-1} \dots \mathcal{T}_2 \mathcal{T}_1, \quad (8.24)$$

or in graphical notation

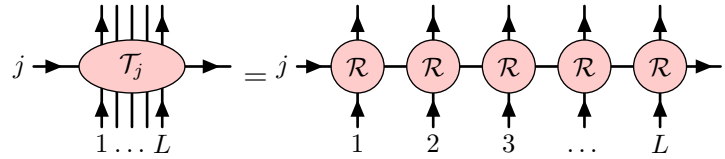


$$(8.25)$$

The row matrices summarise the contribution of a single row j of vertices

$$\mathcal{T}_j = \mathcal{R}_{j,L} \mathcal{R}_{j,L-1} \dots \mathcal{R}_{j,2} \mathcal{R}_{j,1}. \quad (8.26)$$

Note that this is not to be understood as a standard matrix product of the above matrices. The above matrix \mathcal{R} is in fact a tensor of rank 4 and each product merely multiplies along one of the components spaces



$$(8.27)$$

Alternatively, one could decompose the lattice matrix into column matrices $\tilde{\mathcal{T}}$.

So far we have not taken boundary conditions into account. The lattice matrix becomes the partition function after the boundary conditions are implemented appropriately. We shall discuss two relevant boundary conditions further below.

Integrable R-Matrix. We are observing a close similarity to the R-matrix framework for integrable models. The R-matrix of the 6-vertex model has the same form as the R-matrix for the Heisenberg XXZ chain³

$$\mathcal{R}(x, y; q) \sim \begin{pmatrix} a_1 & 0 & 0 & 0 \\ 0 & b_1 & c_1 & 0 \\ 0 & c_2 & b_2 & 0 \\ 0 & 0 & 0 & a_2 \end{pmatrix}. \quad (8.28)$$

The entries of the R-matrix should therefore be interpreted as Boltzmann weights in the statistical mechanics context. The overall scaling of the R-matrix elements

³Note that the R-matrix of the 8-vertex model corresponds to the Heisenberg XYZ chain. Conversely, the Heisenberg XXX chain corresponds to a special case of the 6-vertex model without a reduction of the number of vertices.

is largely irrelevant, and we can adjust it at will. We adjust it such that the coefficients are Laurent polynomials in the parameters.

The coefficients of the R-matrix of the XXZ model take the standard form

$$\begin{aligned} a &= (x/y)q - (y/x)/q, \\ b &= (x/y) - (y/x), \\ c &= q - 1/q. \end{aligned} \tag{8.29}$$

Here x and y are the parameters associated to the two contributing vector spaces.⁴ The deformation parameter q is a global parameter of the XXZ model.⁵ Note that the vertices with opposite directions of all arrows commonly take the same values, i.e.

$$a_1 = a_2 = a, \quad b_1 = b_2 = b, \quad c_1 = c_2 = c. \tag{8.30}$$

However, in some situations one needs more general weights compatible with the constraints

$$a_1 a_2 = a^2, \quad b_1 b_2 = b^2, \quad c_1 c_2 = c^2. \tag{8.31}$$

Most frequently, this generalisation is applied to accommodate for a $c_1 \neq c_2$. This generalisation can always be achieved by an adjustment of boundary conditions, and therefore it is without physical consequences. Generalisations of the type $a_1 \neq a_2$ or $b_1 \neq b_2$ typically have some impact on physics. Note that for the 6-vertex model we are rather free to choose the Boltzmann weights independently while preserving integrability. For higher-vertex vertex models, the configuration of Boltzmann weights for integrable models is very restricted.

The parameters x_j and y_k can be chosen individually per row and per column, respectively. For homogeneous models, however, one would typically choose them to be all equal. In this case the Boltzmann weights are independent of the location of the vertex. Nevertheless, one should allow x and y to take independent values. Furthermore, it may be desirable to have a rotational symmetry for the R-matrix. This is achieved by setting $a = b$.

Parameter Values. In order to investigate the coefficients a, b, c more conveniently, let us choose an overall normalisation such that $b = 1$. Furthermore, split c_1 and c_2 according to

$$\frac{c_1}{c_2} = -q \frac{x^2}{y^2}. \tag{8.32}$$

Finally solve x/y for a

$$\frac{x}{y} = \sqrt{\frac{a - 1/q}{a - q}}. \tag{8.33}$$

⁴The R-matrix is written in a quotient form. The difference form is obtained by setting $x, y = x_0 \exp(u, v)$.

⁵Other parametrisations involve the parameters $\Delta = \frac{1}{2}(q + 1/q)$ and $q = \exp(\hbar)$ or $q = \exp(i\hbar)$. The R-matrix for the Heisenberg XXX model is recovered for $q \rightarrow 1$ with $x, y = q^{u,v}$ and a suitable rescaling of \mathcal{R} .

This leads to the following set of Boltzmann weights

$$b = 1, \quad c_1 = iq^{-1/2} - iaq^{+1/2}, \quad c_2 = iaq^{-1/2} - iq^{+1/2}. \quad (8.34)$$

Let us now consider two of the lattice path models. For the first model (FPL) we would like to have equal weights for all vertices

$$\mathcal{R} = \begin{array}{|c|} \hline \text{[diagram: top-left corner]} \\ \hline \end{array} + \begin{array}{|c|} \hline \text{[diagram: top-right corner]} \\ \hline \end{array} + \begin{array}{|c|} \hline \text{[diagram: bottom-left corner]} \\ \hline \end{array} + \begin{array}{|c|} \hline \text{[diagram: bottom-right corner]} \\ \hline \end{array} + \begin{array}{|c|} \hline \text{[diagram: vertical line]} \\ \hline \end{array} + \begin{array}{|c|} \hline \text{[diagram: horizontal line]} \\ \hline \end{array}. \quad (8.35)$$

This is achieved by setting $a = 1$ and $q = \exp(\pm i\pi/3)$ corresponding to $\Delta = 1/2$.

For the second model we have the directed paths

$$\mathcal{R} = \begin{array}{|c|} \hline \text{[diagram: top-left corner, arrows]} \\ \hline \end{array} + \begin{array}{|c|} \hline \text{[diagram: top-right corner, arrows]} \\ \hline \end{array} + \begin{array}{|c|} \hline \text{[diagram: bottom-left corner, arrows]} \\ \hline \end{array} + \begin{array}{|c|} \hline \text{[diagram: bottom-right corner, arrows]} \\ \hline \end{array} \\ + \left(\begin{array}{|c|} \hline \text{[diagram: top-left corner, arrows]} \\ \hline \end{array} + \begin{array}{|c|} \hline \text{[diagram: top-right corner, arrows]} \\ \hline \end{array} \right) + \left(\begin{array}{|c|} \hline \text{[diagram: bottom-left corner, arrows]} \\ \hline \end{array} + \begin{array}{|c|} \hline \text{[diagram: bottom-right corner, arrows]} \\ \hline \end{array} \right). \quad (8.36)$$

Here we need $a = 1$ for the same reason as above. Now the two vertices c are presented by the four lattice path configurations on the second line. Since these have equivalent links to adjacent vertices, we must set $c_1 = c_2 = 2$. This is achieved by $q = -1$ or $\Delta = -1$.

Note that there is a useful generalisation of the previous model if we keep $q^{1/2} = i\omega$ unspecified. Then the coefficients read

$$a = b = 1, \quad c_1 = c_2 = \omega + \omega^{-1}. \quad (8.37)$$

and we can write the R-matrix as

$$\mathcal{R} = \begin{array}{|c|} \hline \text{[diagram: top-left corner, arrows]} \\ \hline \end{array} + \begin{array}{|c|} \hline \text{[diagram: top-right corner, arrows]} \\ \hline \end{array} + \begin{array}{|c|} \hline \text{[diagram: bottom-left corner, arrows]} \\ \hline \end{array} + \begin{array}{|c|} \hline \text{[diagram: bottom-right corner, arrows]} \\ \hline \end{array} \\ + \left(\omega \begin{array}{|c|} \hline \text{[diagram: top-left corner, arrows]} \\ \hline \end{array} + \omega^{-1} \begin{array}{|c|} \hline \text{[diagram: top-right corner, arrows]} \\ \hline \end{array} \right) + \left(\omega^{-1} \begin{array}{|c|} \hline \text{[diagram: bottom-left corner, arrows]} \\ \hline \end{array} + \omega \begin{array}{|c|} \hline \text{[diagram: bottom-right corner, arrows]} \\ \hline \end{array} \right). \quad (8.38)$$

Here the two terms ω^\pm have been assigned to the two lattice path configurations which contribute to the counting in the same way. Any other distribution leading to the same sum would be equally permissible. This distribution, however, is distinguished because the power of ω is related to the turning number of the paths: For each quarter turn towards the left or right there is a factor of $\omega^{1/2}$ and $\omega^{-1/2}$, respectively. The overall turning number of the first four path configurations is zero, but for the latter four it is half turn in either direction. One can keep track of these factors in the partition function

$$Z = \sum_{k=-\infty}^{\infty} \omega^k Z_k. \quad (8.39)$$

Then Z_k measures the contributions of loops with total turning number $k/2$ towards the left.

By adjusting the Boltzmann weights appropriately, one can try to measure different quantities of the configurations such as the number of loops or the number of self-interactions. One could also use the specific choice $\omega^4 = -1$ to suppress configurations with loops altogether because for every clockwise loop there is a counterclockwise loop with the negative weight.

Periodic Boundary Conditions. We have not yet specified boundary conditions. A convenient choice is periodic boundary conditions in one or in both directions.

If one chooses the horizontal direction to be periodic, the row matrix can be turned into a row transfer matrix by a trace (potentially after inserting a twist matrix)

$$\mathcal{F} = \text{tr}_j \mathcal{T}_j \quad (8.40)$$

or in figures

$$\mathcal{F} = \mathcal{T} = \text{tr}_j \mathcal{T}_j \quad (8.41)$$

When also the vertical direction is periodic, the partition function is given by

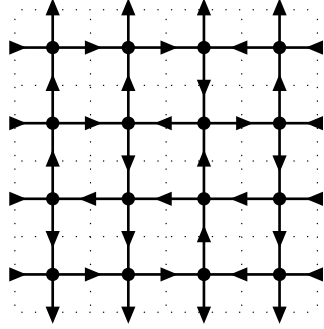
$$Z = \text{Tr } \mathcal{F}^K. \quad (8.42)$$

Therefore, the partition function is determined by the eigenvalue spectrum of the row transfer matrix. In particular, this leads to useful approximations for a very long lattice in the vertical direction. In this case, the largest eigenvalues yield the dominant contributions. The former correspond to the lowest-energy configurations, so this statement makes perfect physical sense, and it allows to derive more concrete statements.

The techniques of quantum integrable systems can now be applied to the system. Here it often makes sense to keep the values of the parameters x_k, y_j arbitrary during the calculation. This allows to investigate the analytical dependence of the observables on them. After having gained a good understanding of the analytical behaviour, one can use it towards construction of the answer. In the answer one can then adjust the parameters to the desired values.

Domain Wall Boundary Conditions. Another boundary condition that has been heavily investigated is domain wall boundary conditions. Here one restricts to a square lattice of size L . All the external links of the vertices are forced in equal configurations along each side of the square. In the 6-vertex description, the horizontal external arrows all point inwards. Consequently, the vertical arrows must point outwards in order to have a conserved flow through the lattice. An

example is given by the configuration:


(8.43)

This partition function for this problem is described by the \mathcal{B} element of the row matrix \mathcal{T} discussed earlier in the context of the algebraic Bethe ansatz. The partition function takes the form

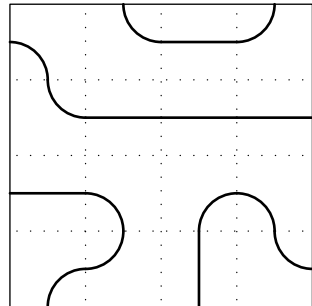
$$Z = \langle \bar{0} | \mathcal{B}^L | 0 \rangle. \quad (8.44)$$

This problem can again be attacked by quantum integrable methods. The result is reminiscent of a determinant formula.

This set of boundary conditions is relevant to alternating sign matrices as one can easily convince oneself. For example, the above pattern corresponds to the alternating sign matrix

$$\begin{pmatrix} 0 & 0 & + & 0 \\ 0 & + & - & + \\ + & 0 & 0 & 0 \\ 0 & 0 & + & 0 \end{pmatrix}. \quad (8.45)$$

Razumov–Stroganov Duality. We are now in the position to introduce the Razumov–Stroganov duality which is a curious relationship between two different lattice path models: On the one hand, there is the FPL model with domain wall boundary conditions on an $L \times L$ square. Its configurations


(8.46)

can be viewed as link patterns on the disk. A link pattern is a configuration of lines which connect $2L$ marked point on the boundary without crossing.


(8.47)

On the other hand, there is the CPL model on the semi-infinite cylinder of circumference $2L$. The states of this model also connect the boundaries according to a link pattern.⁶ The duality relates the probability of finding a state of the CPL model with a given link pattern to the number of states of the FPL model with the same link pattern. Note that the former can be addressed by the wave function of the ground state of the transfer matrix \mathcal{F} .

⁶Paths starting at the boundary and ending at infinity are suppressed.

Schedule of Lectures

The following table lists the locations in the text at the beginning of each lecture:

28.09. 1 [45]:	0. Overview
28.09. 2 [35]:	1.2. ... § Example.
05.10. 1 [35]:	1.3. ... § Quadrature.
05.10. 2 [50]:	1.4. Comparison of Classes
12.10. 1 [30]:	2.3. Spectral Parameter
12.10. 2 [35]:	2.4. ... § Riemann Sheets.
19.10. 1 [45]:	2.5. Dynamical Divisor
19.10. 2 [55]:	3. Integrable Field Theory
26.10. 1 [40]:	3.2. Structures of Integrability
26.10. 2 [50]:	3.3. Inverse Scattering Method
02.11. 1 [40]:	3.3. ... § Inverse Scattering Transformation.
02.11. 2 [50]:	3.4. ... § Riemann Sheets.
09.11. 1 [35]:	3.4. ... § Periods and Moduli.
09.11. 2 [55]:	4. Integrable Spin Chains
16.11. 1 [55]:	4.3. Coordinate Bethe Ansatz
16.11. 2 [40]:	4.4. Bethe Equations
23.11. 1 [55]:	4.5. Generalisations
23.11. 2 [40]:	4.5. ... § Bethe Ansatz at Higher Rank.
30.11. 1 [50]:	5. Long Chains
30.11. 2 [50]:	5.2. ... § Spectral Curve.
07.12. 1 [50]:	5.3. ... § Integral Equations.
07.12. 2 [40]:	6. Quantum Integrability
09.12. 1 [55]:	6.2. Charges
09.12. 2 [45]:	6.2. ... § Multi-Local Charges.
14.12. 1 [55]:	7. Quantum Algebra
14.12. 2 [45]:	7.2. ... § Classification and Construction.
21.12. 1 [45]:	7.3. ... § Universal R-Matrix.
21.12. 2 [40]:	7.4. ... § Magnon States.